

**REPORT for the
Transportation Pooled Fund Program TPF-5(445) Research**

**DESIGN GUIDELINES AND MITIGATION
STRATEGIES FOR REDUCING SEDIMENTATION OF
MULTI-BARREL CULVERTS**

Submitted to:
**Research Program Manager
Iowa Department of Transportation
Office of Research & Analytics
800 Lincoln Way, Ames, Iowa 50010**

Date: December 17, 2024

Submitted by:
Marian Muste (Principal Investigator)
Research Professor (IIHR-Hydrosience & Engineering),
Adjunct Professor (Civil & Env Engineering Department),
The University of Iowa
marian-muste@uiowa.edu; Ph. 319 384 0624

Institution: University of Iowa, IIHR-Hydrosience & Engineering
100 C. Maxwell Stanley Hydraulics Laboratory
Iowa City, IA 52242-1585; <http://ihr.uiowa.edu>; Phone: 319-335-5237

Disclaimer Notice

The contents of this report reflect the views of the authors, who are responsible for the facts and the accuracy of the information presented herein. The opinions, findings, and conclusions expressed in this publication are those of the author and not necessarily those of the project sponsor(s).

The sponsors assume no liability for the contents or use of the information contained in this document. This report does not constitute a standard, specification, or regulation.

The sponsors do not endorse products or manufacturers. Trademarks or manufacturers' names appear in this report only because they are considered essential to the objectives of the document.

Statement of Non-Discrimination

Iowa DOT ensures non-discrimination in all programs and activities in accordance with Title VI of the Civil Rights Act of 1964. Any person who believes that they are being denied participation in a project, being denied benefits of a program, or otherwise being discriminated against because of race, color, national origin, gender, age, or disability, low income, and limited English proficiency, or needs more information or special assistance for persons with disabilities or limited English proficiency, please contact Iowa DOT Civil Rights at 515-239-7970 or by email at civil.rights@iowadot.us.

TECHNICAL REPORT DOCUMENTATION PAGE

1. Report No. TPF-5(445)	2. Government Accession No.	3. Recipient's Catalog No.	
4. Title and Subtitle Design Guidelines and Mitigation Strategies for Reducing Sedimentation of Multi-Barrel Culverts		5. Report Date December 2024	
		6. Performing Organization Code: N/A	
7. Author(s) Marian Muste ORCID - 0000-0002-5975-462X		8. Performing Organization Report No. N/A	
9. Performing Organization Name and Address University of Iowa IIHR-Hydroscience & Engineering 100 C. Maxwell Stanley Hydraulics Laboratory Iowa City, Iowa 52242-1585		10. Work Unit No.	
		11. Contract or Grant No.: TR - 760	
12. Sponsoring Agency Name and Address Iowa Department of Transportation 800 Lincoln Way Ames, Iowa 50010 Federal Highway Administration U.S. Department of Transportation 1200 New Jersey Avenue SE Washington, DC 20590		13. Type of Report and Period Final Report for May 1, 2020 – December 15, 2024.	
		14. Sponsoring Agency Code CFDA/ALN 20.205	
15. Supplementary Notes: None			
16. Abstract The accumulation of sediments at culverts is a chronic operational issue, frequently occurring at multi-barrel culverts located in erosion-prone watersheds. Sediment deposits can develop rapidly, impairing the culvert's capacity to convey design flows and potentially leading to damage to both transportation infrastructure (e.g., road and culvert overtopping) and upstream areas (e.g., flooding). Current culvert design protocols focus primarily on flood flow conveyance, with less attention given to assessing the potential for sedimentation due to the limited understanding of the complex erosion and transport processes leading to culvert sedimentation. Consequently, costly culvert cleaning is often required to maintain operational functionality. The overarching goal of this experimental study, funded by the Iowa, Mississippi, Missouri, New Mexico, and Utah Departments of Transportation (DOT), is to develop mitigation solutions for reducing or eliminating sediment accumulation at three-barrel culverts. The study builds on the experience garnered through pioneering research initiated by the Iowa DOT to substantially advance the understanding of complex flow and sediment transport through culverts located in various hydrological and geomorphological conditions. The proposed mitigation solutions are based on the Self-Cleaning-Culvert (SCC) concept, which relies on the stream's hydraulic power to pass sediment carried by the stream through culverts. The laboratory study entails 180 stand-alone tests conducted in two flume arrangements: Iowa-Mississippi-Missouri (IMM) and New Mexico-Utah (NMU). The tested SCC designs demonstrated satisfactory sediment conveyance efficiency for the IMM culverts, with more than half of the designs increasing sediment conveyance capacity by 50 to 72%. However, the addition of the SCC at the NMU culvert entrance displayed reduced conveyance (less than 25%) due to changes in geometry that further hampered the structure's capability to handle the much heavier sediment load carried by typical NMU flash floods compared to the extreme precipitation events occurring in the IMM landscape.			
17. Key Words: culvert hydraulics, multi-barrel culverts, sediment transport, sedimentation, self-cleaning culvert design		18. Distribution Statement No restrictions	
19. Security Classification Unclassified	20. Security Classification Unclassified	21. No. of Pages 119	22. Price N/A

This page left intentionally blank

Executive Summary

Sedimentation at culverts is an issue frequently occurring at multi-barrel culverts located in erosion-prone watersheds. The intensification of the human activities on hillslopes, floodplains, and in streams compounded with the impacts of the climate change aggravate the chronicity of the culvert sedimentation problem raising considerable operational concerns and maintenance issues across many areas of the United States. Sediment deposits can develop quickly impairing the culvert capacity to convey design flows and potentially leading to damages to both the transportation infrastructure (e.g. road and culvert overtopping) and upstream areas (e.g. flooding). The current culvert design protocols are based on the analyses of hydrologic, hydraulic, and geomorphological conditions at the culvert site with the focus on flood flow conveyance. Less attention is given to the assessment of the potential for sedimentation as the knowledge on the complex erosion and transport processes leading to culvert sedimentation is scarce. These knowledge gaps preclude formulation of guidelines for culvert sedimentation forecasting and mitigation that in turn require to make recourse to costly cleaning methods that often need to be repeated to keep the culverts operational.

The present study builds on the experience garnered through pioneering research initiated by Iowa Department of Transportation (DOT) in 2006 to more substantially advance the understanding the complex flow and sediment transport through culverts located in a variety of hydrological and geomorphological conditions. The overarching goal of this new study funded by the Iowa, Mississippi, Missouri, New Mexico and Utah DOTs is to identify and evaluate the performance of mitigation solutions for reducing or eliminating sediment accumulation at three-barrel culverts. The proposed mitigation solutions are based on the Self-Cleaning-Culvert (SCC) concept that relies on the use of the stream hydraulic power for passing sediment carried by the stream through culverts.

This laboratory study entails 180 stand-alone tests conducted in two flume arrangements, i.e., Iowa-Mississippi-Missouri (IMM) and New Mexico-Utah (NMU). Abundant quantitative and qualitative data and information was acquired for as-is and SCC-modified flume arrangements exposed to precipitation events realistically replicated in the model with precisely controlled experimental protocols. The sedimentation patterns and areal distributions obtained for the as-is IMM and NMU culverts consistently display different sedimentation patterns across the tested hydro-morphological conditions. Specifically, the IMM culverts favor sedimentation in the outer areas of the culvert entrance and culvert body while the NMU culverts display a much more uniform sediment distribution at culvert entrance and throughout the culvert. Based on these preliminary inferences, we designed and tested 8 IMM and 6 NMU SCCs by changing the geometry of the transition areas leading to the culvert inlet with streamlined shapes that directed the flow through the central barrel.

The tested SCC showed a satisfactory sediment conveyance efficiency for the IMM culverts with more than half of the tested SCC designs increasing the sediment conveyance capacity between 50 and 72%. The addition of the SCC at the NMU culvert entrance displayed reduced conveyance (less than 25%) as the change in the geometry in this area further hampered the capability of the structure to handle the much heavier sediment load carried by typical NMU flash floods compared with the extreme precipitation events occurring in the IMM landscape. Nevertheless, the NMU SCCs display beneficial impacts by elevating locally the stream bed layer that in turn enhances the stream power during subsequent storms and by retaining large volumes of sediment upstream the culvert from where it can be easier removed in case of culvert operation failure. The qualitative and quantitative data and information accumulated through the experimental research enabled to straightforwardly distinguish the self-cleaning potential of individual SCC designs allowing to confidently rank the structures using various criteria, i.e., hydraulic and sediment transport efficiency, upfront and during operation costs, or secondary-induced effects on stream aesthetic appearance and ecological aspects.

The vast amount of data and information delivered by the study is analyzed with the end-user

interest in mind focusing mostly on the practical needs of engineers (notably from state and federal transportation agencies, and consultancies in the US) engaged in the design, monitoring, or troubleshooting culvert maintenance. As culvert design requires data on the site hydro-morphological and meteorological conditions in addition to specifications on the culvert structure and setting at the road-culvert crossing, the practical recommendations synthesized through this study should be used with caution and tempered by engineering judgement as the results rely only on a limited number of experiments applied to a subset of possible hydraulic conditions at the culvert-road-stream crossings. Until new experimental evidence of this kind becomes available, the suggested considerations can be helpful for better informing the SCC preliminary design and culvert operational practice. The experimental evidence garnered through the study is a great data resource for further explorations of sediment transport through culverts, a complex and understudied topic in hydraulic engineering.

Keywords: culvert hydraulics, multi-barrel culverts, sediment transport in unsteady and nonuniform flows, self-cleaning culvert design, complex experimental protocols,

Acknowledgements

The project research team (i.e., the Principal Investigator and the 14 research assistants) are grateful to the project Technical Advisory Committee members (S. Claman, J. Ellis, K. Clute – Iowa DOT; V. Wilson, T. Buie – Mississippi DOT; J. Harper – Missouri DOT; S. Morgenstern, S. Lokey – New Mexico DOT; B. Cox, C. Alberts – Utah DOT) for the active role in the investigation and for continuously shaping the development of the research path through direct and virtual communication during the 3 annual project meetings, 6 online coordination sessions, and 8 surveys.

Table of Contents

Section	Page Number
1. RESEARCH BACKGROUND	1
1.1. Substantiation of sedimentation-at-culvert problem	1
1.2. Culvert sedimentation processes	2
1.3. Guidance and relevant research on culvert sedimentation	2
1.4. Iowa studies on culvert sedimentation & mitigation	8
2. TPF PROJECT SCOPE, OBJECTIVES, AND TASKS	12
3. PHYSICAL MODELING CONSIDERATIONS	13
3.1. Overview of the modeling strategy	13
3.2. General principles for designing self-cleaning culvert configurations	19
4. EXPERIMENTAL ARRANGEMENT, PROTOCOLS, AND DATA PROCESSING	22
4.1. Overview of the TPF experimental plan	22
4.2. Experimental facility and instrumentation	22
4.3. Hydraulic similitude	28
4.4. Experimental phasing and associated protocols	29
4.5. Data acquisition & processing protocols	36
4.6. Experimental matrices targeted by the study	40
5. EXPERIMENTAL RESULTS FOR PRODUCTION TESTS	48
5.1. Overview	48
5.2. Results of the IMM production test	49
5.3. Results of the NMU production tests	63
6. SENSITIVITY AND SYNTHESIS ANALYSES	71
6.1. Overview	71
6.2. Sensitivity tests	71
6.3. Additional hydro-morphological considerations on the IMM & NMU tests	82
6.4. Closing comments on the experimental results	93
7. PRACTICAL RECOMMENDATIONS	95
7.1. Inferences from the experimental tests	95
7.2. Culvert design considerations	99
8. CONCLUSIONS	103
REFERENCES	104

List Figures

Figure 1. Samples of multi-box culverts in US Midwest	1
Figure 2. End-to-end culvert sedimentation processes	3
Figure 3. Definitions for characterizing the degree of sedimentation at culvert inlet	4
Figure 4. Illustration of sedimentation progress at a 3-box culvert	5
Figure 5. Multi-box culvert with low flow barrel	7
Figure 6. Culvert modifications for expanding the culvert design sustainability	7
Figure 7. Self-cleaning culvert (SCC) solutions identified through previous research for 3-barrel culverts	9
Figure 8. Iowa multi-culvert study location	10
Figure 9. Self-cleaning culvert solutions	11
Figure 10. Flow configuration at culvert sites: a) Iowa-Mississippi-Missouri culvert setting; stream-to-culvert transition	15
Figure 11. Hydrologic/hydraulic variables recorded at a three-box culvert	17
Figure 12. Sedimentation patterns at the culvert	17
Figure 13. Sensitivity of the hydraulic model to the type of sand used for the experiments	18
Figure 14. Sedimentation conditions at three-box culverts	19
Figure 15. Flow aspects relevant to TPF study	20
Figure 16. Flow patterns targeted by IMM self-cleaning culvert design	21
Figure 17. Iowa-Mississippi-Missouri experimental facility	23
Figure 18. New Mexico-Utah experimental facility	24
Figure 19. Essential items for flow control and experiment execution for the IMM and NMU tests	26
Figure 20. Webcam system	27
Figure 21. Laser surveys	27
Figure 22. Sedimentation patterns for various steady flows	30
Figure 23. Sample tests for various steady flows in the “as-is” IMM culvert	31
Figure 24. Water and sediment hydrographs for storms modeled in the IMM flume	33
Figure 25. Sample results for steady and unsteady flows tested in the IMM flume with coarse sand and protocols described in Table 7 and Figure 24b (bottom) for the flood wave	34
Figure 26. Water and sediment hydrographs for storms modeled in the IMM flume	35
Figure 27. Additional flow conditioning devices for NMU flume	35
Figure 28. Sample results for steady and unsteady flows tested in the “as-is” 0.3 degree stream-to-culvert NMU flume with coarse sand	36
Figure 29. Photo-documentation of individual tests	37
Figure 30. Documentation of individual tests	37
Figure 31. Processes applied to images to obtain the 2-D mapping using Photoshop software	38
Figure 32. Sequence of procedures used to determine the volume distributions in the culvert vicinity using the Lidar surveys	39
Figure 33. Comparison of the areal sediment accumulations obtained with analysis of images and Lidar survey	40
Figure 34. Ranking of the SCC for the IMM flume layout	49

Figure 35. Delineation of the areas for the analysis of sedimentation in the vicinity of the culvert body for the IMM flume layout	50
Figure 36. Snapshots of the first 3 ranked SCC tested for the IMM flume layout acquired during the tests at $\frac{1}{4}$ (the first row), $\frac{1}{2}$ (the second row), and at the end of the experimental runs (the third row) using time-lapsed movies captured with the webcam	52
Figure 37. Sample still photos for two IMM CSSs subjected to an aggressive storm (1RE)	53
Figure 38. IMM SCCs tested with: a) one light & long storm flow (1LL), and b) one aggressive storm scenario (1RE)	54
Figure 39. Synoptic view of all IMM SCC production tests	55
Figure 40. Synoptic view of all IMM SCC production tests	56
Figure 41. Ranking of the SCC for the NMU flume layout	63
Figure 42. Production test results for the ranked NMU SCC sedimentation pattern distribution extracted from the group of tests with a stream-to-culvert angle of 2 degrees	65
Figure 43. Ranking of NMU SCCs for two types of storms	66
Figure 44. Lidar survey maps for the stream and culvert slopes set at a 0.3 degree	67
Figure 45. Ranking of NMU SCCs for one aggressive storm in the 4-degree stream-to-culvert angle	68
Figure 46. Synoptic view of all NMU SCC production tests in the 0.3 degree slope layout	69
Figure 47. Synoptic view of the NMU SCC production tests in the: a) 2 degree stream-to-culvert flume layout, and b) 4 degree stream-to-culvert flume layout	70
Figure 48. Sensitivity test to illustrate differences in depositional patterns between suspended and bedload transport.	72
Figure 49. Stress tests for increased sand loads applied to IMM flume SCCs	73
Figure 50. Long-tapered curtain wall efficiency	74
Figure 51. Partitioning of the sediment deposit footprint per IMM culvert areas	75
Figure 52. Sensitivity tests for highlighting the sand characteristics impact on sediment footprint in the IMM flume layout	76
Figure 53. Stress tests for increased sand loads and simulated culvert clogging applied to NMU flume SCCs	81
Figure 54. Definition sketches for sampling the depth and velocity field in the vicinity of the culvert	83
Figure 55. Numerical simulations results used for relating the central point velocity acquired in the model and mean velocities used for determining the Fr and Re numbers corresponding to model discharges of: a) 50 gpm, and, 100 gpm	83
Figure 56. Numerical and graphical representation of the depths and velocities in the IMM SCCs' vicinity along with the Fr and Re numbers for the flow in the incoming stream. For varying flows, the Fr and Re are only provided for the initial test stage	84
Figure 57. Pairing of the sedimentation footprint with the spatial distributions of depths and velocities in the culvert vicinity for selected flow and SCC combinations	90
Figure 58. Definition sketches for sampling the depth and velocity field in the vicinity of the culvert	91
Figure 59. Numerical and graphical representation of the depths, velocities, Fr and Re for NMU tests	92
Figure 60. Terminology for defining culvert road crossing The presence and degree of flow nonuniformity	95
Figure 61. Illustration of the flow nonuniformity effect in the transition area from the stream to the IMM and NMU culvert entrance	97
Figure 62. Flowchart for SCC design with considerations on sediment transport	100

List of Tables

Table 1. Hydro-geomorphologic variables driving sedimentation at culverts	3
Table 2. Comparison of the three self-cleaning culvert (SCC) designs	10
Table 3. Project technical advisory committee	12
Table 4. Objectives (O) and final tasks (I) for the TPF Project-5(445)	13
Table 5. Scaling of essential variables for $L_r = 1:25$	28
Table 6. Phasing of the experimental program	29
Table 7. Steady flow scenarios for supporting phases PH2, PH3 and PH4 of the study	31
Table 8. Self-cleaning configurations for the IMM flume arrangement	41
Table 9. Modeled hydrographs and sediment characteristics for the IMM flume arrangement	42
Table 10. Sensitivity tests for various storms, sand types and loads for the IMM flume arrangement	42
Table 11. Sensitivity tests with fine sediment in the IMM flume arrangement	43
Table 12. Experimental matrices for the 0.3, 2 and 4 degrees NMU flume arrangement	44
Table 13. Sensitivity tests for various culvert configurations, event hydrographs, and stream-to-culvert slope for the NMU flume arrangement	47
Table 14. Summary of the experimental tests conducted through the study	48
Table 15. Froude and Reynolds numbers for NMU SCCs tested for one aggressive storm (1RE)	92

1. RESEARCH BACKGROUND

1.1. Substantiation of sedimentation-at-culvert problem

The vast majority of the U.S. secondary roads entails culverts to enable stream crossings. Different designs are used to accommodate the hydraulics of the culvert site and the hydrology of its drainage area (FHWA, 2012). Multi-barrel (a.k.a. multi-box) culverts are often deployed at stream crossing with larger flows and higher road embankments. Typically, multi-barrel culverts are sized to handle specific return flows (i.e., 25 or 50 years) in culvert design process (Cafferata et al., 2017; Pyles et al., 1989). There is no substantial evidence to suggest that culverts operation and failures are related to limited capabilities to convey design discharges (Cafferata et al., 2017). A more prevalent cause in operations is the accumulation of sediment and/or debris at the culvert inlet. These sediment deposits partially block the culverts, and, when become severe, can lead to culvert overtopping flooding during extreme events (Furniss et al., 1998; Foltz et al., 2008; MacDonald & Coe, 2008).

Ideal operation (as designed) for a multi-box culvert is indicated by a stable stream geometry in the culvert vicinity over time, as illustrated in Figure 1a. Situations such as those shown in Figure 1a are however rare across the U.S. landscape. Surveys conducted by our research team in 2009 and 2013 indicate that about 95% of Iowa culverts are silted in various degree of severity (Ho, 2010; Muste & Xu, 2017a). Sediment accumulations at culvert inlets develop quickly reducing considerably their capability to handle significant flow events, as the partial blockage of the structures may severely impair their hydraulic capacity (see Figure 1b). Impairing the culvert capacity to convey design flows leads to damages to the transportation infrastructure and the surrounding areas.

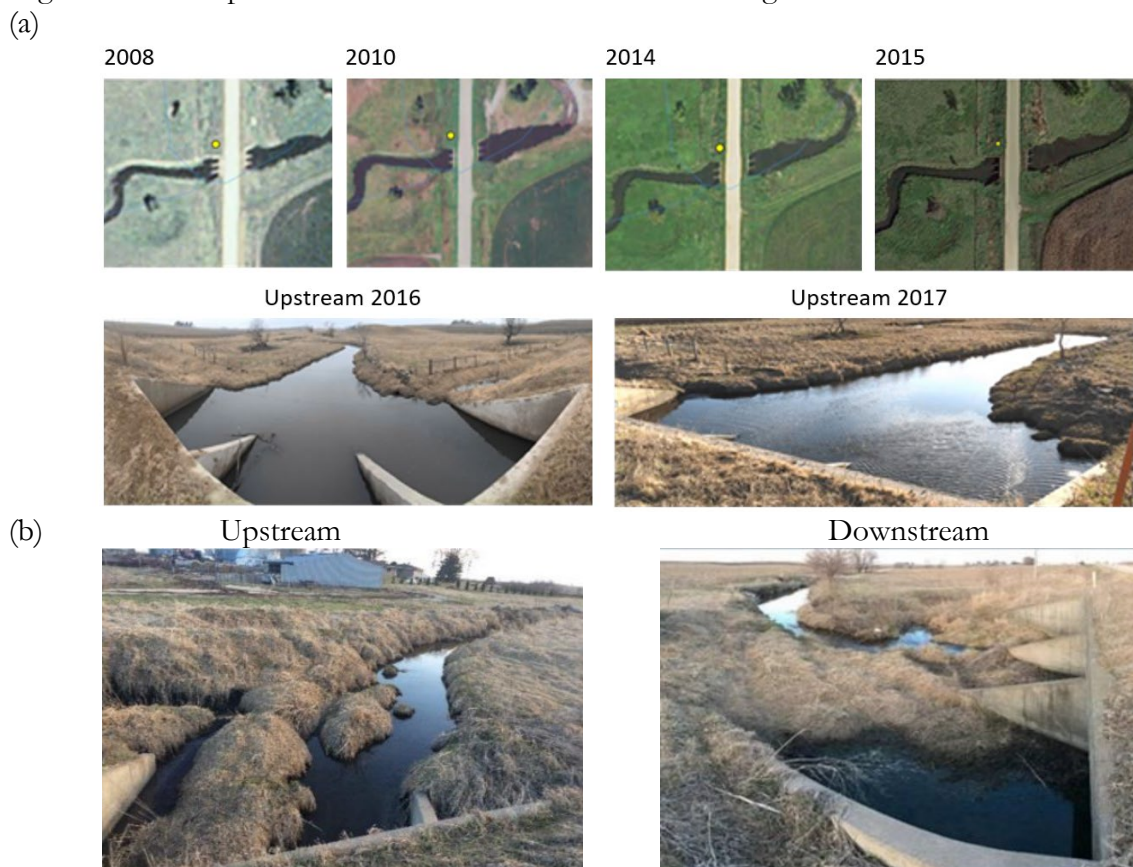


Figure 1. Samples of multi-box culverts in US Midwest: a) culverts without sediment accumulations (less than 5% of the culverts in Iowa); b) silted culvert (about 95% of Iowa culverts)

Obstruction at the culvert inlet may cause both damage to the transportation structure (due to culvert and road overtopping) and/or in its vicinity (by creating a ponding area during floods). The high degree (severity) of culvert sedimentation observed in many regions stems from the fact that the main, and, in many cases, the only culvert design criteria, is to ensure the passing of the design flow. Limited attention is paid to the sediment transport processes in the uphill areas and the vicinity of culverts. Another detrimental factor not accounted in the culvert design is the aggravation of sedimentation due to the vegetation growth over the freshly created sediment deposits.

Culvert sedimentation concerns are widespread in the nation, from California to Pennsylvania and from Wisconsin to Florida (Rowley, 2014), with direct bearing on the culvert's ability to maintain normal operation during extreme flows when the structure is essential for the communities they serve. Despite its ubiquitous presence, the mitigation of sedimentation at culverts is a peripheral activity called upon only for extreme situations or when specific requests are placed by concerned land owners. Systematic research efforts for mitigating culvert sedimentation are limited, despite the availability of many technical means that enable the comprehensive observation, understanding, and mitigation of the involved processes (Muste & Xu, 2022).

Given that currently sedimentation at culverts does not benefit by well-established mitigation solutions, the only alternative for DOT maintenance offices is repeated cleaning. Culvert cleaning is one of the costliest maintenance operations for Iowa culverts due to the cleaning frequency, the range of equipment used, and the labor required for the cleaning (one-time cleaning cost for a 3-box culvert ranges between \$15,000 and \$20,000). The socio-economic costs associated with culvert sedimentation are unlikely to diminish, as recent studies predict that the frequency and intensity of storms will likely increase in the contiguous United States (Villarini et al. 2013).

1.2. Culvert sedimentation processes

While sedimentation at culvert is a localized in-stream process, it is highly dependent on the processes occurring in the drainage area leading to the road structure. The dynamics of the sediment movement from source to the deposition location depends on multiple factors. These factors include culvert location in the drainage area, the culvert's configuration, and its structure positioning with respect to the stream. For the same culvert location, the sediment transport regimes can be different depending on the characteristics of individual storm events and the type of the culvert's hydraulic control. For example, at an inlet control culvert, the sediment-prone area is upstream near the culvert's entrance. For a culvert with outlet control, its barrels and downstream area can be more silted.

Conceptually, the processes generating culvert sedimentation can be grouped into three major categories as depicted in Figure 2: (a) soil detachment (i.e., erosion, sediment supply, and sediment production, as illustrated in Figure 2a), (b) sediment transport (overland and in-stream demonstrated in Figure 2b), and (c) sediment deposition (settling at culvert structure and stabilization due to vegetation growth, as shown in Figure 2b). The three categories of sedimentation processes are tightly related in an end-to-end spatial continuum that connects the sedimentation sources (in drainage basins) and their transport pathways (through watersheds and stream networks) with the deposits formed at the culverts (Haan, 1994; Schumm, 1977; Merritt et al., 2003, and Lord et al., 2009).

As physical-based investigations of culvert sedimentation through simulation are scarcely reported in the literature, this section discusses some salient features of the end-to-end sedimentation process to substantiate the variables that are contributing most to the culvert sedimentation process. A data-driven study by Xu (2019) investigated the origin and interconnections among the processes involved in forming sediment deposits at culverts. More than 800 Iowa culverts have been analyzed using machine learning to determine sedimentation causality and dependencies. The most relevant variables are summarized in Figure 2 and Table 1, along with the sources of information about specific data.

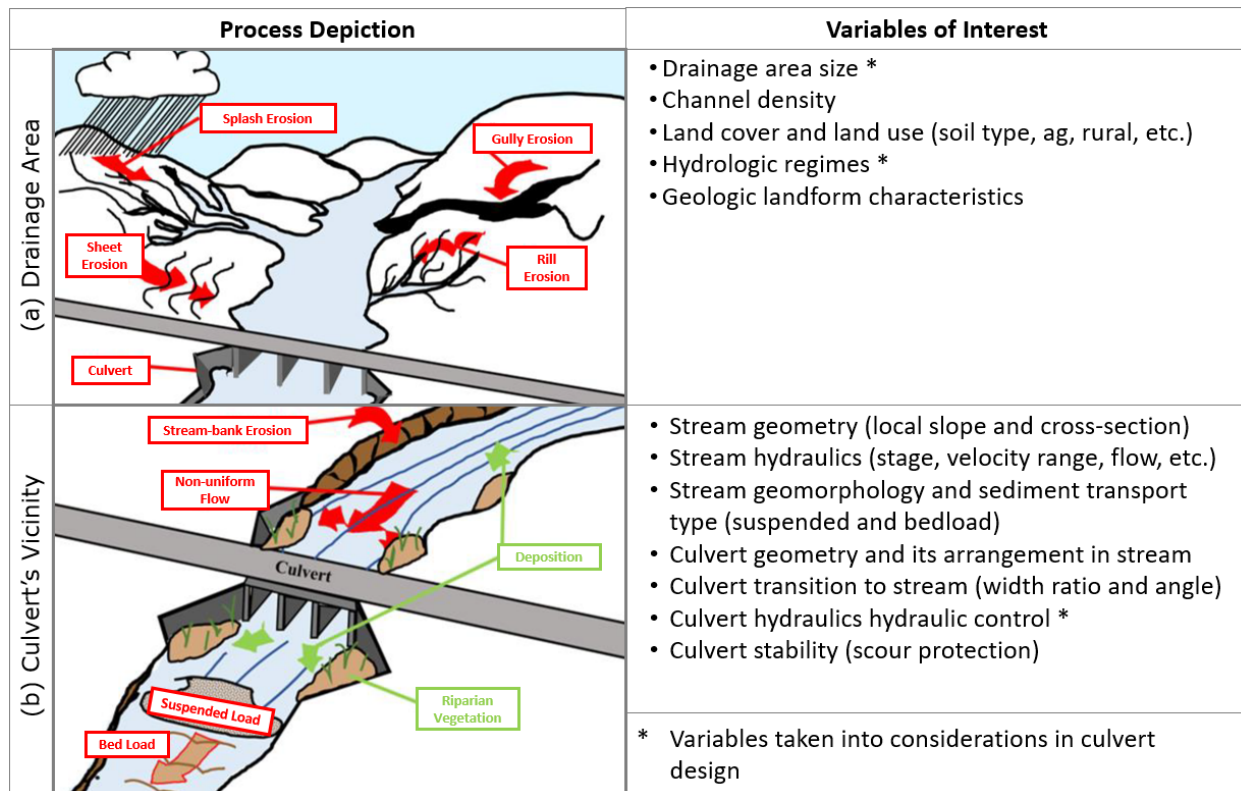


Figure 2. End-to-end culvert sedimentation processes: a) soil detachment in the drainage area; b) in-stream sediment transport in the culvert vicinity (Muste and Xu, 2017a).

Table 1. Hydro-geomorphologic variables driving sedimentation at culverts (Muste & Xu, 2022)

Variables of Interest	Data Source(s)
Watershed characteristics	
Drainage basin area	NHD - Plus, StreamStats
Sediment sources	SSURGO, RUSLE
Hydrologic regimes	USGS flood-frequency analysis
Localized erosion processes	On site reports (if available)
River corridor characteristics	StreamCAT, Land Use and Land Cover (LULC)
Geomorphologic characteristics	e.g., historical landform regions
Culvert vicinity	
Stream geometry	Aerial imagery, topo surveys
Stream hydraulics	Stage & free-surface slope monitoring
Stream geomorphology & sediment transport types	Coring, topoc surveys, suspended sediment monitoring
Culvert geometry & siting	Design manual and field surveys
Culvert transitions to stream at inlet and outlet	SIIMS*, Aerial imagery
Culvert hydraulics	Design specs, in-situ measurements
Vegetation presence	Aerial and local imagery
Culvert stability	Design & field inspections
Culvert flow controls	SIIMS*
*SIIMS – Iowa’s Department of Transportation Structure Inventory & Inspection Management System	

The findings published in the literature along with our recent study results indicate that the variables governing the flow-sediment interaction locally (i.e., the “Culvert vicinity” group of variables in Table

1) are the most significant contributors to the deposition of sediment at culverts. Our studies found that the most important local factors leading to sedimentation at culverts include the Stream-to-Culvert Width (SCW) ratio, the type of culvert flow control (i.e., inlet or outlet), and the stream geomorphological and ecological aspects at culvert location (Ho, 2010, Xu et al., 2019b). The SCW ratio is defined as $SCW = B/W$, where B is the width of the undisturbed stream and W is the total span of the culvert, as illustrated in Figure 3 for a three-box culvert. The culvert span and its height are dictated by the value of the design flows that they have to handle (i.e., typically storm events having a 25- or 50-year return period). In most of the cases, the design procedure requires culvert spans that extend beyond the width of the natural channel; therefore, channel transitions are required to convey drainage flow to and from the culvert. Normally, a channel expansion is located upstream of the culvert and a contraction is downstream of the culvert, as shown in Figure 3.

These transitions disturb the natural channel regime, producing nonuniform flows that during propagation of storm events are also unsteady. During low flows (that dominant throughout the year), only one barrel carries the stream flow. Often, the preferred barrel is not the central one.

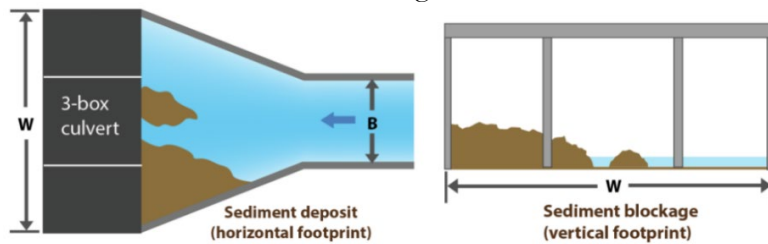


Figure 3. Definitions for characterizing the degree of sedimentation at culvert inlet (Xu, 2019)

Two indicators were used in our previous studies to quantify the sediment deposits extent: the areal degree of sedimentation, and the blockage at the culvert entrance, as illustrated in Figure 3. The degree of the sedimentation defines the ratio between the area occupied by sediment deposits at any given time and that of the original clearance between the inlet and outlet in relation to the natural stream at the time of the culvert construction. The degree of sediment blockage characterizes the reduction of the culvert's inlet cross-section, which directly affects the structure's capacity to convey high flows.

The widely different types of flows carrying with them sediment in suspension and as bedload trigger an unwanted effect during the transition through the multi-barrel culverts: sedimentation (Tsihrintzis, 1995; Kosicki & Davis, 2001; and Charbeneau et al., 2002). The localized sediment depositions at 3-box culverts are initiated at the culvert inlet and within the culvert barrels when flow rates are smaller than the design flow. Deposits occur in these enlarged stream areas because the sediment transport capacity of flow is less than in the undisturbed stream due to the flow non-uniformity. During the sediment deposition, various degrees of compaction of the settled materials are attained depending on the nature of the material in the deposit, flow duration, ponding in the culvert area, and other factors. It is rare that the deposits are removed by subsequently occurring large flows moving over the compacted deposits. Additional complexities favoring sedimentation are formation of point bars due to stream bends, abrupt changes to a flatter grade in the culvert or in the channel adjacent to the culvert, and the presence of woody or leafy debris.

There is no question that unsteady flows enhance the sediment movement compared with an equivalent steady flow counterpart (Rowinski & Czernuszenko, 1998; Suszka, 1987). The increased intensity of turbulence on the rising limb of the hydrograph entrains more sediment than on the falling limb. In the middle of the falling limb, the sediment in suspension reaches a minimum and then increases to the value for a steady flow condition (Rowinski & Czernuszenko, 1998). The amount of sediment entrainment depends on the magnitude of hydrograph in the first place and its shape (e.g., steeper or wider) in the second, resulting in more sediment carried out by steeper hydrographs than the flatter ones. What is still less understood, is the fractional contribution of the suspended and bedload during the propagation of the storm following a precipitation event (De Sutter et al., 2001).

It can be concluded that the shape of the area leading to the culvert inlet (defined by the presence or absence of oblique wingwalls) is a prime factor in determining the hydraulics regimes occurring upstream and inside the culvert seconded by the flow condition in the expansion area at the culvert outlet. The flow nonuniformity determined by the inlet shape in combination with the intensity of the storm (magnitude normalized with its duration) are the dominant drivers affecting the culvert capacity to convey sediment. Ensuing from the above considerations, is that sediment transport theories should be involved while designing culverts in streams loaded with sediment. After the deposits are established, the flow and sediment conveyance are further changed commensurate with the amount and patterns of deposition. Larger amount of sediment deposition at the culvert entrance elevates the headwater in comparison to culvert free of sediment disregard of the size of sediment in the deposit (as long as the sediment is moving, not blocking the culvert entrance).

The sedimentation at culverts evolves with each incoming storm and can be aggravated between storms when another concern might come into play: the vegetation growth on the initially created sediment deposits. The vegetation growth stabilizes the sediment deposits further complicating both the flow conveyance and the stability of the culvert structures over time. Information assembled during field visits and from aerial photographs collected over successive years by our research team across the state of Iowa has revealed that the process of sedimentation at culverts can attain a stable form of the sediment deposits in no more than four to five years (Muste & Xu, 2017a). A sample of repeated survey documented by our research team is shown in Figure 4.

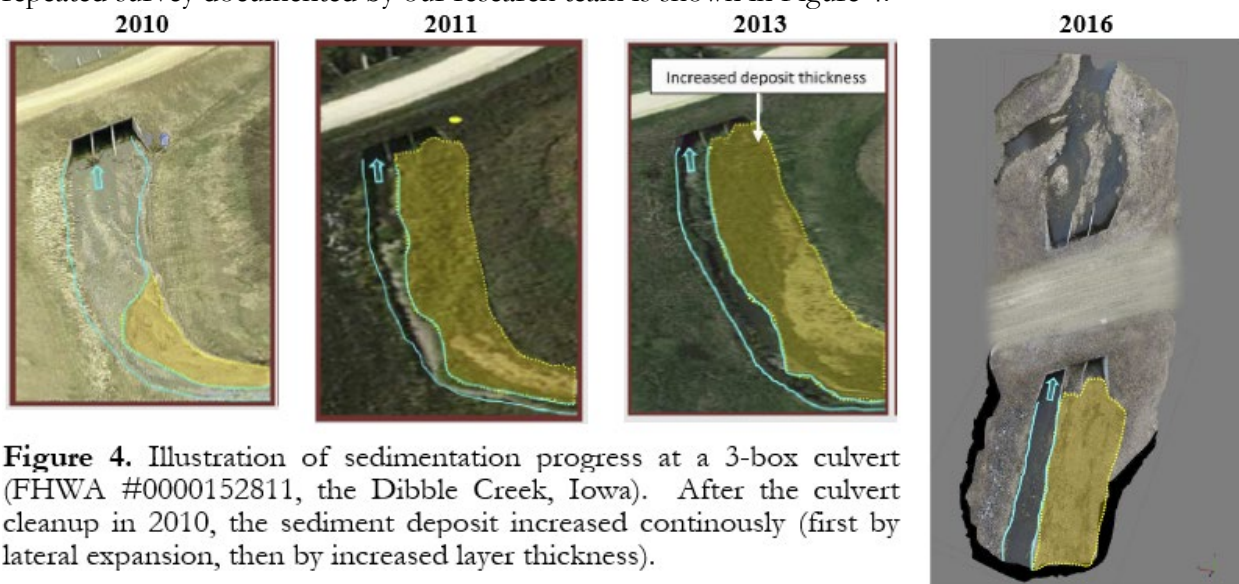


Figure 4. Illustration of sedimentation progress at a 3-box culvert (FHWA #0000152811, the Dibble Creek, Iowa). After the culvert cleanup in 2010, the sediment deposit increased continuously (first by lateral expansion, then by increased layer thickness).

The rate of development of the sediment deposits depends on the geological characteristics, practices implemented in the drainage area upstream the basin, and intensity and sequencing of the strong meteorological events. The increasing intensity and frequency of precipitation combined with the human interventions in watersheds of the last decades have drastically altered the natural sediment regime in watersheds over the whole contiguous US (Solomon et al. 2007). These changes in the watersheds trigger imbalances of the water cycle that in turn accelerate upland erosion (sediment production) and in-stream sediment transport (through aggradation, scouring, and deposition). The formation of sediment deposits negatively affects the stability of river morphology, the vulnerability of the riverine structures, and sustainability of aquatic biology (Tetreault et al., 2018). The insights provided by the above-mentioned observations enable a more comprehensive understanding of the processes leading to culvert sedimentation hence better informing managerial decisions and the development of methods towards the effective mitigation of this operational nuisance.

1.3 Guidance and relevant research on culvert sedimentation

Engineers tackle stream-roadway crossings by designing and installing a bridge or culvert structure. While they share similar hydraulic behavior, bridges are typically associated with larger streams while culverts are viewed as a small-stream crossing solution. The criterion used by for distinguishing between the two structures is the size of the opening width (Shall et al., 2012): a bridge is recommended if a single-culvert span determined from design exceeds a 20 ft (6.1 m). Culverts resemble tunnels of short spans embedded in the soil, while bridges have support structures beneath them with open areas preserving the bed of the river practically undisturbed. Culverts entail some specific features (Lyn et al., 2024): (1) standardized inlet geometry; (2) large streamwise length relative to opening dimensions (the span and rise are kept small to ensure earthen embankment cover); (3) a prismatic barrel geometry sloped all along its length; and (4) absence of piers (or similar structures).

The U.S. design specifications for culverts follow the HDS-5 guide (Shall et al., 2012) supported by the HY-8 software (<https://www.fhwa.dot.gov/engineering/hydraulics>). Bridge design is guided by the HEC-RAS bridge model (Brunner, 2016). Given that both models are used for culvert design, Lyn et al. (2024) tested through laboratory and numerical simulations the HEC-RAS and HY-8 software concluding that their predictive performance is similar. Additional guidance for culvert design is provided in numerous publications (e.g., AASHTO, 1975; FHWA, 1972; FHWA, 2012; NCHRP, 2011; NCHRP, 2019). Customized versions of these publications exist at state levels (e.g., ODOT, 2014). The HDS-5 leading guidance for culvert design is based on Bernoulli equations with empirical adjustments for box culverts established in 1960s through modeling work (e.g., French, 1966a, 1966b, and 1967). The equations are applied for two types of flow (i.e., inlet and outlet controls) that are sufficient for designers in choosing the appropriate cross section. Less guidance is available on selecting the roughness of the materials, wingwall angles or culvert slopes. Consequently, some of these aspects were tackled through additional studies (e.g., Jones et al., 2019 and Jaeger et al., 2019).

Some of the current guidance on culvert design are weakly-posed assumptions: e.g., “the total discharge is equally divided among the barrels.” The evenly divided discharge assumption is not accurate as demonstrated by experimental studies illustrating the strong non-uniform nature of the flow at the multi-box culvert inlet (Charbeneau et al., 2006; Muste & Xu, 2017b). Another limiting factor is the focus on only the conveyance of “clear” water (no sediment transport) under the assumption that the site morphology does not change over time as the large storms propagating through the structure “clean” the accumulated sediment. This assumption is rarely fulfilled in natural-scale conditions as repeated storms passing through the culvert can dramatically change the local geomorphology of the "as constructed" situation. Moreover, the transitions from stream to culvert geometry for multi-barrel culverts are not typically part of the design despite that the streamflow in these areas is non-uniform with enhanced vorticity and even reverse flows (Muste et al., 2010). The ubiquitous vegetation presence is also overlooked in the culvert design specifications. Leaving all these factors out of the design of multi-barrel culverts has unintended consequences. The sedimentation of culvert is one of them, as the channel transitions leading toward and away from the culvert structure entail considerable changes of the cross-section geometry in comparison with bridges that in turn create conditions for significant geomorphological and ecological changes in the culvert vicinity.

The issue of the accumulation of sediment deposits at culverts is only marginally and superficially referred to in the existing design guidelines. For example, Section 5.3.3 of the HDS-5 shortly discusses the culvert sedimentation problem for single- and multiple box-culverts by relating it to the natural stream aggradation/degradation processes, discontinuity between culvert and stream slopes, and stream-to-culvert angle. While all mentioned factors are contributing factors, our field observations show that sedimentation is considerable even if these factors are absent as found with field observations in the state of Iowa (Muste and Xu, 2017a), as well as in the states of Mississippi and New Mexico (based on the input from partnering DOT's surveys garnered through this TPF project).

The remediation measures suggested by the HDS-5 are very limited for single-box culverts, while for multiple-box culverts they refer to the often-invoked barrel setting illustrated in Figure 5 with scarcely documented design aids (HDS-5, Section 5.4.3). This configuration encourages the conveyance of the flow and sediment through the lower barrel reducing the sediment and debris accumulation in the other barrels that become active only during higher-than-normal flows. The implementation of this innovative culvert is made ad-hoc as many details on the hydraulic features of this modified culvert geometry are missing or are not detailed at the level required by practical situations.

One a more general note, the published studies exploring sedimentation at culverts is quite limited entailing a handful of works conducted in laboratory (e.g., Goodridge, 2009; Faqiri, 2014; Kozarek & Mielke, 2015) or in situ (e.g., Howley, 2004; Rowley, 2014). The studies that attempt a more holistic approach for the investigation of river sediment dynamics are even less (Fuller et al., 2014) due to the data-rich background required to track sediment movement over a range of scales. The major problem faced by detailed and holistic investigations of culvert sedimentation is that the available information on the process is episodic and incomplete. This shortcoming is related to the fact that the current periodic inspections of the waterway structures conducted by the transportation agencies are mostly targeting their hydraulics and structural integrity while tracking sedimentation is neither complete nor well-organized (FHWA, 2014). There is a need to offer tools and protocols that allow to access, integrate, and synthesize the third-party relevant datasets on sedimentation with the purpose to better understand this complex hydraulic transport process and subsequently support the new design approaches that are both operational and sustainable. More customized studies on sedimentation at culverts, similar with those conducted on debris accumulation at culverts (e.g., Iqbal et al., 2023; Miranzadeh & Hossein, 2023), are needed to transfer research results in design specifications.

Overlooking the issue of sedimentation at culverts cannot be continued as it is not aligned with modern design concepts that include the long-term sustainability of the structures in addition to a robust hydraulic functionality (Epicum et al., 2021). Newer perspectives of culvert design ask for approaches that mimics natural flow conditions for the full spectrum of flows (normal flow to design flood) as well as attaining sustainable goals (e.g., Armstrong et al., 2012), as illustrated in Figure 6.

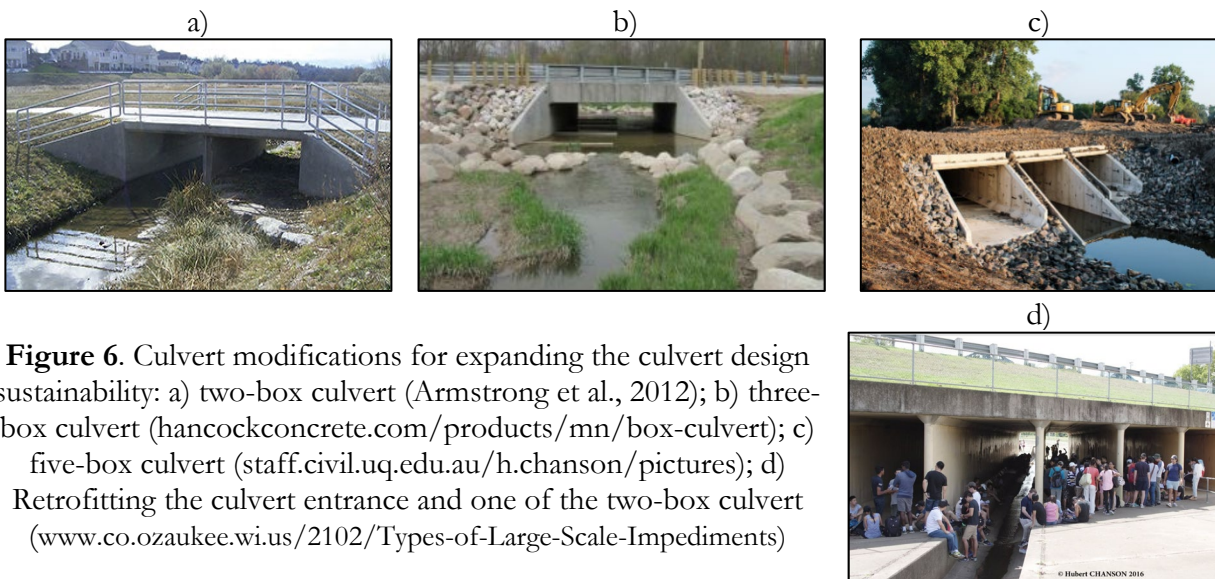


Figure 6. Culvert modifications for expanding the culvert design sustainability: a) two-box culvert (Armstrong et al., 2012); b) three-box culvert (hancockconcrete.com/products/mn/box-culvert); c) five-box culvert (staff.civil.uq.edu.au/h.chanson/pictures); d) Retrofitting the culvert entrance and one of the two-box culvert (www.co.ozaukee.wi.us/2102/Types-of-Large-Scale-Impediments)

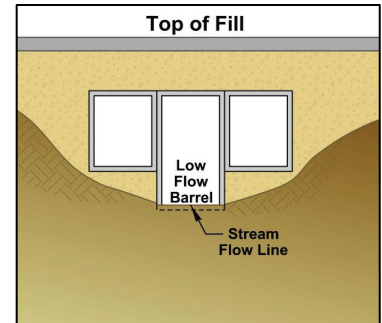


Figure 5. Multi-box culvert with low flow barrel (Shall et al., 2012)

These more sustainable guidelines suggest to innovatively approach the culvert design with a broader scope adapted for the specific conditions at each culvert location in addition to fulfilling the basic role of conveying flow and transported materials. The sample of innovations in the design of multi-barrel culverts targeting both operational and sustainable aspects are well demonstrated in Figure 6. Among the targets of the nature-based culvert design are: promoting a more natural transport regimes for both sediment and bedload, reducing routine maintenance needs, reducing the upstream and downstream impact on the waterway, protecting the normal conditions for ecological habitat (by enabling fish passage and keeping the benches favorable for native vegetation establishment), and (when appropriate) facilitating traffic on and under the culvert. To date, there is limited guidance on alternatives to standardized ones with many of the technical details for designing sustainable culvert configurations are missing.

1.4 Iowa studies on culvert sedimentation & mitigation

The highly erosive Iowa soil and the increase in the frequency and intensity of the storm events in the most recent decades (e.g., Slater & Villarini 2016) resulted in a fast-paced culvert sedimentation that become of concern both from socio-economic as well as flood hazard perspectives. Site visits at more than 250 three-box culverts in the State of Iowa conducted by our research team have revealed that the vast majority of multi-box culverts in the state experience severe blockage due to sedimentation. Since 2006, the Iowa DOT has provided funding to IIHR – Hydrosience and Engineering (IIHR), The University of Iowa for: 1) understanding the sedimentation progression mechanisms; 2) searching for efficient solutions for mitigation of culvert sedimentation; 3) developing design guidance for reducing the potential for sedimentation at multi-barrel culverts; 3) providing supporting tools for guiding the maintenance operations and the design of sediment-free culverts. The initial research was focused on 3-box culvert build with IDOT standards and entailed: a) site visits and measurements; b) numerical simulations, and c) an extensive set of laboratory measurements. In an attempt to facilitate a better understanding of the end-to-end process of sedimentation at multi-barrel culverts and supporting their maintenance and design, parallel research has been carried out to develop a customized web-platform for sedimentation at culverts (Xu, 2019). The platform provides systematic procedures for storing culvert inventory information, assessing culvert sedimentation status, analyzing and forecasting culvert sedimentation potential. As the web-portal was built with generic databases, it can be easily extended for any stream location in the U.S. that is prone to sedimentation.

Early self-cleaning culvert solutions. The self-cleaning culver (SCC) concept behind the newly developed designs relies on the use of the stream hydraulic power for passing the suspended and bed loads carried by the stream during storms downstream the culvert. The implementation of SCC designs does not affect the as-designed culvert hydraulics as the changes are made outside the culvert constructed areas. Specifically, the transitions at the culvert inlet and outlet are modified to enhance flow and sediment transport, without affecting the hydraulics losses thought the culvert.

During more than 18 years of research on various aspects of sedimentation mitigation at multi-barrel culverts, our team identified three possible self-cleaning culvert configurations to reduce, or, completely eliminate the formation of sediment deposits at three-box culverts (see Figure 7): a) filled-based (Design A); upstream curtain wall (Design B; upward or downward curtain), and downstream weir (Design C). Notably, the SCC solutions for three-box culvert are only applicable to three or higher odd numbers of multi-box culverts. Single-box culverts and any even number of multi-box culverts requires different solutions that those currently developed.

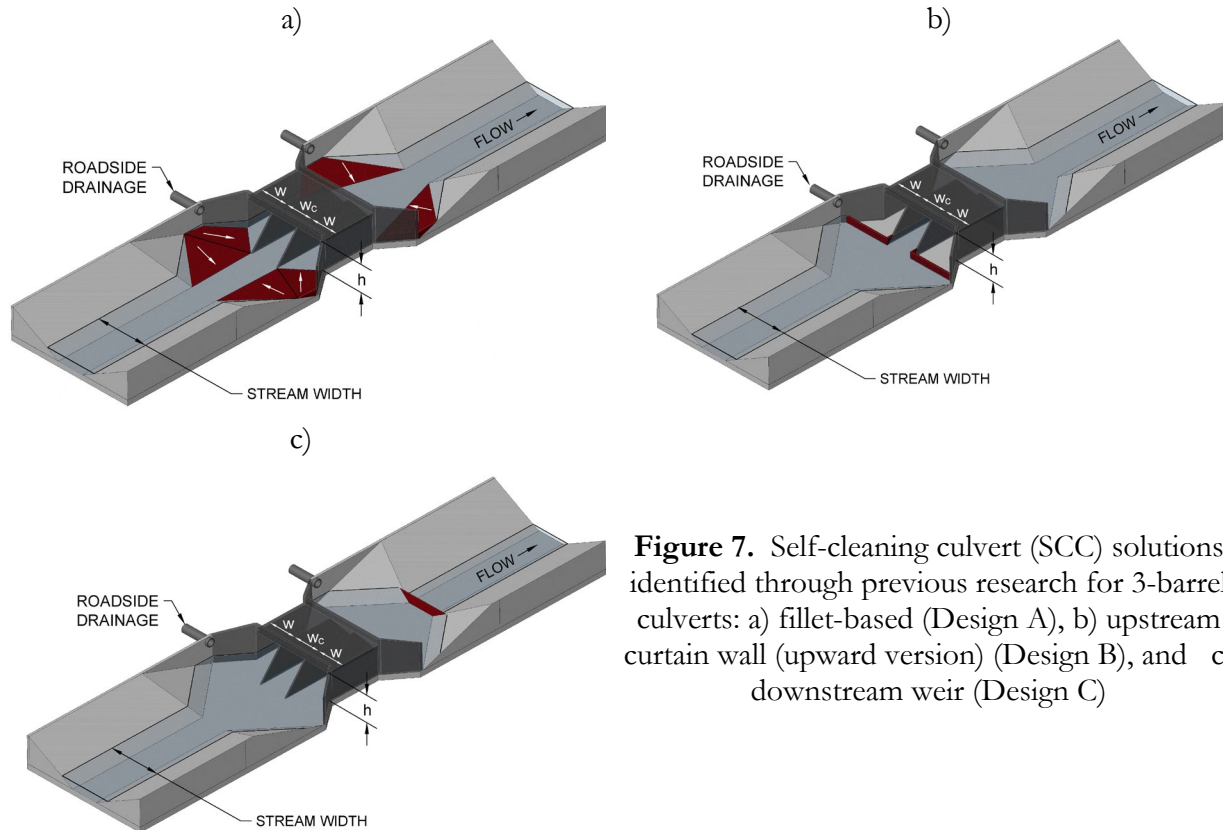


Figure 7. Self-cleaning culvert (SCC) solutions identified through previous research for 3-barrel culverts: a) fillet-based (Design A), b) upstream curtain wall (upward version) (Design B), and c) downstream weir (Design C)

Self-cleaning culvert design efficiency. Based on a series of studies and observations following the installation of the self-cleaning designs shown in Figure 7, the Iowa research team found that all the aforementioned culverts performed well in a variety of geomorphological and hydraulic conditions. The three retrofitted designs have not been investigated with the same level of detail, but continuous in situ-observations were carried out for each of them starting with 2010 on. Design A has been fully investigated through laboratory and numerical studies and implemented at a culvert site since 2013 (Muste and Xu, 2017a). Design B has been adopted for sedimentation mitigation purposes at culverts in several Iowa Counties and Cities. Design B has not been investigated with hydraulic studies but was observed at several culvert locations (Muste & Xu, 2017b). Design C has been randomly found at few Iowa culvert sites (mostly under the form of obstructions created by beavers). Observations and measurements at culverts acquired at four 3-barrel culverts (out of each three entail designs A, B, and C) were made on a reach of 1.5 miles over the same stream (e.g., Willow Creek in Iowa City, Iowa) as illustrated in Figure 8. Between Site #1 and Site #3 (retrofitted with designs A and C, respectively) on this stream reach another 3-box culvert was identified that was not modified since its construction in 2006. Given the “as is” status of the culvert located at site #2, it was used as a reference for assessing the performance of the other solutions located on the same stream.

Preliminary evaluations of the SCC designs for three-box culvert are summarized in Table 2. Many of the garnered inferences are considered preliminary requiring further quantitative assessments. The innovation brought by the Iowa SCC design has been nationally recognized with two awards: a) the IDOT received funding from the FHWA’s State Transportation Innovation Councils (STIC) for implementing the SCC design as standard practice throughout the state of Iowa, and, b) the American Association of State Highway and Transportation Officials (AASHTO) Research Advisory Council designated the SCC design project as one of the “Sweet Sixteen” High Value Research Projects for 2016 during the 2017 Transportation Research Board annual meeting.

Table 2. Comparison of the three self-cleaning culvert (SCC) designs.

Design concept	Hydraulic principle	Protected area	Sensitive to approach angle	Relative cost*	Relative efficiency**	Applicable
Fillet-based (Design A)	sediment transfer	Upstream, downstream	yes	highest cost	-	anytime
Curtain wall (Design B)	sediment transfer	Upstream	yes	relatively high	relatively limited	anytime
Downstream weir (Design C)	sediment trapping	Upstream, downstream	no	-	Similar (unknown lifetime)	anytime

* Reference: Design C; ** Reference: Design A

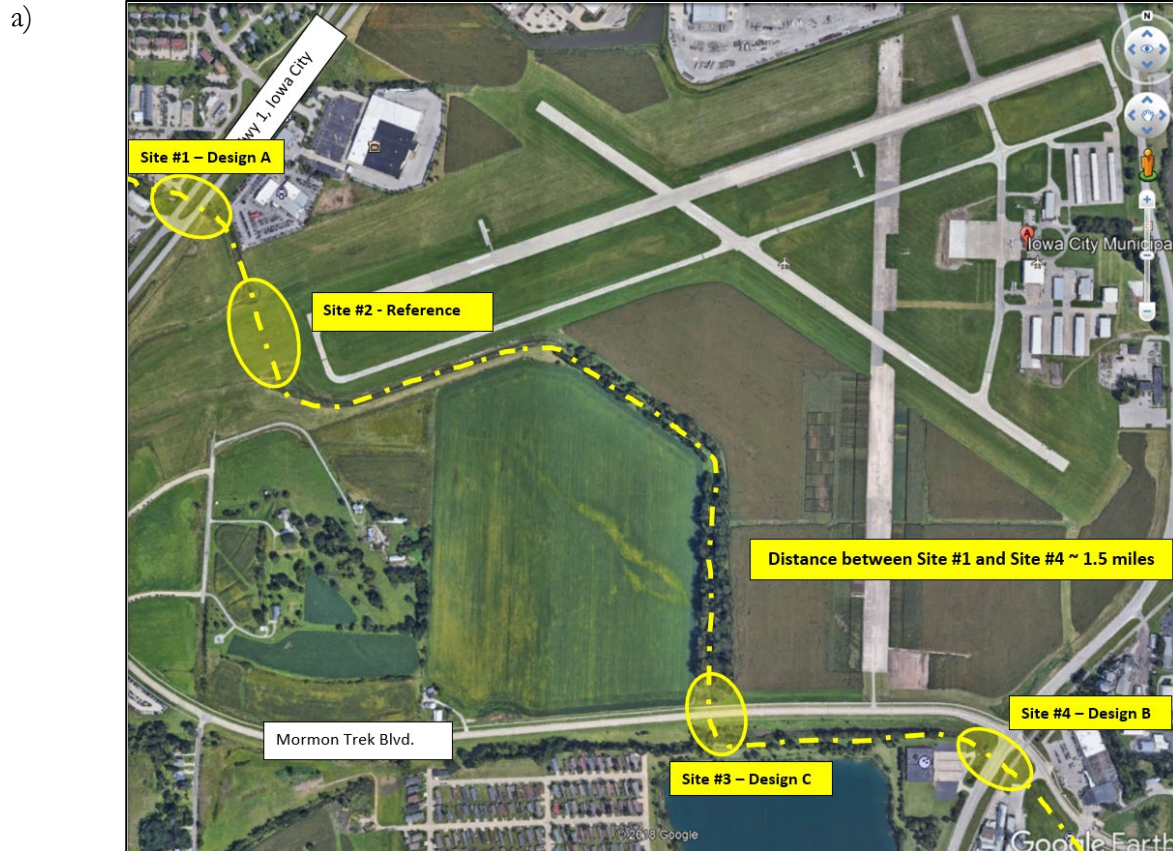


Figure 8. Iowa multi-culvert study location: a) the layout of the four observed culverts, b) view of the reference culvert inlet; c) view of the location for the reference culvert outlet

A photo-documentary of the culvert status before and after retrofitting for Designs A and B and for the as-is culvert Design C from the beginning of its operation is provided in Figure 9. Designs A and C operate well during the observation periods. Design B (Site #4) developed by the Iowa City engineers has been continuously clean since its construction.



Figure 9. Self-cleaning culvert solutions: a) Design A (fillet-based) applied to a triple 15'-18'-15x12' ~ 170-ft long culvert; b) Design B (upstream downward curtain) applied to a triple 15'-18'-15x12' ~ 800-ft long culvert; c) Design C (downstream weir) used for a Triple 15'-18'-15x12', ~ 200-ft long culvert

2. TPF PROJECT SCOPE, OBJECTIVES. AND TASKS

Ensuing from the introductory considerations presented in Section 1 is that sedimentation at multi-barrel culverts is an ongoing maintenance issue in erosion-prone watersheds located in various U.S. states. Despite the widespread presence of this operational nuisance and the costly and labor-intensive cleaning efforts, currently there are no systematic efforts for mitigating detrimental effects of sediment blockage at multi-barrel culverts. The culvert design protocols continue to be guided by hydrologic and hydraulic analyses of water free of sediment or debris with limited attention given to the conveyance of the transported materials. Overlooking sedimentation matter in culvert design is not deliberate. Rather, it is the consequence of gaps in our knowledge on the processes leading to sedimentation and their complexity that entails interlinked environmental processes that are difficult to investigate and solve with conventional approaches (e.g., experiments or physical modeling).

The scope of this study is to initiate research focused on mitigating sedimentation at multi-barrel culverts using comprehensive laboratory investigations entailing new modeling features. The experimental study adopts a fast-track engineering approach whereby the fundamental aspects of the sedimentation are observed using the best available information on the processes involved with the main priority being the search for practical solutions to mitigate sedimentation by altering the standard design specification for multi-barrel culverts. The research builds on the outcomes of the IIHR between 2006 and 2019. The guiding principles and best practices for mitigating sedimentation of this study complement the current design guidelines for culvert hydraulics.

The overall goal of the Transportation Pool Fund project TPF-5(445) project is to screen and evaluate various changes in the geometry of the stream entering the culverts based on the comparative analysis of the accumulations of sediment in areas of the culvert vicinity where stabilized deposits were observed during field visits. This primary goal is accomplished through a phased experimental program. The secondary goal of the TPF project is to suggest design aids on the mitigation measures for reducing sedimentation at existing and proposed culvert locations. The guiding principles and best practices for mitigating sedimentation will complement the existing hydraulic design guidelines. The second goal can be leveraged if the experimental studies are followed by in-situ implementation of the top ranked solutions to eliminate the effect of the factors that are not present in the laboratory experiments (e.g., impact of various types of hydrographs, effect of series of events for various seasons of the year, sediment compaction and aggregation, vegetation growth, effect of weather-related processes, etc.). Given that the research on sedimentation at culverts is relatively new and sparsely tested investigation area, there have been unknown aspects of the project at its inception that required clarifications as the project evolved. Consequently, the initial research plan has built-in flexibility to enable adjustments based on the data and experiences garnered from all project participating partners. Prior to the first meeting of the partnering states, the Technical Advisory Committee (TAC) was formed to ensure the prioritization and coordination of the project activities. The TAC members acting during the project execution are listed in Table 3. The initial research plan was re-aligned based on the partnering states input in the March 11, 2020 meeting. The initial plan offered several alternative investigative approaches to choose from in order to meet the project objectives. Subsequently, the research plan was re-adjusted several times to respond to the new aspects revealed by the ongoing investigation. The PTF project goals and the final tasks are listed in Table 3.

Table 3. Project Technical Advisory Committee

Name	Affiliation
Wilson V.; Buie T.	Mississippi DOT
Morgenstern S.; Lokey S.	New Mexico DOT
Cox B.; Alberts C.	Utah DOT
Harper J.	Missouri DOT
Claman D; Ellis J.; Clute K.	Iowa DOT
Kerenyi K.	FHWA
Muste M.	U. Iowa, Project PI

Table 4. Objectives (O) and final tasks (T) for the TPF Project-5(445)

#	Description
O1. Assemblage of knowledge on sedimentation at culverts & mitigation measures	
T1	Evaluation of self-cleaning culvert (SCC) solutions developed through previous research and investigation of local culvert configurations that mitigate sedimentation at culverts.
T2	Survey of partnering state DOT-s on the types, extent and degree of sedimentation at multi-box culverts to account for regional issues related to sedimentation. The survey includes inventory of regional practices for mitigating sedimentation. Assemblage of the survey information and development of the study road map.
T3	Screening and compiling culvert-related data resources (e.g., aerial photos, culvert National Bridge Inventory databases, etc.) for assessment of the degree of sedimentation of selected culverts in project partnering states.
O2. Laboratory experimental investigations	
T4	Development of metrics for assessment of sediment transfer/removal efficiency by SCCs.
T5	Selection of the hydrologic/hydraulic regimes leading to sedimentation
T6	Development of the experimental protocols with specifications on the flow and sediment regimes and procedures for documented the results of individual tests (photo- and video-documentation, sediment deposit survey using qualitative and quantitative measures)
T7	Assess the efficiency of self-mitigating culvert configurations & rank optimal candidates
T8	Screening and sensitivity analysis of the SCC solutions identified in task T7
T9	Prescribing guidelines for best practices for preventing sedimentation at culverts in conjunction with current hydraulic design guidelines. Verification of the hydraulic losses for the produced by various types of mitigation solutions operating in various setting scenarios (e.g., stream-to-culvert angle, sediment type).
O3. Synthesis of knowledge and design aids for reducing/eliminating sedimentation	
T11	Preparation of design guidelines for sedimentation mitigation measures applicable to culvert configurations and sites in partnering states.

3. PHYSICAL MODELING CONSIDERATIONS

3.1. Overview of the modeling strategy

The expansion upstream of a culvert is the focus of this research as the TPF partnering state experience undesirable consequences related to sedimentation occurring in this area. This section briefly overviews considerations related to the screening of the multiple possible combinations of factors leading to sedimentation at culverts to a set of hydrologic, hydraulic, sediment transport, and culvert geometry conditions that are relevant to the study's partners and attainable with the available resources. Guiding principles for developing SCC solutions are also included in this section.

As summarized in Section 1.2, sediment deposition at culverts is influenced by many factors, including the hydraulic characteristics generated under different hydrologic events, the size and characteristics of material of which the channel is composed, and the type of native vegetation in the culvert vicinity. The geometry of the culvert and channel transitions and the type of hydraulic control are established to allow the passage of natural and storm flows through roadway embankments on smaller streams. The final culvert geometry can be a single or multiple openings shaped as ovoid (i.e., pipe structures) or rectangles (box structures). Choosing multi-box culverts is cost efficient over

single-box culverts low headwater at the structure is required. The normal setting of the culverts involves contraction of the channel upstream of the openings, and expansion to the natural channel width on the downstream side (i.e., SWC ratios ≤ 1). In cases where in the design calculations suggest that the required size and geometry extend beyond the width of the natural channel, channel transitions are also required to convey water to and from the structure openings (i.e., SWC ratios > 1). During the design phase, culverts are analyzed for operating under inlet and outlet control. The final culvert configuration is set for the condition that requires the largest headwater value (Shall et al., 2012). Based on the survey on our project partners, the culvert of interest for our study are those of small stream entering embankments with limited rise and unobstructed downstream area. *Consequently, the scope of the current TPF project is limited to multi-box culverts located on channels that are much narrower than the culvert span and operating under inlet control with small headwater (unsubmerged) without considering vegetation presence.*

The transitions associated with multi-box culverts located on small streams display a SCW ratio $\gg 1$ (see Figure 10a) producing flow non-uniformity characterized by the divergence/converge of the streamlines for all flow regimes and, eventually, flow areas of widely different velocities (see Figure 10a). The low-velocity areas are prone to sedimentation as they favor the sediment deposition on a continuous basis. Most of the time the culverts are conveying only a fraction of the designed flow passing through the structure as a non-uniform steady flow. Even in these extreme cases, flow recirculation procedures are developed and 10c1 (laboratory experiments conducted by Ho et al., 2013). The most energetic sedimentation events ensue during the propagation of unsteady flows following the storms incoming from the culvert drainage area. The amount of bed load is small compared with suspended load, making up only 5-10% of the total sediment load (Richardson et al., 1990). Site inspections conducted at culverts have confirmed this aspect, finding most of the sediment in deposits as fine-grained soils that are not present in the bed load material. Disregard of the type of transport, the culvert design discharge and sediment transport rate for culverts with SCW ratio $\gg 1$ display a positive correlation (Howley, 2004; UDOT, 2017). The underlying mechanism of this correlation is explained by the equilibrium between sediment load and stream power (Lord et al., 2009). According to Howley (2004), flood discharge and sediment transport rate are also positively correlated, i.e., larger design discharges normally imply larger sediment loads. Furthermore, culverts that require a large design discharge are susceptible to oversizing. The knowledge and information on culverts with SCW ratio ≈ 1 (see Figure 10b) are limited and, to the best knowledge of these authors, this PTF study will provide some pioneering insights.

It is common knowledge that the unsteady flows occurring following storms produce hydrographs that are different on the rising and falling limbs of the hydrograph (see Figure 10c2). This flow process property, labeled hysteresis, is rarely accounted in current flow monitoring (Muste et al., 2020), hence it is also neglected in the design and analyses of river structures such as culverts. The unsteady flow associated with the storms entrains the sediment in suspension and activates the bed load transport. The sedimentation at culverts mostly occurs on the falling stage of the hydrographs, when the stream power diminishes. The rising phase of the hydrograph is characterized by a dynamic sediment transport phase followed by a falling stage when the sediment rates return to normal transport regimes, as shown in Figure 10c3. Specifically, the maximum total sediment load passing through a section during a storm event precedes the peak flow, disregard of the discharge magnitude. The flow's non-uniformity combined with its inherent dynamics during the transitions decides where and when the sediment settling in the culvert vicinity will occur. Currently, there are considerable gaps in theory regarding the non-uniform, unsteady, sediment-laden flows developing in three-dimensional culvert geometry. Lack of understanding of the complexities of this combination of local processes preclude

making accurate predictions without proper analytical tools. *Given the complexity of the local processes and the nature of the transported materials through culverts, only a handful of studies have focused on the stream and structural attributes that will affect sediment deposition at culverts (Cafferata et al., 2017; Ho et al., 2013; Howley, 2004). In this study, only the impact of the unsteady non-uniform flow passing through culverts with SCW ratio $\gg 1$ and ≈ 1 will be reported without making reference to hysteresis effects.*

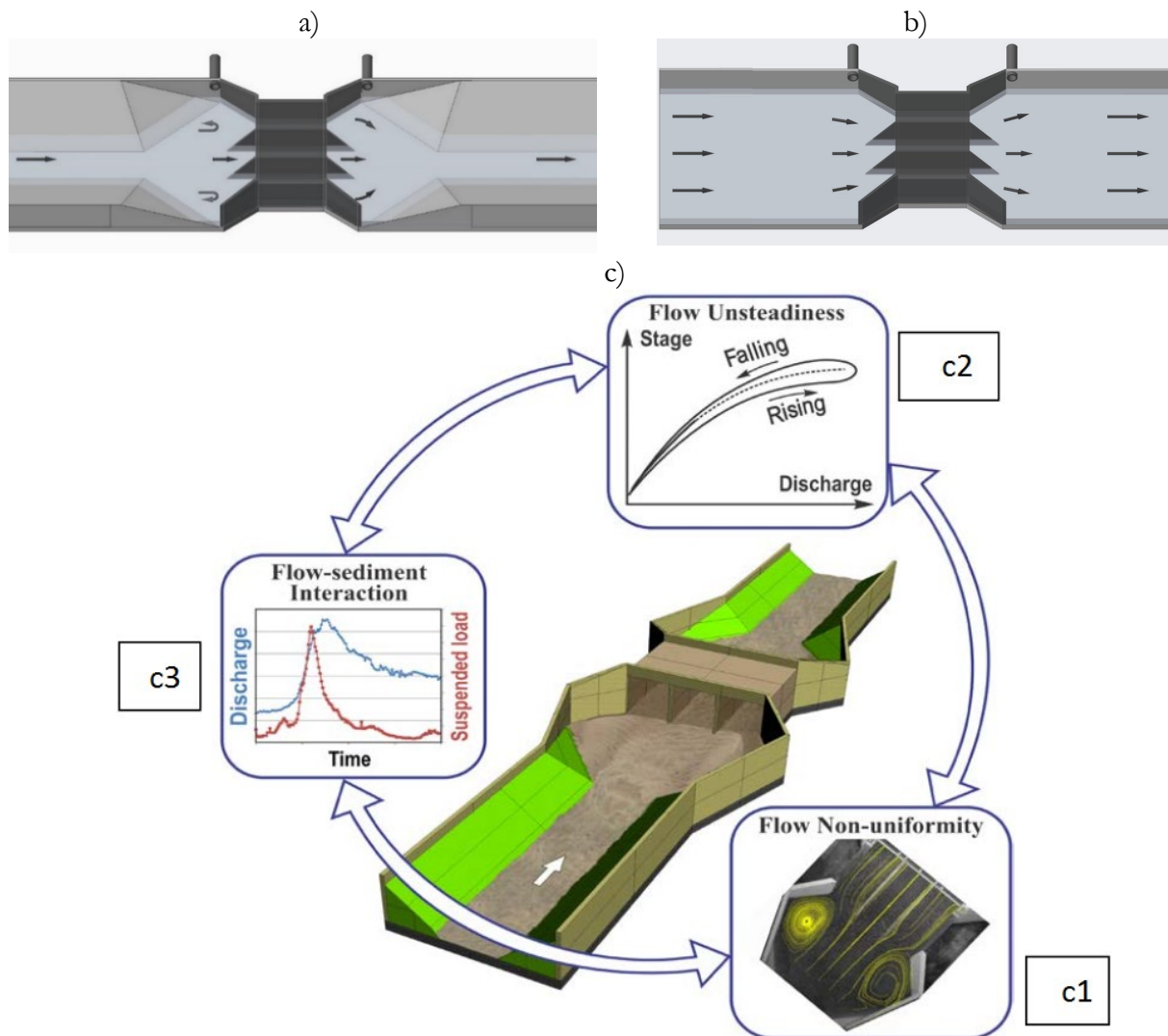


Figure 10. Flow configuration at culvert sites: a) Iowa-Mississippi-Missouri culvert setting; stream-to-culvert transition; b) New Mexico-Utah culvert setting; c) flow complexities due to flow unsteadiness (Muste & Xu, 2020)

The premises for this TPF-5(445) project have been to leverage the IIHR extensive research on the combination of parameters on self-cleaning culvert concepts applied to three-box culverts between 2006 and 2012. More specifically, during this interval extensive laboratory experiments have been conducted in physical (hydraulic) models of various scales to observe the sedimentation patterns for the self-cleaning culvert alternatives mentioned in Section 1.4 as documented in Muste et al., 2009; Ho, 2010; Muste et al., 2010; Muste & Ho, 2012. The major role of the previous laboratory studies was to accurately replicate the dynamics of the sedimentation at culverts for testing self-cleaning culvert solutions and providing benchmark data for numerical simulation validation. The common

denominator for IIHR studies was the focus on triple reinforced box culvert with flared walls (IDOT design TRRCB-G1-01) displaying a SCW ratio $\gg 1$. This culvert configuration is common in the states of Iowa, Mississippi and Missouri. In the previous hydraulic models, the channel approaching the culvert was centered on the culvert axis intersecting the road at a normal angle. Given that the culvert vicinity (i.e., expansion and contraction) develops strong non-uniform flows that favorize sedimentation, most of the observations and measurements were focused on this area. *In this study, the same type of culvert (i.e., TRRCB-G1-01 IDOT design with a SCW ratio > 1), roadway crossing setting, and layout of the experimental flume as in previous IIHR studies is tested to allow comparison with our and other previous studies (e.g., Charbeneau et al., 2006) and identifications of self-cleaning culvert design for the states of Iowa, Mississippi and Missouri. In the second part of the TPF study, a three-box culvert (TRRCB-G1-01 IDOT design) is tested displaying a SCW ≈ 1 to more realistically replicating the sedimentation scenarios in the states on New Mexico and Utah.*

The above-mentioned combination of regional and hydrologic factors involved in sedimentation at culverts results in a complex physical modeling undertaking. The most challenging modeling task regarding the regional factor is selecting representative flow conditions approaching the culvert. The most challenging tasks regarding the local factors involved in modeling of the sedimentation process is the type of entrainment occurring in the vicinity of the culvert. *Decisions on the regional and local factors to be used in the present study required additional data gathering and experimental tests regarding: a) the type of water and sediment hydrographs passing thorough the culvert; b) the type of sediment transport to be modeled (i.e., suspended vs. bedload), c) specification of the size distribution of the modeled sediment.*

Modeled water and sediment regimes. To ensure a realistic input for the hydraulic model, we searched for realistic data on the flow and sediment transport (i.e., flow and sediment hydrographs) of culverts. Given that the simultaneous measurements of this kind are rare, we used instead measurements and observations acquired at a three-box culvert (FHWA #364790) located in Iowa City, IA investigated through a previous IDOT project (Muste & Xu, 2020). The site was instrumented with stage sensors located upstream and downstream the culvert as well as a turbidity sensor installed upstream the culvert (see Figure 11a). The readings of the stage sensors were adjusted by their elevation (determined with a topographic survey) to estimate the free-surface slope through the culvert area (Figure 11b). Surrogate data about suspended sediment concentrations were obtained by correlating the measured water turbidity via a locally calibrated relationship (Figure 11c). The overall shapes of the water and suspended sediment hydrographs acquired in-situ were used as rough guides for modeling the protocols for water and sediment feeding in this modeling study. Given that similar information was not available for New Mexico and Utah sites, these protocols were kept the same across all the tests for this TPF study.

Deposition patterns created by suspended sediment and bedload transport. Clarification of this modeling aspect is critical as the hydraulic modeling with both sediment in suspension and bedload are difficult to scale to realistically replicate prototype conditions. Fulfilling the similitude criteria for the flow and sediment fractions can be fully attained only if the transported materials and the working fluid are different from natural sand and water, respectively. Conducting experiments using such a scenario has exceeded resources available for this TPF project. In order to overcome this procedural obstacle, we conducted qualitative tests with identical flows carrying only suspended load and bed load in separate experiments and we compared the test results (Ho et al., 2013). For this purpose, the same reference flows was established in the experimental flume and loaded with two widely different properties: crushed walnut shells ($d_{50} = 0.76$ mm, specific gravity 1.2 – 1.4) and silica sand ($d_{50} = 0.54$ mm, specific gravity 2.65). The crushed walnut shell was carried by the flow as only suspended fraction. The natural sand was exclusively carried as bed load. Sample results from the suspended vs. bedload test series are illustrated in Figure 12.

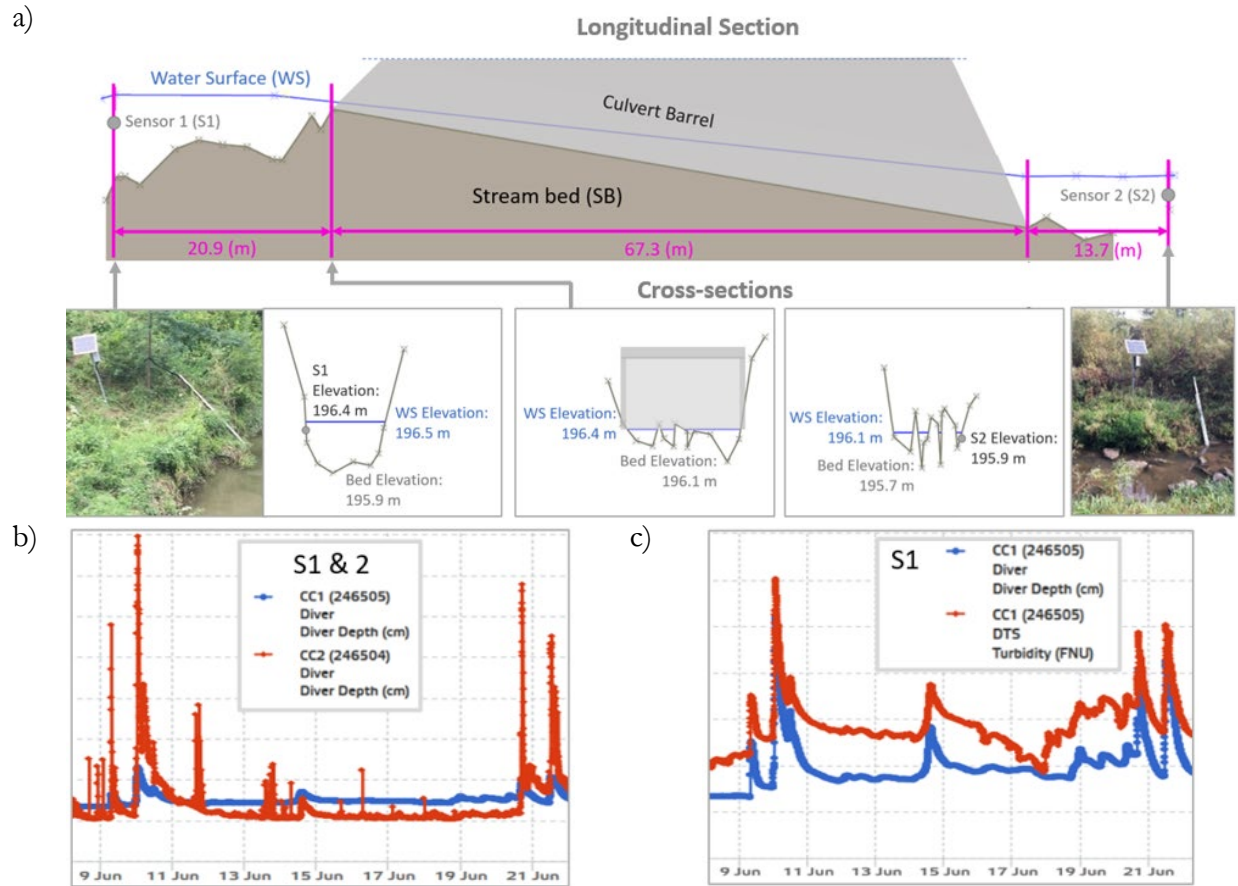


Figure 11. Hydrologic/hydraulic variables recorded at a three-box culvert (Muste & Xu, 2022): a) topographic survey of the culvert and sensors installed for measurement of water stage and turbidity (vertical scale of the plot is intentionally distorted to visualize the culvert vicinity features; b), c) stage and turbidity measurements acquired at culvert inlet and outlet.

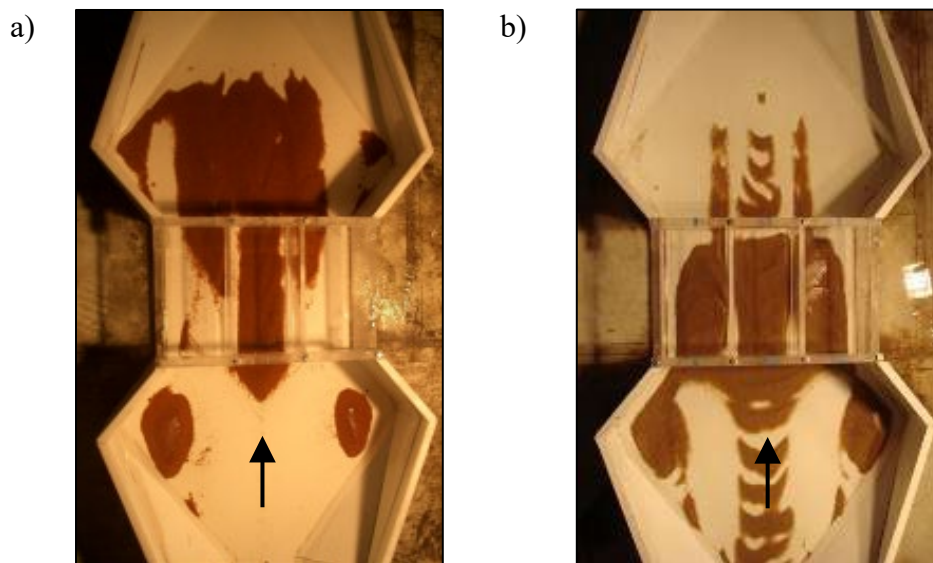


Figure 12. Sedimentation patterns at the culvert (Ho et al., 2013): a) using suspended load (crushed walnut shells), and b) using bed load (silica sand)

The deposition patterns in the figure display similarity in the expansion area leading to culvert, and different patterns within and downstream the culvert. It is deemed that in the presence of a combined suspended-bedload transport, a similar sediment depositional pattern will develop in the upstream area of the culvert and an augmented build-up of sediment will occur in the downstream area of the culvert. Given that sedimentation in the upstream area is the triggering factor for increased flow non-uniformity and flow obstruction, it was decided that for this study goals the use of bed load will suffice. In other words, although the mechanisms for bed load and suspended load are different, it can be assumed that the sediment mitigation measure designed for bed load will be also effective for suspended load, especially in the area upstream the culvert.

Selection of the modeled sediment size distribution. The prior project conducted by our team (Muste and Xu, 2020) included a detailed analysis of the layering and particle size distribution in the sediment deposits accumulated at FHWA #364790 three-box culvert. Visualization of the sampled cores revealed that most of the sediment in the deposits is of the silty-loam nature. Figure 13a shows the particle size distribution resulting from sieve analysis of multiple samples collected in situ from the upper layers of the deposits. Prior to execute the production tests for the TPF project, we conducted a sensitivity analysis to the impact of depositional patterns created by two types of sands, labeled internally as the “coarse) and “fine” sand. The sieve analyses for these two types of sand are shown in Figure 13b and 13c, respectively.

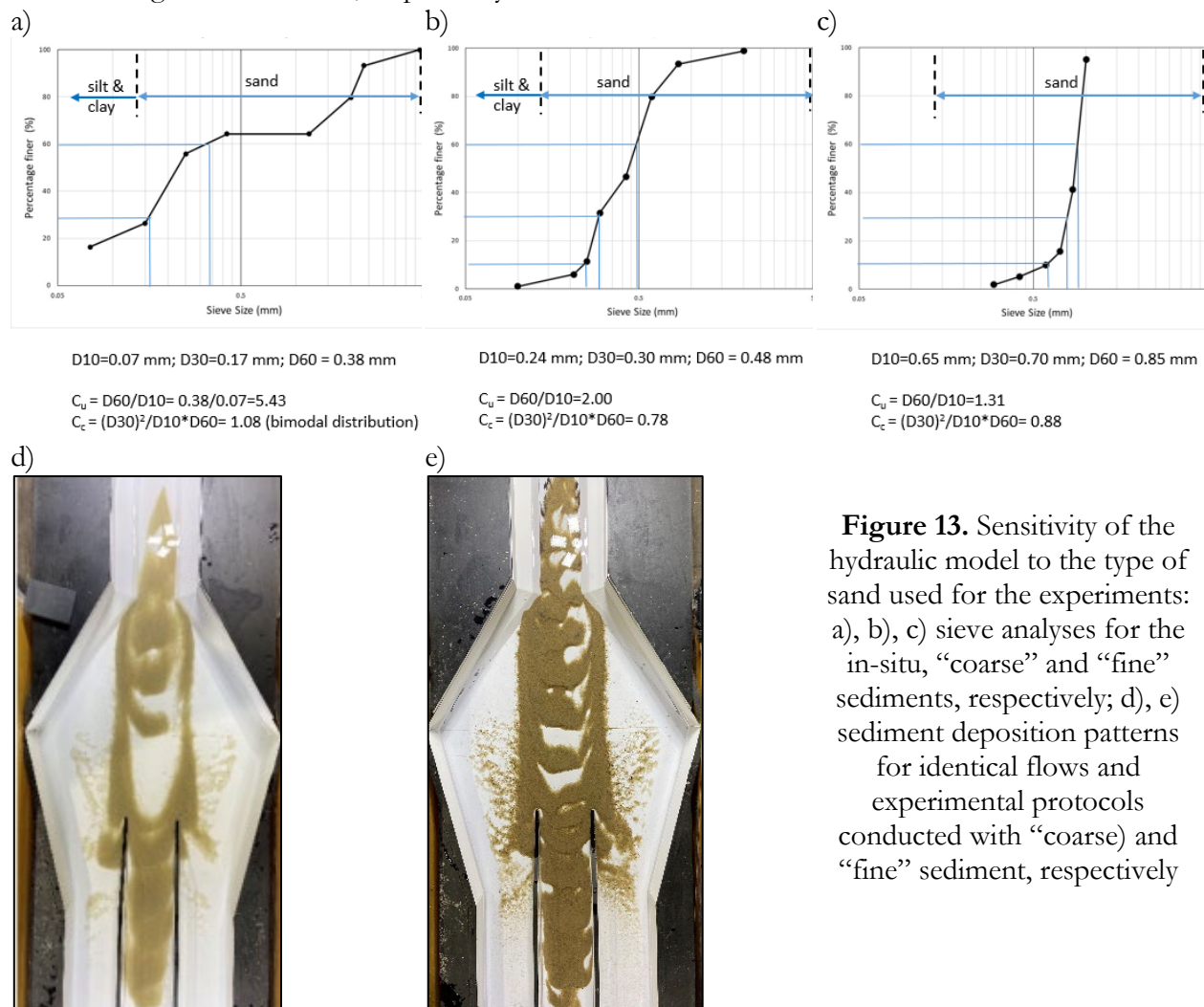


Figure 13. Sensitivity of the hydraulic model to the type of sand used for the experiments: a), b), c) sieve analyses for the in-situ, “coarse” and “fine” sediments, respectively; d), e) sediment deposition patterns for identical flows and experimental protocols conducted with “coarse) and “fine” sediment, respectively

Samples of sedimentation patterns obtained from identical tests with the “coarse” and “fine” sediment are illustrated in Figures 13d and 13e. The similarity between the patterns in those photos is obvious with slight differences in the amount of carried load and the coloring of the pattern (attributed to the different nature of the sand). In the initial stages of the project, we conducted several tests like these for various flow scenarios to conclude that the similarity between patterns is prevalent. Following those initial parallel tests, the TPF TAC concluded to continue the rest of the tests with only the “coarse” sand characterized by sediment distribution properties illustrated in Figure 13b.

3.2. General principles for designing self-cleaning culvert configurations

The TPF experimental strategy has been tailored to accurately reflect the local hydro-geomorphological conditions at the TPF project partnering states. These conditions can be broadly grouped around two stream-to-culvert configurations: Iowa-Mississippi-Missouri (IMM) and New Mexico-Utah (NMU). Figure 15 provides essential elements for the two set of conditions.

- a) IMM conditions entail: perennial rivers, well-defined initial stream bed, typically expansion areas from stream to culvert, small incremental sedimentation pockets are deposited with every storm, sediment deposits are fossilized over time by vegetation, a fraction of the culvert span still open
- b) NMU conditions entail: ephemeral rivers, weakly-defined stream path, funnel like area upstream the culvert, large amounts of sediment conveyed by individual storms, sediment deposits lack vegetation hence they are partially mobilized by subsequent storms, uniform loss of cross-section area over the culvert span.



Figure 14. Sedimentation conditions at three-box culverts: a) IMM group; b) NMU group

At the time of this study, the observations available on the hydrological conditions occurring at culverts in the IMM group are by far more substantial compared with the NMU group. Anecdotal evidence collected during extreme flows illustrates that the combination of factors for the two groups of culvert settings leads to similar appearances during extreme flows, as illustrated in Figure 15. The range of variation and the rated of change of the discharges occurring during storm events for the NMU conditions is larger than the one for IMM as the former culverts are located in semi-arid landscapes therefore lacking the resistance posed by the vegetation for the overland runoff progression. While the runoff flows for the IMM group are typically confined to the stream banks, similar flows passing through NMU culverts are carrying considerably larger amount of sediment as the area washed by the flow upstream the culverts is order of magnitude larger for NMU conditions than the in IMM ones. The NMU incoming flows are typically loaded with log/debris at their front. As the events develop, a gradual decrease of the debris concentration occurs followed by an increase

in sediment loads. It is deemed that the IMM culverts are carrying largely suspended load while the NMU culverts are dominated by bedload transport. Despite that debris transport and accumulation occur occasionally, for the present study this added complexity was not considered as most of the visited sites at the TPF partnering states indicate that debris is a secondary factor.

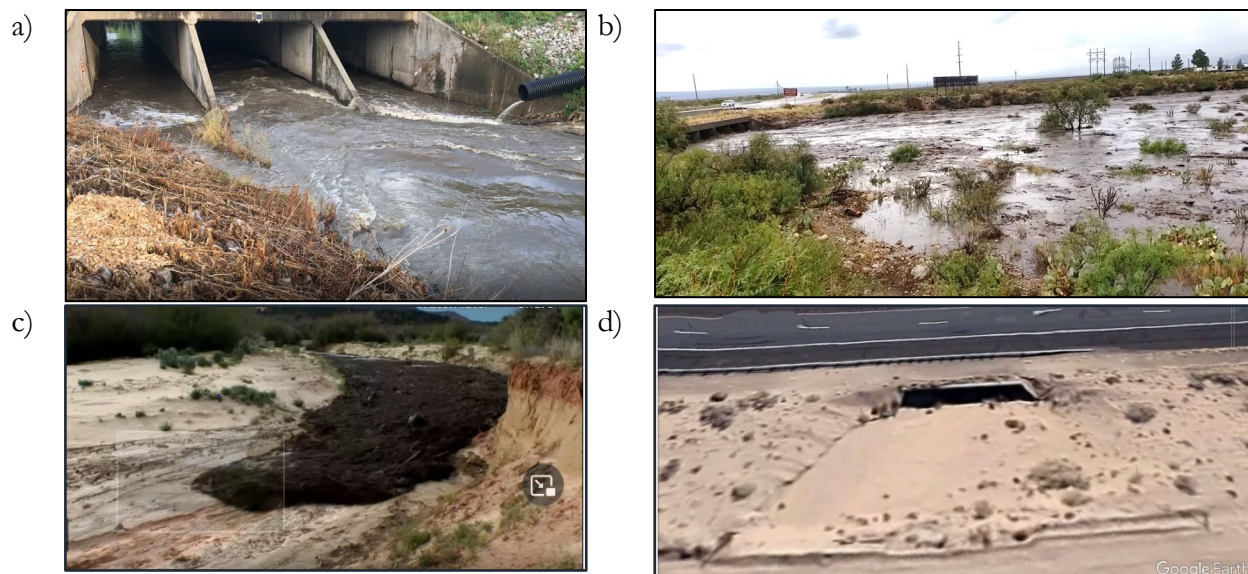


Figure 15. Flow aspects relevant to TPF study: a) culvert in Iowa City, Iowa during an extreme event (personal photo); b) culvert in Carlsbad Caverns National Park, New Mexico during an extreme event ([youtube.com/watch?v=h4N0I3kc2ls](https://www.youtube.com/watch?v=h4N0I3kc2ls)); c) inception of flash flood in Buckskin Wash, Utah ([youtube.com/watch?v=aZp_1KtrzjQ](https://www.youtube.com/watch?v=aZp_1KtrzjQ)); d) culvert # 7202 in New Mexico (photo captured from Google Earth)

The proposed self-cleaning culvert designs are conceived to suit the local sedimentation situations at the state partners' culverts (sediment conveyance for Iowa-Mississippi-Missouri culvert settings vs. sediment blockage & limited conveyance for New Mexico-Utah settings). Consequently, the hydraulically-propelled sediment mitigation designs are different as succinctly described below.

Iowa-Mississippi-Missouri (IMM) culvert settings. Sedimentation at IMM multi-barrel culverts is practically unavoidable given the nonuniformity of the velocity distributions through individual culvert boxes during high and low flows (Ho et al., 2013). The transition of the cross-section geometry from channel to culvert in the upstream expansion area typically used for these conditions produces a change in the flow distribution that ensures the passing of the design flow but hampers the continuity of sediment transport. Completely eliminating sedimentation is a desirable target but not attainable in practice, therefore ensuring culvert's capacity to convey water and sediment is an appropriate target. Doing so by working with the flow as it approaches a culvert based on merely hydrodynamic action is also desirable for a robust solution.

Our general strategy for retrofitting the IMM culverts for mitigating sedimentation involves modifications of the initial ("as designed") channel geometry immediately upstream from the culvert without changing the "as-designed" culvert geometry. The prescribed modifications should ensure that they can be applied for both new and existing culverts (as they do not require structural changes to the culvert geometry). Our previous experience with this issue identified some basic principles for developing self-cleaning culvert configurations. They entail the following elements:

- Make modifications upstream the culvert that would emulate the shape and functionality of the original stream.

- Concentrate the flow distribution toward the culvert centerline to ensure that most of the sediment transport is conveyed through the high-velocity flow areas, as illustrated in Figure 16.
- Reduce sedimentation in the expansion and contraction areas leading to and out of the culvert structure to (possibly) eliminate the formation of sediment islands formation upstream the culvert that can promote the growth of vegetation that in turn accelerate the sediment deposition rates.
- Enhance turbulence in the low velocity areas to keep the sediment in suspension during the sediment-laden flow movement through the culvert, and,
- Minimization of the waterway disturbance in the culvert vicinity to avoid creation of additional flow complexities (disruption of the aquatic habitat transit, debris retention, ice jamming).

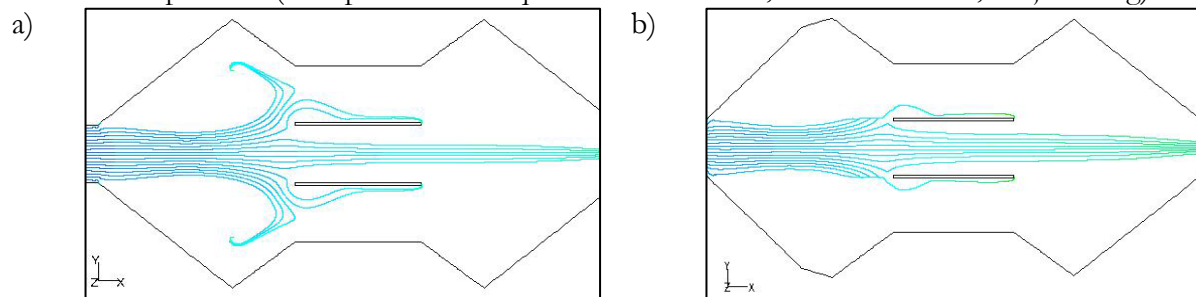


Figure 16. Flow patterns targeted by IMM self-cleaning culvert design: a) "as-is" culvert geometry; b) modified geometry

New Mexico-Utah (NMU) culvert settings While sediment conveyance through culvert is still a desirable target, retrofitting the NMU culverts aims primarily to block the considerably larger amount of sediment collected upstream the culvert. Setting a flow blockage across the section is desirable as it provides a control section upstream the culvert that also enhances the flow uniformity in comparisons with the preferential paths typically created in the undisturbed bed of this area. Combining, flow blockage over the full width of the channel with a central opening in the obstructing wall can partially fulfill both design targets.

4. EXPERIMENTAL ARRANGEMENT, PROTOCOLS, AND DATA PROCESSING

4.1 Overview of the TPF experimental plan

The initial plan for the project experiments entailed a culvert configuration typical for the states of Iowa, Mississippi and Missouri (IMM) set along the same direction with the incoming stream. The initial plan includes tests with two types of sand (see Figures 13b and 13c) and several types of steady flows and hydrographs as described in Section 4.6. During the first TAC annual meeting (December 1-2, 2021), several critical decisions were made that departed significantly from the initial project plan. The major changes made to the initial plan are: a) using only the coarse sand (see Figure 13b) in the subsequent tests, b) introducing Laser-based surveys for mapping and quantification of the amount of sediment deposited in the model using, and, c) addition to the experimental program of a new culvert sitting akin to the conditions pertinent to New Mexico and Utah (NMU). Given the major budgetary implications brought by the TAC decisions in December 2021, in the second phase of the project (starting with January 2022), the number of self-design configurations and the type of flows and hydrographs was reduced to enable the fulfillment of the new requests from the partnering states. In the third phase of the project (July 1, 2024), additional funding was provided by Mississippi DOT to deep dive in some of the initial analyses for providing information of interest regarding the modeled sediment deposits created for various culvert configurations. The impact of these project changes is reflected in a variable number of test conditions for each project phase (see Section 4.6).

The experimental arrangement targets the culvert vicinity with the intent to detect and trace in space and time the location of the incipient sedimentation with special focus on the deposition developed at the culvert inlet. Following the project TAC guidance, the IMM and NMU flumes contain a 3-box culvert with 15°-angled wingwall, symmetrically set along a common axis as shown in Figures 10a and 10b. Our debugging tests on the IMM facility indicated that the velocity distribution at the culvert entrance does not change with the ratio of the length of the expansion area, hence we selected the shortest transition length, which is also the most cost-effective for in-situ installation.

4.2. Experimental facility and instrumentation

The experimental flume was built as an undistorted model at a scale of 1:25. The model scale was established based on the hydraulic considerations described in Section 3.1. This scale has been successfully tested in previous studies both with respect to targeted flow range as well the capability to ensure sediment mobility. The IMM flume contains a TRRCB-G1-01 Iowa DOT culvert design that is widely adopted at partnering states. The NMU culvert is basically the same design without fins for the dividing walls. The IMM and NMU flumes and the setting in the experimental facility are provided in Figures 17 and 18, respectively. A 75 hp pump with variable frequency-drive controller (accuracy of +/- 3% of reading) circulated water in an open loop. The model components are constructed from marine grade plywood (material stable when exposed to water) covered with a mix of fine particles and paint to roughen the interior flume walls. Steel and plastic pipe convey water from the pump to the model inlet. Brass gate valves control the inlet flows to the model headbox.

The culvert model includes a long-enough undisturbed channel length upstream the culvert expansion area to develop uniform flows with capability of transporting sediment. A series of flow conditioning devices (not all of them visualized in Figures 17a and 18a) are set in the flume's head tank and short distance downstream for stabilizing the flow incoming from the inlet pipe, evenly distribute the flow in the channel, and triggering the required turbulence levels for the flow. Downstream from the undisturbed channel reach, the expansion to the culvert, the culvert body, and the contraction returning the flow to the undisturbed channel are tightly set, as illustrated in Figure 17b,c and 18b,c for IMM and NMU flumes, respectively. Figures 17d,e,f and 18d,e,f provide additional details about the modeled culvert area for the IMM and NMU flume arrangements, respectively.

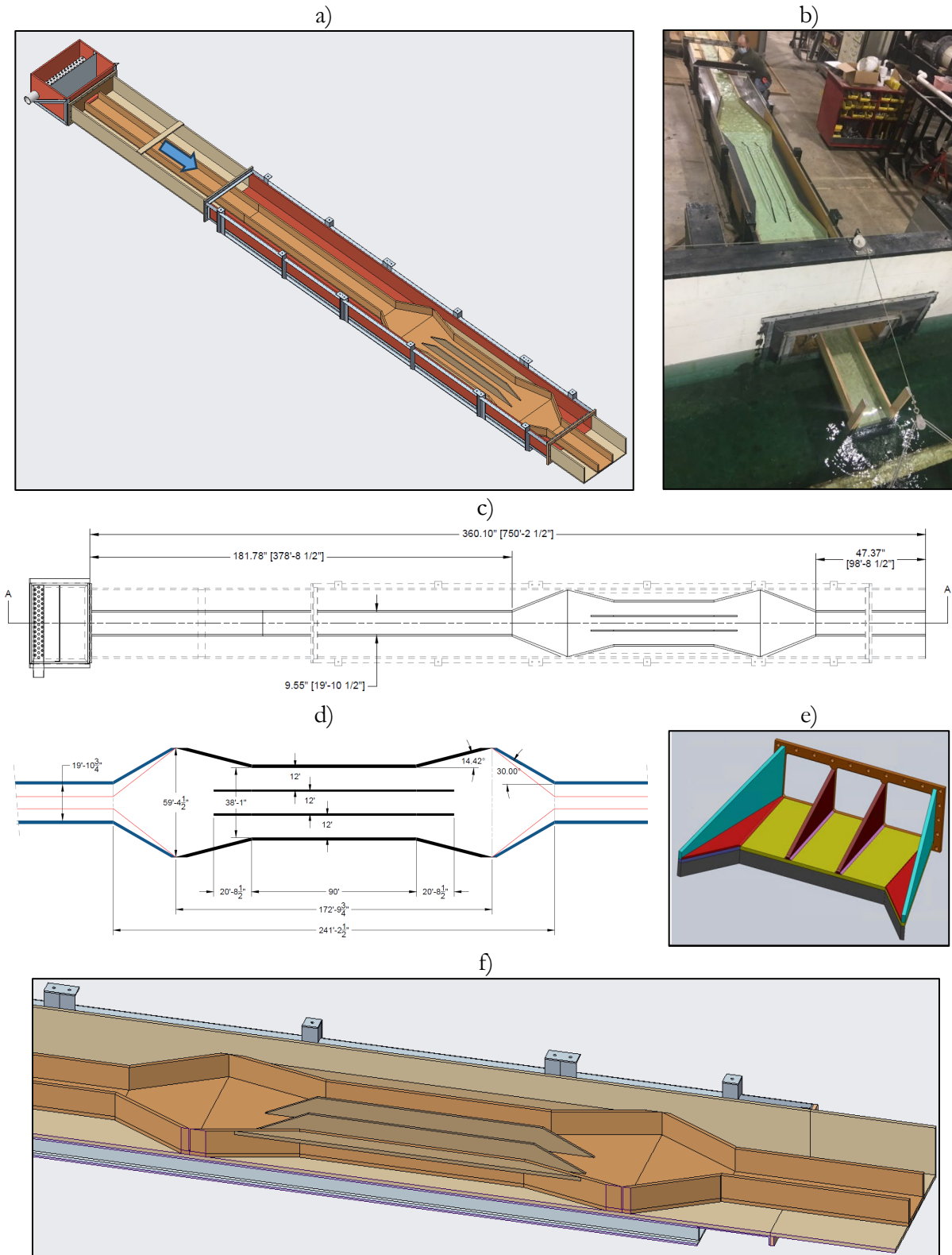


Figure 17. Iowa-Mississippi-Missouri experimental facility: a) overall view; b) facility photo; c) facility dimensions; d) culvert prototype dimensions; e) culvert inlet; f) view of the culvert area

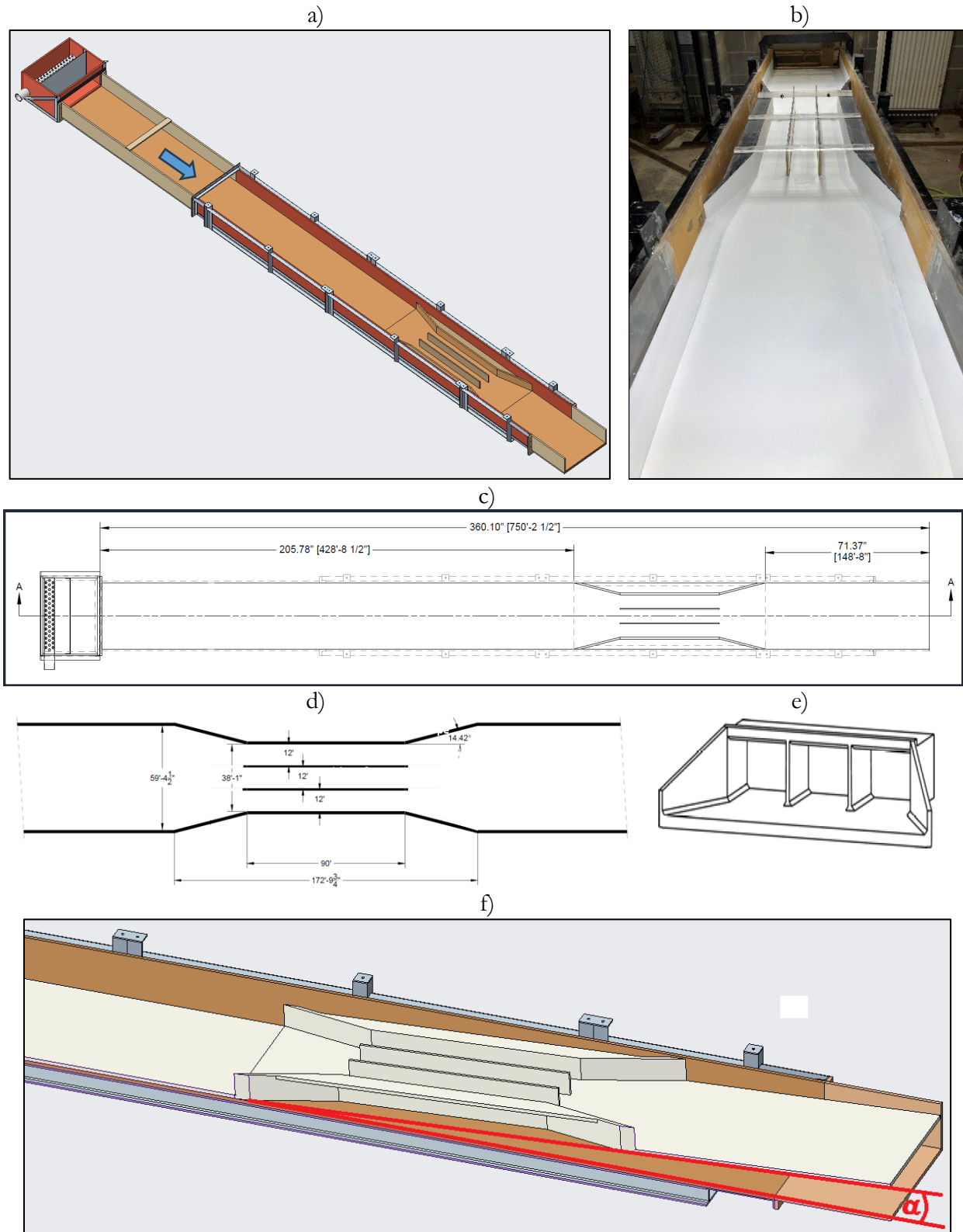


Figure 18. New Mexico-Utah experimental facility: a) overall view; b) facility photo; c) facility dimensions; d) culvert prototype dimensions; e) culvert inlet; f) view of the culvert area

The shape of the approaching channel is typically left to the decision of the modeler as the prototype cross-section shapes vary widely. In our study, we used a rectangular cross-section shape with beveled edges along the channel floor for IMM flume. The bed of the IMM flume was set at a slope of 0.3 degrees (equivalent to 0.52%) for all the tests. Despite that the geometry of the IMM flume was symmetric and the flow distribution in the approach channel was uniform, random non-symmetric flow patterns were developing at the entrance of the culvert due to a phenomenon called “stall flow behavior” (Smith & Kline, 1974). The diffuser-like area of the culvert expansion triggers a flow regime that is self-excited by the large-scale vortices created at the expansion entrance that in turn produce large stalls building up and washing out in a quasi-periodic fashion. The flow instability occurs when a certain combination of geometric and flow regime factors is produced (intentionally or not) in the expansion area (Fearn et al., 1990). As this flow instability would have had adversely impacted the execution of the tests, especially for the sediment-laden flows (Kantoush, 2008), we iteratively had to alter the entrance area geometry up to the point that the instability was eliminated.

The NMU flume has a rectangular cross-section without bevels at the floor edges. This flume has been constructed to enable the change of the stream-to-culvert angle by changing the slope of the reach approaching the culvert entrance in the 0-8 degree range. The planned succession of tests was 0.3, 4, and 8 degrees. However, during the 4-degree bed slope tests, a fast flow (supercritical) was developed that washed out the sediment released in the channel. Additionally, a hydraulic jump was developed close to the flume entrance that would have deviate considerably from the type of flow targeted by the modeling. A longer flume or smaller scale model could avoid the hydraulic jump occurrence, but the construction of an additional facility was out of discussion at this point of the project lifetime. Consequently, the TAC decision was to test the NMU flume with 0.3 (same as the single bed slope used in the NMU flume), 2 and 4 degrees for all tested self-cleaning designs.

The NMU flume experiments used underlying flows twice larger and sediment quantities up to five times than the ones used in the IMM experiments. Consequently, the conditioning of the flow (especially at the higher bed slopes) required installation of additional flow conditioning devices such as flow straighteners, weirs, and screens set across in the upstream area of the channel. Additional changes to the NMU model compared with the IMM configuration were made to bring the flows akin to those in New Mexico and Utah conditions. Specifically, the ephemeral streams in these semi-arid areas are changing from fast shallow, supercritical flow to slow deeper flows toward the end of the storm events, as observed in exiting recordings available on internet (e.g., [youtube.com/watch?v=K7iHjce9ePE](https://www.youtube.com/watch?v=K7iHjce9ePE); [youtube.com/watch?v=JcJhbDoMbVI](https://www.youtube.com/watch?v=JcJhbDoMbVI)). The stalling flows were not present at all in the NMU tests as there was no expansion area for this configuration.

Both flumes were equipped with a tailwater gate that can be raised and lowered with a crank, cable, and pulley system to control the flow depth upstream. The experimental flume for both culvert configurations were equipped with instrumentation for flow control (see Figure 19). Specifically, an electromagnetic flowmeter (Manifold Flow Meter – www.banjovalves.com.aspx) was used to continuously check the flow discharge in the flume, and a point velocity meter paired with a point gage were used to capture the velocity and depth distribution throughout the flume. A Streamflo 440 propeller-based instrument (velocity range 0.05 – 3 m/s) manufactured by Nixon (nixonflowmeters.com/streamflo-velocity-meter) was used for velocity measurements and a built in house point gage was used for stage measurements (accuracy, 0.0001 ft). Metallic beams set on rails running along the model walls allowed to position the instruments in area of the flume.

The most complex aspect of the modeling work was the replication of realistic sediment transport conditions using a live-bed experiments. Sediment was run in the flume using an open-loop approach, whereby the sediment was released in the upstream area of the flume and retrieved in the model tailbox. Several approaches for feeding sediment into the flume were tested prior to the production tests (e.g., conveyor belt, rotating perforated drums). Eventually, a pair of commercially-available

variable-rate feeders, distinct for IMM and NMU flumes, were adapted for releasing sand (see Figure 19). The sediment feeding rates for various settings of the feeders were calibrated before the start of the tests. Combining the two separate feeders and varying the feeding rates with prescribed timing enabled our team to accommodate the rates of sediments for various flow events simulated in the IMM and NMU. The sediment supplied to the channel was recovered in the flume tailbox where removable sand-retaining containers were installed at the flume outlet. The sand catchers allowed to quantify the amount of sand washed out from the flume after conducting each individual test.



Figure 19. Essential items for flow control and experiment execution for the IMM and NMU tests

In addition to the above-mentioned instrumentation, two other installations were used for globally recording the test results: a webcam and a laser-based scanning system. The webcam system recorded continuously images from the beginning to the end of the experiments. The webcam selected for the study was an off-the-shelf webcam with real-time communication (<https://www.moultriemobile.com>) that allowed to conveniently watch and record high-resolution still images (see Figure 20a). At the time of project initiation, we could procure a Moultrie Panoramic 120i Trail Camera (120° field of view, 20 megapixel resolution) that currently is discontinued. Operating the webcam in multi-shot mode enabled to create useful time-lapse videos of the experiments during their progression. The camera and local illumination bulbs were set on a dedicated platform centered on the flume with their position kept identical throughout the experimental runs (see Figure 20b). Series of multi-shot image recordings acquired during one experimental test are shown in Figures 20 c-f.

The three-sensor camera covered the entire area of interest, but due to the lens distortions and sensor positioning in the camera housing it produced geometrically distorted images. An in-house software was used to correct for the geometric distortion based on algorithms pertaining to the Large-Scale Particle Velocimetry (LSPIV) technique (Fujita et al., 1998). The LSPIV implementation requires identification of homologous points in the raw image (see Figure 20g) and in real-world coordinates (see Figure 20h) followed by an orthorectification of the images using a geometrical transformation applied pixel-by-pixel over the entire imaged area. These homologous points, labeled Ground Reference Points, are indicated with red dots in Figures 20g and 20h. Once this transformation is implemented, two-dimensional quantitative estimation of the sediment accumulation areas can be conducted with various image analysis software package. These estimations are preserving the actual areas of the sediment deposits as the images are now scale to reality. The process of evaluating quantitatively the areas occupied by sediment deposits is presented in Section 4.5.

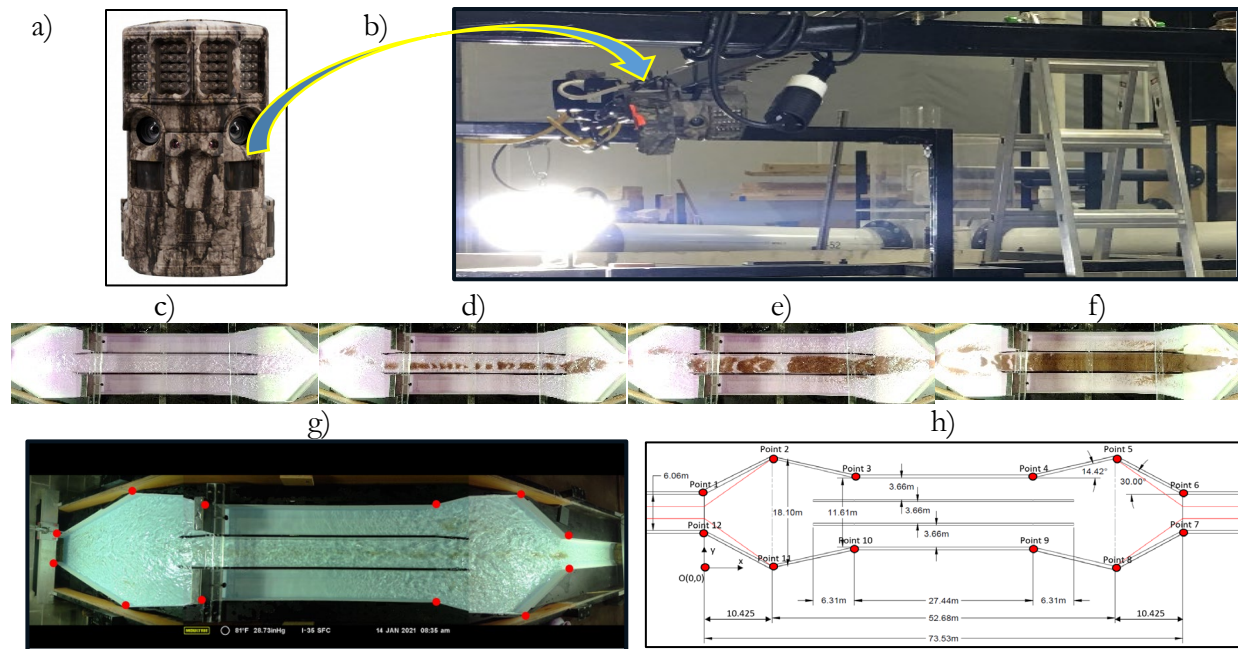


Figure 20. Webcam system: a) panoramic webcam; b) camera and illumination supporting beam; c) – d) time-lapse photography; g) webcam frame (IMM raw image) with marked ground-reference points (GRP are red dots); h) GRP positioned in a reference system

The laser-based system is an even more powerful tool as it maps the three-dimensional (3D) maps of the sediment accumulations. Our surveys were entailed a Faro Focus Laser Scanner (www.faro.com), see Figure 21a. During the data acquisition, the laser scanners do not need special preparations besides identifying a set of fixed points in the scanned area that can be tied in the scans taken from several viewing angles. The fixed points for our surveys were rigidly set of the framing surrounding the experimental flume, i.e., white sphere in the image shown in Figure 21a.

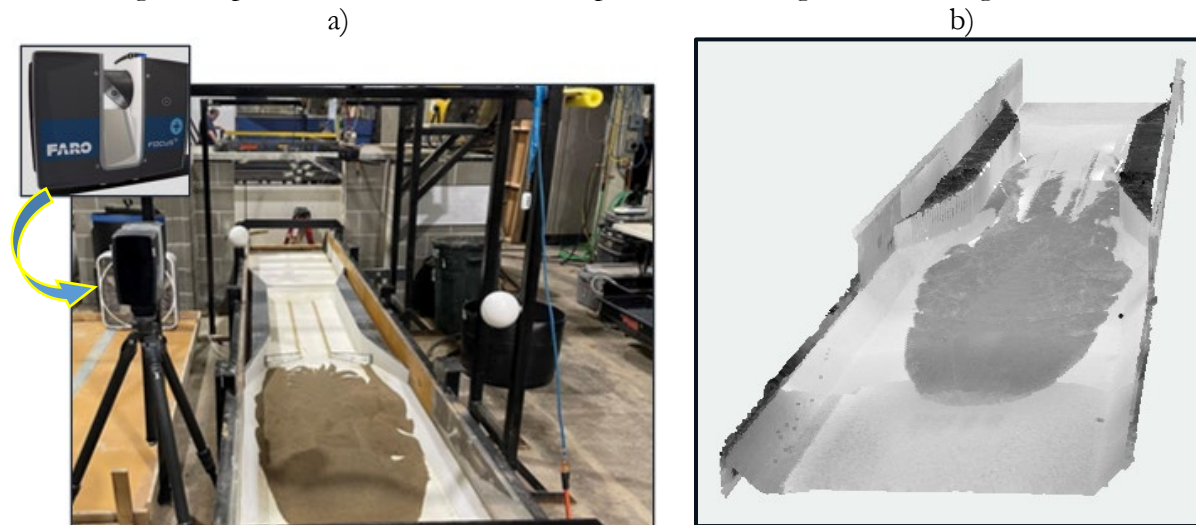


Figure 21. Laser surveys (NMU case): a) scanner and surveying platform; b) raw point-cloud map

The scans acquired from different angles are subsequently processed with proprietary software to first obtain the raw point-cloud map that assembles all laser points collected during the survey (see Figure 21b). Section 4.5 describes the step-by-step process to create accurate, photorealistic 3D representations of volumes of sediment accumulated in the culvert area.

4.3. Hydraulic similitude

Section 3.1 of this report highlights the challenges associated with the hydraulic modeling of sedimentation at multi-barrel culverts. This process is governed by complex flows under the hydraulic label of sediment transport in nonuniform and severe unsteady flows. Investigation of any of the flow complexity involved in these flows is a difficult task in itself, but when combined they create a daunting task for modelers, who have to decide on the most important hydraulic similitude criteria that ensure a reliable replication of the actual flows. The task difficulty is exacerbated as our knowledge on these highly variable (in time and space) flow and transport processes is not supported by reliable data from monitoring and modeling investigations. While modeling and monitoring have continuously advanced, only laboratory modeling can address the fundamental knowledge gaps on these processes and provide the information needed for developing superior models and informing the design of in-situ monitoring. This study is an effort along this line by providing useful insights and quantitative information on the overall development of sedimentation at multi-barrel culvert.

The chief similitude criteria for hydraulic modeling of sediment transport are the Froude and Shields scaling relationships (ASCE, 2000, ASCE, 2008). The former criterion is the dominant similitude parameter for free-surface flows and it is typically sufficient for modeling clear-water open-channel flows if the Reynolds criterion (another essential similitude number) is large enough (e.g., fully turbulent flow). The Froude scaling relationships is defined as $Fr = U/\sqrt{gH}$ where U - mean flow velocity, H - flow depth, and g - the gravitational acceleration constant. Appropriate similitude is achieved if $Fr_m = Fr_p$ (subscripts p and m stand for prototype and model dimensions, respectively). Defining the geometrical scale by L_r for our undistorted models display a $L_r = L_m/L_p=1/25$.

Table 5 lists the scaling factors for the main model variables ensuing from Froude similitude criterion. Also listed in the table are ranges of interest for the main variables targeted through the present study.

Correctly scaling the size and distribution of the sediment in the model is important to capture the transport behavior. This scaling relationship is governed by the Shields stress, τ^* , dimensionless parameter which characterizes the

bed shear stress relative to the resistance of the grains to motion. The Shields stress is defined as (Kozarek,2015): $\tau^* = \tau_0/[(\gamma_s - \gamma_w)D] = (\gamma_s HS)/[(\gamma_s - \gamma_w)D] = HS/1.65D$ where γ_s and γ_w are the specific weights of sediment and water, respectively, τ_0 is the bed shear stress, S is the channel bed slope (equal to the free-surface slope in steady flow), and D is the particle size. Similarity between model and prototype is attained if $\tau_m = \tau_p$. The Shields criterion, a.k.a. Froude densimetric number or particle mobility, is useful for characterizing the condition of incipient motion of particles on the bed. When mass rate of sediment transport is of concern, a useful parameter is Φ which relates the mass and volumetric rates of sediment (ASCE, 2000). The parameter is defined as: $\Phi = \rho_s/[\sqrt{g(\Delta\rho/\rho_w)}D^3]$ where, ρ_s and ρ_w are the density of sediment and water.

Ideally, our hydraulic modeling study should seek to achieve all the above-mentioned similitude criteria fulfilled, i.e., $Fr_m = Fr_p$; $\tau_m = \tau_p$; and $\Phi_m = \Phi_p$, but this might be impossible to simultaneously achieve. Our experimental study is limited in attaining the desired hydraulic similitude by various practical aspects such as scale effects (e.g., a larger scale for the model), material limitations (e.g., using

Table 5. Scaling of essential variables for $L_r=1:25$

	Prototype values		Scaling factor	Scaling factor
	Min	Max		
Water Depth	1ft	10ft	L_r	0.04
Culvert width	36 ft	(for 3 culvert boxes)	L_r	0.04
CX area	36 sqf	360 sqf	L_r^2	0.0016
Bed slope	0.01		1	1
Velocity	3 ft/s	10 ft/s	$L_r^{1/2}$	0.2
Discharge	108 cfs	3,600 cfs	$L_r^{5/2}$	0.00032

other than water and natural silica sand particles), available instrumentation (e.g., using distributed instrumentation network rather than point measurements), and (not least important) the funding level available for carrying out such demanding experiments. As multiple studies have done before, we adopted a more flexible modeling approach without compromising the reliability of the results produced from the experiments. In this “hybrid” modeling approach (Heller, 2011) we observed the similitude criteria defined above augmented with additional observations made during our field studies (Ho, 2010; Ho et al., 2013; and Muste and Xu, 2020). Specifically, our main modeling goal for all the study experiments was to obtain a loose bed sufficiently mobile to uniformly convey the sediment through channel and culvert and creating deposition geometry and areal distributions similarly with what we found from the field surveys. As a result, our modeling approach placed a greater emphasis on sediment mobility criterion than on Froude number similarity.

4.4. Experimental phasing and associated protocols

The experimental program for the study entailed a phased progressing of the tests, with each of the test group targeting specific modeling goals. The phasing of the experimental program is provided in Table 6. The experimental protocols for each phase were shaped to attain the goals of individual project phases. The changes occurred during the progression of the project (see Section 4.1) led to a variable number of tests for each phase to accommodate the priorities sought by the partnering states and the resources available for the project at specific times. This section provides sample experiments carried out in various phases to test the performance of the model for various purposes. The “production” tests leading to the final recommendations of this study are described in Chapter 5.

Table 6. Phasing of the experimental program

#	Experimental Phase	Role of the experiments
PH1	Model debugging	Preliminary tests for commissioning the model in the “as-is” IMM and NMU models (checking the flow distribution and stability, firming the flow range for the tests, sediment mobility))
PH2	Baseline tests	Testing modeled sediment transport scenarios using alternative sand types
PH3	Screening of self-cleaning culvert (SCC) designs (i.e., “Production tests”)	Series of successive tests conducted uniformly for each SCC design to document the patterns of sediment accumulations in the culvert vicinity for various. These tests included all the data acquisition and processing steps described in Section 4.6.
PH4	Sensitivity tests	Applied to best ranked solution in PH3 to test the performance of SCC designs in atypical conditions (see Section 4.6)

The high degree of complexity for the hydraulic modeling of sediment transport through culverts and the presence of multiple factors that could affect the final configuration of the sediment deposits required implementation of rigorous protocols for each study phase and across all culvert designs tested in the IMM and NMU flumes. Specific experimental protocols were developed for exploring: a) the behavior of steady flows in the “as-is” culvert configurations; b) steady flow regimes of different intensities, durations, and, repetition number; c) the establishment of realistic hydrographs for storm events and prescribing the change in the rates of flow and sediment and their timing.

The steady flow tests conducted in phase PH1 were aimed at observing and firming the flow conditions that are within the bounds of the similitude modeling but also replicate the actual processes observed in field conditions. Figure 22a compares patterns of sediment deposition in the as is IMM model for a range of discharges (tests with the same amount of the fine sand). It can be observed that

an initially tested low flow [i.e., 25 gallon/minute (gpm) in the model] mobilized the bedload but did not practically result in sedimentation in the side barrels. With the increase of the discharge, the deposition in the side barrels is taking shape. The larger the flow, the more sediment moved downstream the central barrel and more sediment protrudes in the side barrels. Balancing similitude criteria with the appearance of the sediment deposits at the end of the experiment led to the decision to set the range of flows for the storm hydrographs in the IMM model for 25 - 100 gpm. Similar tests were conducted for the NMU model, as illustrated in Figure 22b (tests with the same amount of the coarse sand). Accordingly, the range of flows for storm hydrographs was set from 50 gpm to 200 gpm. We deem that the above-described trade-off between experimental approaches is justified as long as the self-cleaning designs were compared based on the same set of flows for each flume configuration.

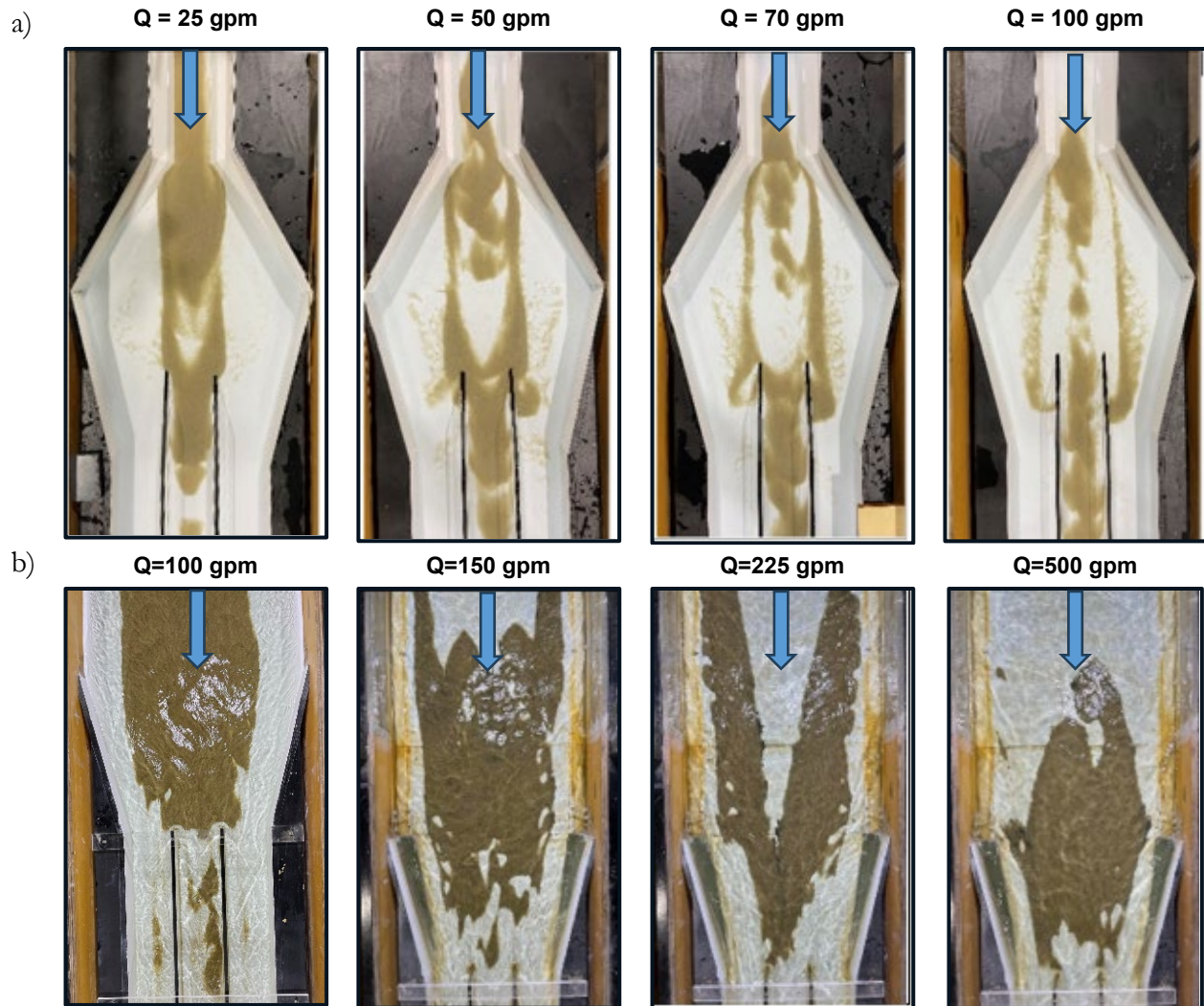


Figure 22. Sedimentation patterns for various steady flows: a) IMM flume, and, b) NMU flume

In Phases PH2 and PH3 of the study, we investigated the impact of various types of steady flows on the sedimentation patterns accumulated at the culvert entrance. These tests were carried out with the intention to assess the impact of flow duration on the mobilization of the sediment in the model and provided essential elements for building the storm hydrographs used in phases Ph3 and Ph4. Table 7 lists the types of steady flows tested for the IMM flume tests. The sieve analysis of the “coarse” and “fine” sediment is provided in Figure 13. The base flow for the IMM flume tests was deemed to be at 25 gpm as while conveying sediment in the channel, it barely contributed to accumulation of

sand in the culvert (see Figure 22a, $Q = 25\text{gpm}$). The “light” and “heavy” storms differentiate flows based on the discharge magnitude (i.e., 50 vs. 100 gpm). The amount of sand released for the two opposite storms was the same to differentiate the stream power impact. The distinction between “short” and “long” was made based on the duration of the storm. The amount of sand released in the flume for the long storms was kept the same as for short storms. In addition to the exploratory tests reported above, repeated light and heavy storms were also tested. Testing various type of sand discussed in Section 3.1 and will be expanded on in the sensitivity tests discussed in Section 4.6.

Figure 23 hints to the information that can be inferred from the photos of this type of tests (e.g., impact of flow power, amount of added sediment to the flow, and repeated flows). The tests were conducted with “fine” sand (see Figure 13). The sequence of images allows to qualitatively observe that light storms can be more detrimental than heavy storms, light and long storms are also detrimental, and that repeated flows are not considerable adding to the spread of the accumulations.

Table 7. Steady flow scenarios for supporting phases PH2, PH3 and PH4 of the study

Experimental setup	Flow scenarios	Flow & sediment rates
<ul style="list-style-type: none"> • various culvert designs • various sediment types: <ul style="list-style-type: none"> ○ “coarse” sand (0.2 -2.0 mm) ○ “fine” sand (0.3 -0.85 mm) ○ crushed walnut shells 	One light & short storm	50 gpm steady flow & steady sediment rate
	One light & long storm	50 gpm steady flow & steady sediment rate
	One heavy & short storm	100 gpm steady flow & steady sediment rate
	Two light storms	2X 50 gpm steady flows & steady sediment rate
	Two heavy storms	2 X 100 gpm steady flows & steady sediment rate

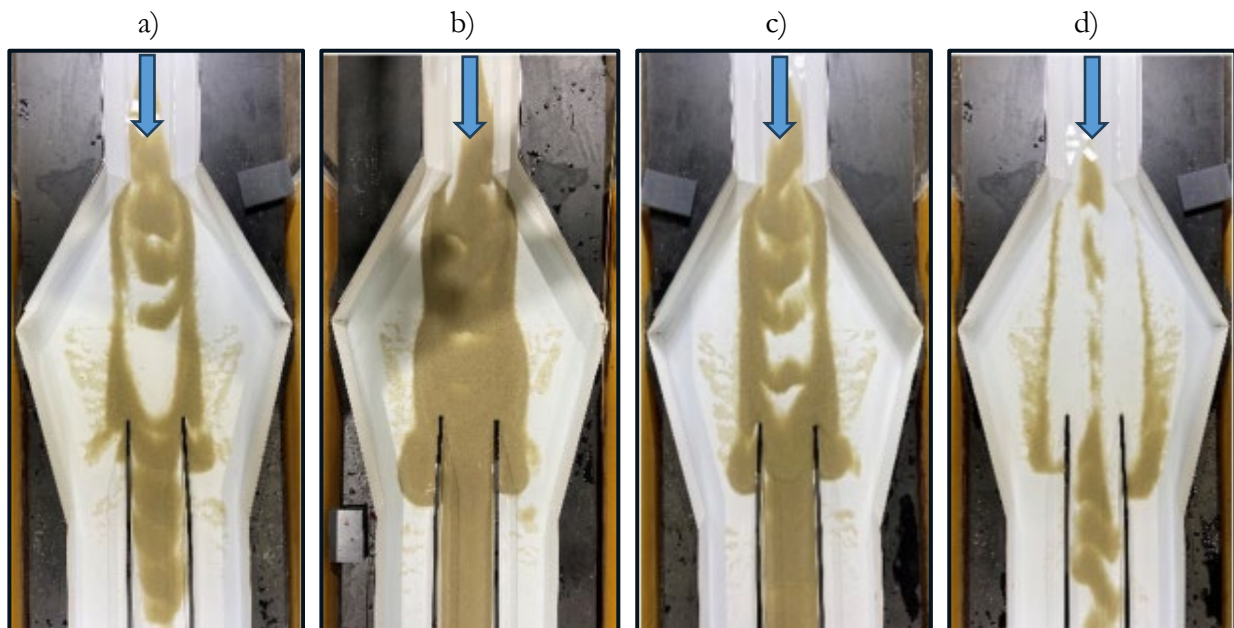


Figure 23. Sample tests for various steady flows in the “as-is” IMM culvert: a) 50 gpm light & short; b) 50 gpm light & long; c) 2 repeated 50 gpm light & short; and, d) 100 gpm heavy & short

All the steady flow cases in Table 7 were fully documented with such images but it is beyond the scope of this study to illustrate all the tested cases in the body of the report. The raw data and information are available upon request. It is deemed that the sequence of tests with steady flow regimes enables to account for various climatic and morphologic conditions specific to the geographic areas of the TPF partnering states (i.e., perpetual vs. ephemeral streams). Due to changes in the experimental program occurring in the study progression, the NMU flume tests were not equally extensive covered with steady flow alternatives, as it would have drastically affected the available resources. It is deemed

that the inferences obtained from the phases 1 and 2 tests carried out for the IMM flow scenarios are also relevant for NMU ones.

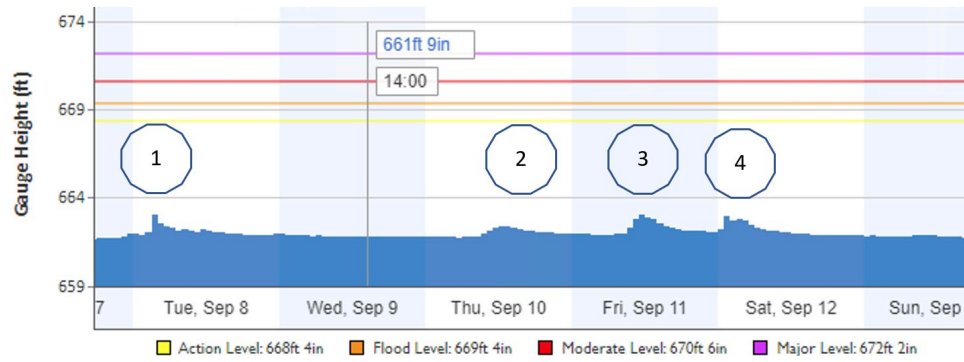
Critically important for the hydraulic modeling conducted in the study is the replication of the realistic transport of water and sediment fraction occurring during hydrologic events as this is the driver for the sedimentation process at culverts. The most detrimental events for sedimentation are the rapidly-varied storms known as flash floods (www.weather.gov/phi/FlashFloodingDefinition). These events are triggered by heavy rains that produce fluvial waves that peak within 6 hours from the rain start. Simulation of fluvial wave propagation cannot be attained in the model by a simple superposition of steady flows of various magnitudes. Rather, fluvial waves are complex physical processes described in Muste et al. (2024).

As no data could be found for average regional hydrologic characteristics, the water and sediment hydrographs during storms were developed based on observations from our own field study (Muste & Xu, 2022) mentioned in Section 3.1. The observations garnered from repeated measurements of the stream stage and turbidity acquired at the inlet and outlet of the culvert FHWA #364790 in Iowa City (see also Figure 11) over a series of storms during September 2020 are illustrated in Figure 24a. Synthesis of these measurements enabled us to quantify the water and sediment hydrographs characteristic for this culvert and representative for the IMM conditions, as illustrated in Figure 24b (top). The inferred hydrographs for the unsteady tests used a “stepped” approach for the water and sediment progression following the timeline shown in Figure 24b (bottom). Selection of the 1:3 ratio between the rising and falling stages for the water hydrograph was made for the storms as this ratio is more closely resembling a flash flood.

An important feature of the hydrographs is the phase shift between the peaks of sediment and water which indicates that most of the sand entrainment occurs on the rising limb of the hydrographs. This is a well-documented feature associated with unsteady flows, whereby the total amount of sediment transported during the flood wave propagation is higher than the equivalent steady flow counterpart (Li et al., 2015; Mrokowska & Rowinski, 2019). It has been demonstrated that the total sediment yield was up to an order of magnitude higher for the naturally-shaped hydrograph than for the equivalent steady flow of the same duration as the unsteady flow hydrograph. The final experimental protocol for setting the water and sediment hydrograph is shown in Figure 24b (bottom). In this figure the non-dimensional representation of the storm hydrograph was inserted in the context of an end-to-end test. This protocol for storm hydrograph was kept the same for all IMM unsteady tests (a.k.a. flood wave or “ramping” for brevity).

Comparison of test results on the sedimentation patterns of steady and unsteady flow tests are shown in Figure 25. The steady flow tests compared in this figure were executed with the protocols described in Table 7 but, in contrast with the results presented in Figure 23, they are using the “coarse” sand (see Figure 13). The visual comparison of the test cases in Figure 25 indicates that the light storms are more detrimental with respect to the amount and distribution of sediment than the heavy storms. The comparison also shows that the light and long storm is close with respect to sediment deposition with the flood wave storm. This is not surprising as the flood wave storm is a combination of light and heavy storm of longer duration for the first type and shorter for the second type of storm (see also Figure 24b bottom).

a)



Storm #	Stage change			Timing			Duration (h)		
	start	Max	Delta h	start	peak	end	peak	total	ratio
1 (typical)	661.75'	663'	1.25 ft	7/23:00	8/3	9/5:00	10	29	1:3
2	661.75'	662.33'	0.58 ft	10/8:00	10/13:00	11/3:00	5	31	1:6
3	661.83'	663'	1.17 ft	11/6:00	11/12:00	11/23	6	17	1:2.8
4	662'	662.92'	0.92 ft	11/23:00	12/1:00	12/22:00	3	23	1:7

b)

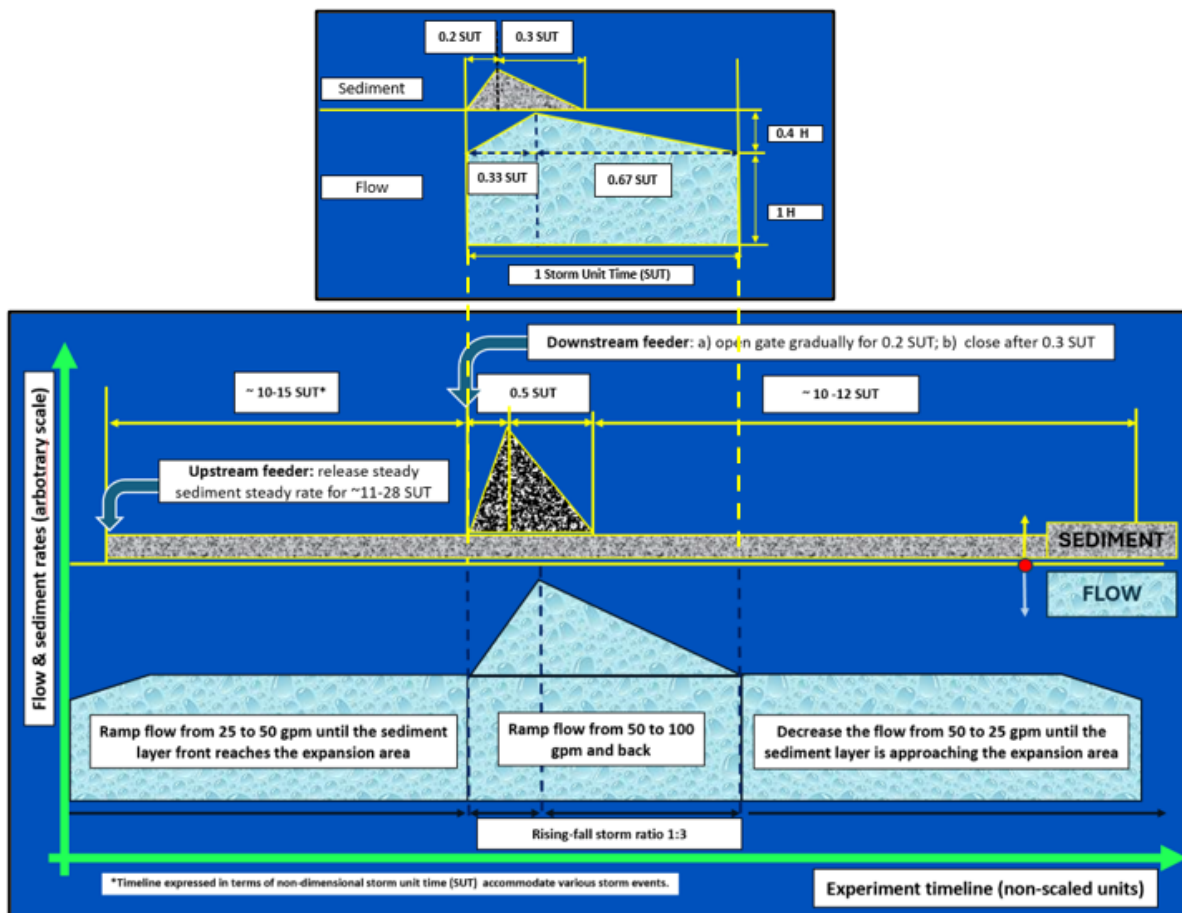


Figure 24. Water and sediment hydrographs for storms modeled in the IMM flume (plots in arbitrary scales): a) observations made on a series of storms at a 3-box culvert within IMM region during September 2020; b) synthesis of the filed measurements for informing the experimental protocols (top) and water and sediment hydrographs with timing from left to right (bottom)

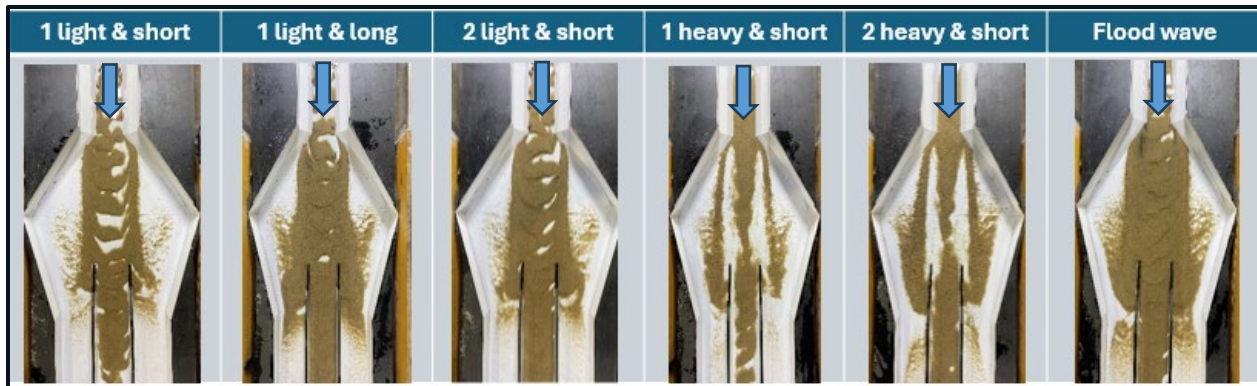


Figure 25. Sample results for steady and unsteady flows tested in the IMM flume with coarse sand and protocols described in Table 7 and Figure 24b (bottom) for the flood wave.

In the absence of similar data for NMU hydrologic conditions, we used essentially the same water and sediment hydrographs as for IMM (see Figure 24b, bottom). Additional information on the flood wave dynamics was obtained from third-party videos recorded during flash floods in New Mexico region and subsequently posted on the internet (e.g., www.youtube.com/watch?v=K7iHjce9ePE). Using LSPIV concepts applied to the available video recordings allowed to reconstruct the velocity profile of the heavily-loaded wave front propagating in the ephemeral streams, as illustrated in Figure 26a. Combining field-inspired evidence from various sources with our own filed observations, we eventually established the water and sediment hydrographs illustrated in Figure 26b. These hydrographs, developed in the 0.3 degree flume arrangement, were slightly changed for the other two stream-to-culvert angles tested in the NMU model. The water and sediment hydrographs established for one of the stream-to-culvert angles were uniformly applied for all culvert configurations to ensure that the behavior of the self-cleaning designs is assessed under the same sediment transport conditions. The NMU tests required considerably higher water discharges and sediment volumes than the IMM tests. Handling the increased water and sediment quantities required in turn replacing the sediment feeders with larger capacity ones (see Figure 19) and additional means for controlling the water distribution upstream of the culvert, as illustrated in Figure 27.

The additional costs incurred with retrofitting the flume for the NMU tests and its repositioning for different stream-to-culvert angles along with the addition of the 3D quantification of the sediment deposits using the lidar scanner required adjustment of the research plan tasks and of the project timeline. Surveys #5, 6 and 7 of the project TAC members (provided in Table 3) document the sequence of steps taken for this purpose. Using inferences drawn from IMM tests on the types of flow and sediment that were the most relevant for the study the overall number of NMU tests was considerably reduced. More specifically, for the 0.3 degree stream-to-culvert arrangement only the light & long storm (one of the most detrimental hydrograph for the IMM conditions, as illustrated in Figure 25) and the flood wave scenarios were tested. For the 2 and 4 degree stream-to-culvert arrangement only the flood wave scenario was tested. Some of the initially planned self-cleaning designs were not tested. Moreover, most of the NMU tests were conducted with the “coarse” sand (see Figure 13) as the “fine” sand could be controlled only for the 0.3 degree stream-to-culvert angle because the high velocities and hydraulic jump developed in the flume. Consequently, the assessment of the performance of the self-cleaning designs for the NMU flume was based on the flood wave scenario using coarse sand, as reported in Section 5. Also reported in this section are the results of the customized experimental protocols conducted for sensitivity analysis. Samples of the steady and unsteady flows tests for the NMU flume (not reported in Section 5) are illustrated in Figure 28.

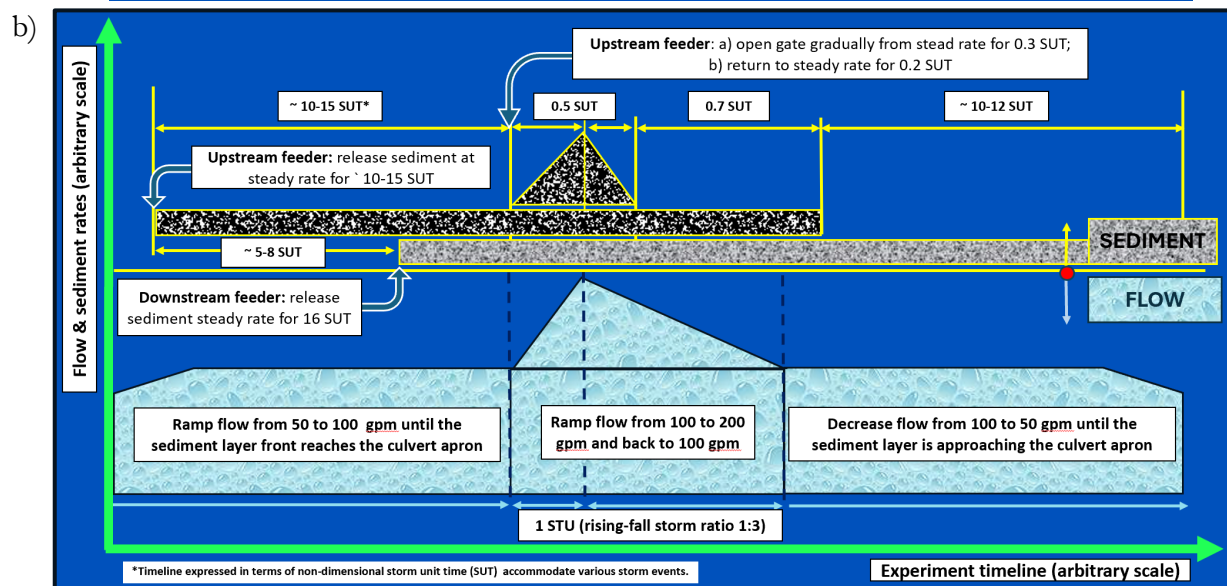
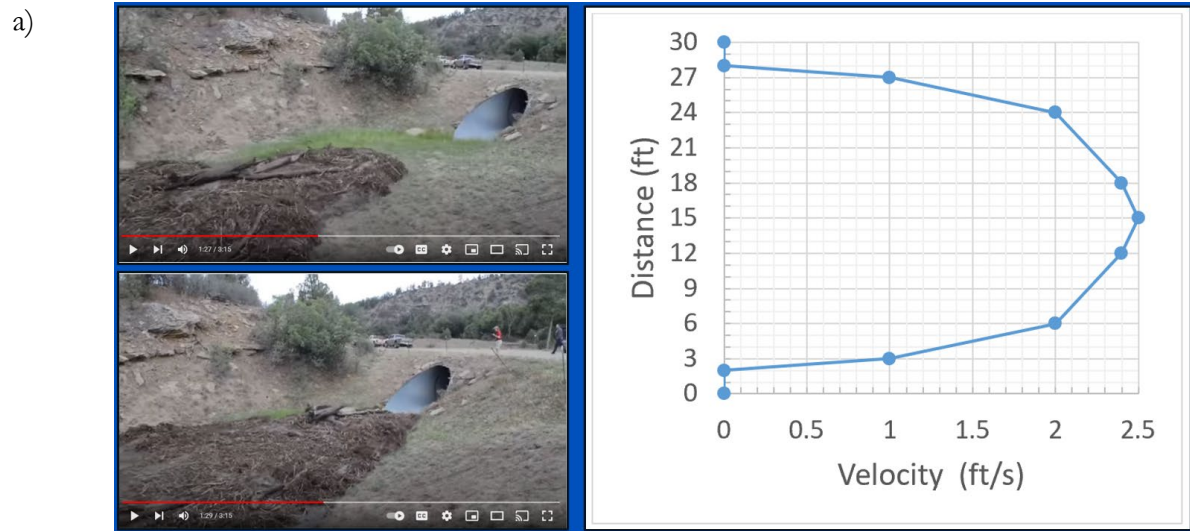
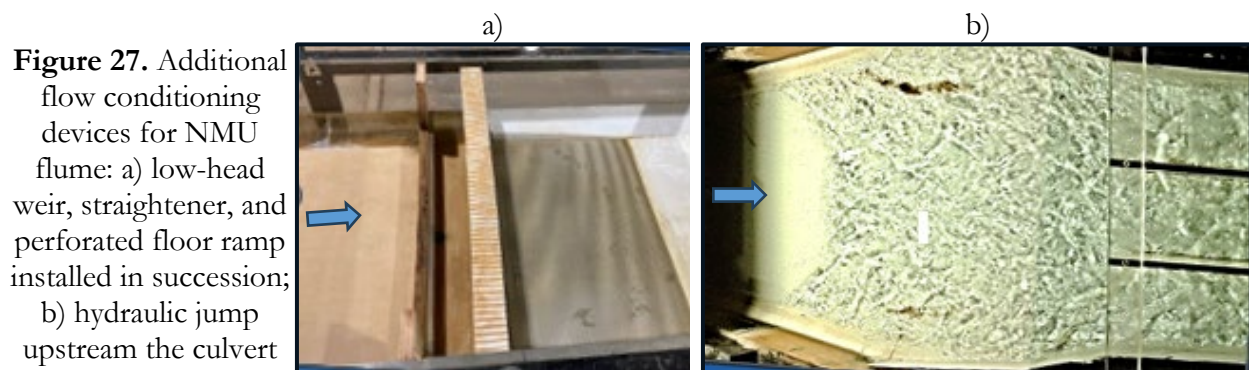


Figure 26. Water and sediment hydrographs for storms modeled in the IMM flume (plots in arbitrary scales): a) quantitative estimation of the flood wave front from video-recordings on a flash flood event in New Mexico; b) water and sediment hydrographs (timing from left to right)



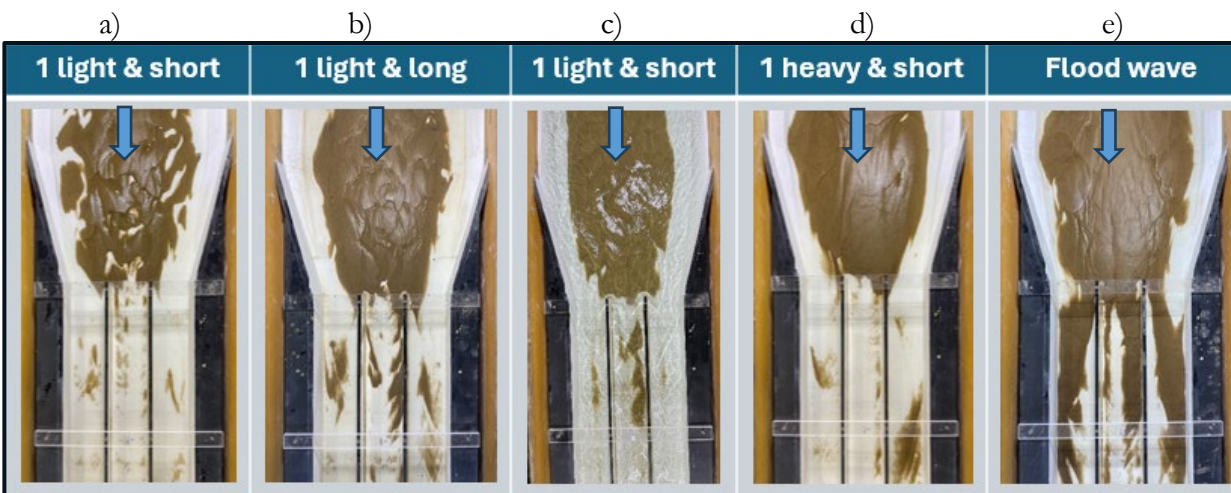


Figure 28. Sample results for steady and unsteady flows tested in the “as-is” 0.3 degree stream-to-culvert NMU flume with coarse sand: a) steady light & short steady ($Q = 100$ gpm); b) steady light & long ($Q 100$ gpm); c) steady light & short ($Q=150$ gpm); d) steady heavy & short ($Q = 300$ gpm); e) flood wave flow scenario ($Q 50$ - 200 gpm & protocol described in Figure 26).

4.5. Data acquisition & processing protocols

The data acquisition and processing protocols were carefully developed to maintain the uniformity of the test execution, assuring the reproducibility of the results, and, enabling unbiased assessment of the developed self-cleaning designs. The complex hydraulic modeling tackled through this study necessitated well-organized workflow, and detailed recording of each step of the tests. Given that in this study we used for the first-time extensive workflows, detailed documentation for the execution of the associated protocols were written to ensure similar quality outcomes when new student assistants joined the research team. Typical operation sequence for a complete screening and/or sensitivity test included (as a minimum) the following steps:

- Preparation of the sediment material (sediment drying, sizing, and quantification)
- Verification of the flume status (integrity of the flume active areas and installed modifications)
- Setting of the targeted flow
- Checking of the clear-water flow conditions within the facility and documentation of the flow distribution throughout the flume
- Acquisition of time-lapse videos and photo documentation at the start and the end of the tests (three fixed camera positions were used for this purpose)
- Application of the flow scenario phasing and timeline and recording of the actual execution of the workflows for each experiment
- Continuous checking of the facility for unwanted flow and sediment patterns
- Closing the experiment with precautions for maintaining the integrity of the sediment deposits formed during the tests
- Drying the model and executing the lidar survey
- Collecting and weighing sediment from the areas of interest and sand washout from the model
- Logging all particular features of the individual tests for supporting the experimental inferences
- Execution of the Lidar survey
- Processing the acquired data for quantitatively documenting the results

Given the large number of the tests and the similarity of the sedimentation patterns, the photo-documentation of each test was critical as it provided a quick reference to the obtained results.

The photo documentation entailed acquisition of 3 photos taken from the fixed positions for each test, as illustrated in Figure 29. Most of the images in this report contain only the culvert inlet and expansion area (the focus area of the study) to not clutter the presentation flow. Details on the multiple execution steps along with the photographic evidence (see Figure 30) are archived for possible re-analysis.

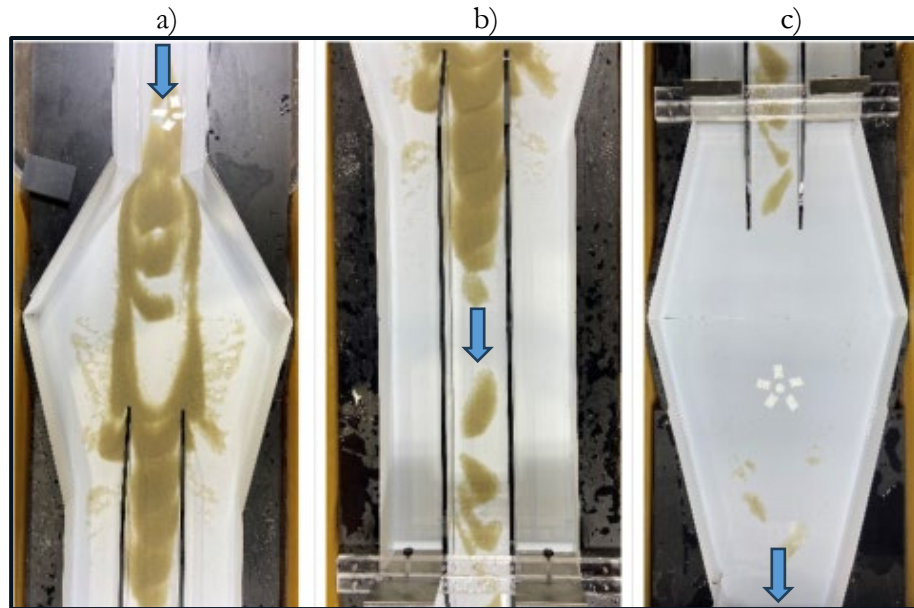


Figure 29. Photo-documentation of individual tests: a) culvert inlet & the expansion area; b) culvert body; c) culvert outlet & contraction area

a)

Facility setup		
Flow setting	Sediment feeding	Comments
Flow regime: Ramping Discharge: 100-200-100 Incoming flow ch. depth: 3.05-4.57-3.05 cm Incoming flow central velocity: 33.5-43.0-33.5 cm/s Inlet flow ch. depth: 3.29-4.36-3.29 cm Inlet flow velocity: 47.0-58.7-47.0 cm/s Run time: 11.5 min	D/S feeder: Position: 0.57m from culvert expansion 14cm blockage from both side ends Vibrator used Opening level: 1.5 Feeding type: continuous Total amount: 15 kg Feeding time: 9 min U/S Feeder: Position: 1.05m from culvert expansion Central opening for feeding: 17 cm Started 2 min earlier than d/s feeder Opening level: 1-2-1 Feeding type: continuous Total amount: 18 kg Feeding time: 9 min	Time to reach expansion after feeding: 5 min Time to reach the contraction after feeding: 6 min Location of incoming flow velocity measurement: 25cm from culvert expansion Location of inlet velocity measurement is at tapered section of the culvert No backwater on both sides Channel configuration: Plexiglass weir with U-shaped wooden weir u/s, small metal weir with wired mesh d/s, and honeycomb u/s Sediment remaining in D/S Feeder: 6.3 kg Sediment remaining in U/S Feeder: 5.25 kg Sediment washed out during experiment: 0.9 kg Sediment in flume: 19.55 kg (23 kg wet) Partial timelapse, initially forgot to turn on camera

b)

Run #/ Date # 2/ Oct 23, 2022 Culvert type: "As Is" Rain Type: Ramping	Depositional pattern at the end of the run			
	At the beginning	At the end of the run (equilibrium)		
		Upstream area	Downstream area	Full Length Photo
	Internal team research info	Photo documentation for reporting		

Figure 30. Documentation of individual tests: a) details on the facility settings and execution steps, b) progressive photo documentation.

Two-dimensional mapping of the sediment deposits was used in the first part of the study to quantify the areal extend of the sediment in the culver vicinity. In the second part of the study, the quantitative sediment mapping was conducted with Lidar surveys described next. The 2-D mapping workflows executed with the Photoshop software (www.adobe.com) are shown in Figure 31.

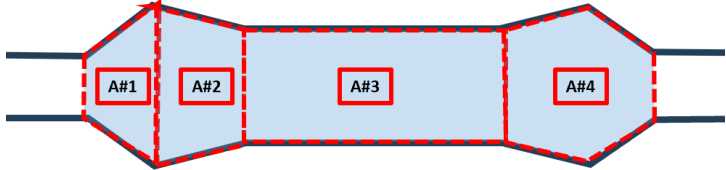
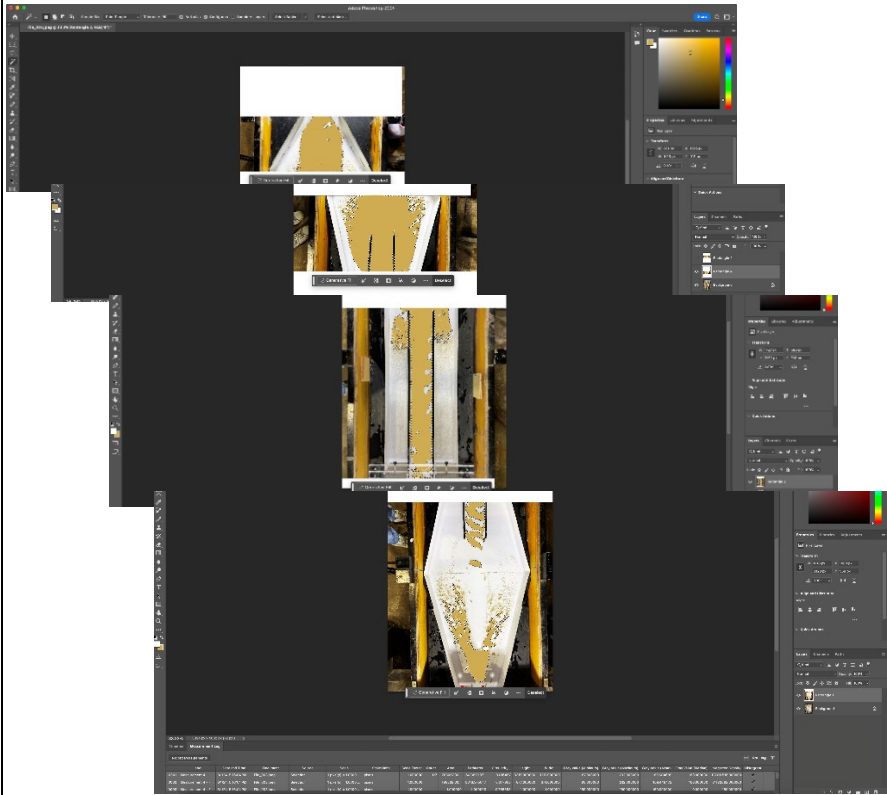
#	Procedure	Details																																													
A.	Delineate the areas of interest for mapping	 <p>Delineation is applied to still or video camera images. The latter images are orthorectified using LSPIV concepts.</p>																																													
B.	Apply Photoshop to the delineated area.																																														
C.	Identify pixels corresponding to sand particles in areas A#1, A#2, A#3, A#4	<ul style="list-style-type: none"> the “Magic Wand” identify pixels of similar color value.tool the “Tolerance” tool applies bounds for the identification process sum up the total number of pixels order to find out its total pixel count 																																													
D.	Scale the mapped areas using model coordinates and evaluate % sand coverage/per area using Excel Compare with Lidar mapping, if available.	<table border="1"> <thead> <tr> <th colspan="5">Model Scale 1:25</th> </tr> <tr> <th>Photoshop Data</th> <th>Width of Expansion (pixels)</th> <th>Width of Expansion (in)</th> <th>Conversion Factor (in²/pixel²)</th> <th>Area (pixel²)</th> </tr> </thead> <tbody> <tr> <td></td> <td>1725</td> <td>28.5</td> <td>0.000272968</td> <td>684134</td> </tr> <tr> <th colspan="5">Old Model Name 22 G#2 w_ FW Coarse Ramping A</th> </tr> <tr> <th>Sediment Area</th> <th>Model Area (in²)</th> <th>Model Area (ft²)</th> <th>Prototype Area (ft²)</th> <th>Prototype Area (m²)</th> </tr> <tr> <td>Photoshop</td> <td>186.7465966</td> <td>1.296851365</td> <td>810.5321033</td> <td>75.30086399</td> </tr> <tr> <td>LIDAR</td> <td></td> <td>0</td> <td>0</td> <td>0</td> </tr> <tr> <td></td> <td></td> <td>Percent Error*</td> <td>#DIV/0!</td> <td></td> </tr> <tr> <td></td> <td></td> <td colspan="2">*Reference value is LIDAR estimation</td> <td></td> </tr> </tbody> </table>	Model Scale 1:25					Photoshop Data	Width of Expansion (pixels)	Width of Expansion (in)	Conversion Factor (in ² /pixel ²)	Area (pixel ²)		1725	28.5	0.000272968	684134	Old Model Name 22 G#2 w_ FW Coarse Ramping A					Sediment Area	Model Area (in ²)	Model Area (ft ²)	Prototype Area (ft ²)	Prototype Area (m ²)	Photoshop	186.7465966	1.296851365	810.5321033	75.30086399	LIDAR		0	0	0			Percent Error*	#DIV/0!				*Reference value is LIDAR estimation		
Model Scale 1:25																																															
Photoshop Data	Width of Expansion (pixels)	Width of Expansion (in)	Conversion Factor (in ² /pixel ²)	Area (pixel ²)																																											
	1725	28.5	0.000272968	684134																																											
Old Model Name 22 G#2 w_ FW Coarse Ramping A																																															
Sediment Area	Model Area (in ²)	Model Area (ft ²)	Prototype Area (ft ²)	Prototype Area (m ²)																																											
Photoshop	186.7465966	1.296851365	810.5321033	75.30086399																																											
LIDAR		0	0	0																																											
		Percent Error*	#DIV/0!																																												
		*Reference value is LIDAR estimation																																													

Figure 31. Processes applied to images to obtain the 2-D mapping using Photoshop software

Three-dimensional Lidar surveys were initiated in the last stage of the IMM experiments with only few culvert designs for this group of tests included. All the NMU tests included the powerful Lidar survey tool. The step-by-step procedures resulting in the final graphical and numerical results are summarized in Figure 32.

#	Procedure	Details
A. Data acquisition (FARO 3D laser scanner)		
A.1	Prepare facility for scanning	Remove extra water from experimental flume, ensure proper lighting (no strong direct or reflected light)
A.2	Install Lidar & reference point	see Figure 21a
A.3	Execute scanning from various locations (each scan covered 360°)	Typically, 3-4 separate scanning positions are needed.
A.4	Retrieve data from probe's memory	
B. Data aggregation (using "SCENE" FARO-compliant software)		
B.1	Load data into SCENE	Software prompts for data transfer
B.2	Register reference points	Manual registration of the reference points
B.3	Project rendering in real coordinates	Locate coordinate system origin and axes orientation
B.4	Verify correct overlay of scans	
B.5	Create raw point cloud	Raw cloud point representation (see Figure 21b)
B.6	Define area of interest from the overall point cloud	Using clipping boxes, isolate the area of interest (i.e., the sedimented area in the culvert vicinity)
B.7	Create and export mesh	Export mesh in .stl format
C. Data Processing (using TecPlot visualization software package)		
C.1	Insert & triangulate baseline data	
C.2	Insert & triangulate sediment data	Append sediment data onto baseline data plot
C.3	Interpolate sediment data onto baseline	
C.4	Scale up correct vertical values	
C.5	Alter data to create a difference plot	
C.6	Value Blanking	Blank all areas that don't have sediment pixels
C.7	Integrate over the sedimented area using the difference plot.	<div style="display: flex; align-items: flex-start;"> <div style="flex: 1;"> <p>a)</p> <p>The final sediment accumulation volumes (plot c) are determined by subtracting the map of the clean "as-is" culvert geometry as determined by the scanner (plot a) from the volume of sand mapped in each individual test scan (plot b).</p> </div> <div style="flex: 2;"> <p>Figure 32 consists of three vertically stacked contour plots labeled a), b), and c). All plots share the same axes: the x-axis is 'Streamwise Distance (m)' ranging from 0 to 100, and the y-axis is 'Distance from Centerline (m)' ranging from -15 to 15. Plot a) is titled '"As is" Bare Bed (absolute values)' and shows a cross-section of a culvert with a central channel. The elevation is color-coded from 9.78 m (dark purple) to 9.84 m (yellow). Plot b) is titled '"As is" Sedimentation (absolute values)' and shows the same culvert cross-section but with a large area of sediment accumulation in the center, indicated by higher elevation colors (green and yellow). Plot c) is titled '"As is" Sedimentation (difference)' and shows the sediment layer thickness. The color scale for this plot ranges from 0 m (blue) to 0.9 m (red), with a legend titled 'Sediment Layer Thickness (m)'. The sediment is most concentrated in the center of the culvert, reaching a thickness of approximately 0.8-0.9 m.</p> </div> </div>

Figure 32. Sequence of procedures used to determine the volume distributions in the culvert vicinity using the Lidar surveys

Attaining the targeted sediment mapping results required a two-phase process: data acquisition and data processing. The Lidar data acquisition required to have the sediment accumulations resulting from the tests totally dry to avoid conducting the scanning with water ponding in the lower areas of the bedforms. Patches of water in the lower regions of the bedforms or saturated sand are not detectable from the Lidar scans, as they produce bright spots in the maps.

A validation test for evaluating the accuracy of the 2-D mapping with Photoshop was conducted using Lidar surveys of the results for the same culvert modifications, as illustrated in Figures 33a and 33b for the cross-section curtain wall, Reference 3 in in Figure 33c. The qualitative and quantitative comparison of the areal coverage of the sand accumulated at the entrance for the IMM culvert modified with various self-cleaning configurations revealed good agreement between the two mapping methods, as illustrated in Figure 33c. Based on these evaluations, it was concluded that the efficiency of the 2-D and 3-D mapping for assessing the performance of the self-cleaning designs are similar.

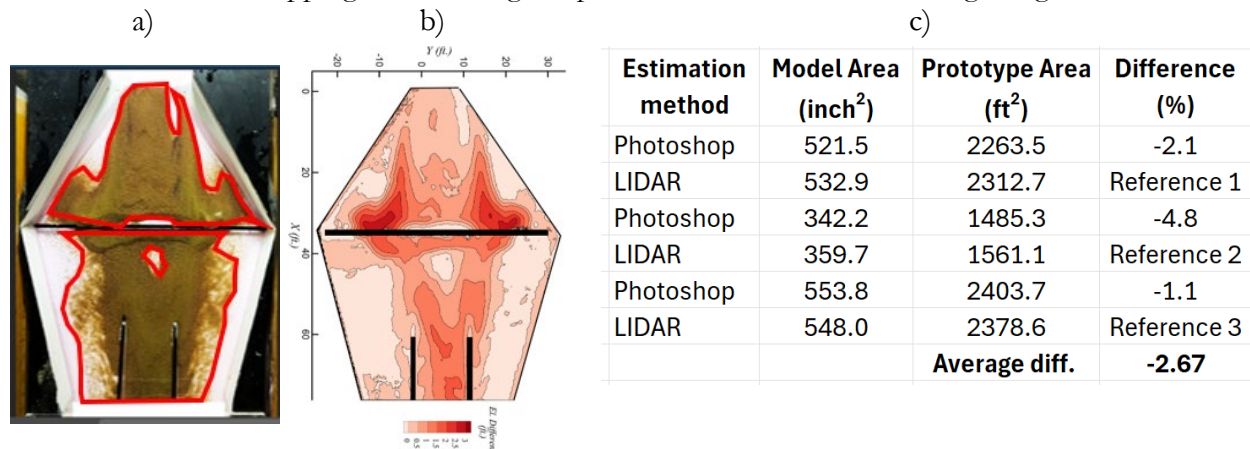


Figure 33. Comparison of the areal sediment accumulations obtained with analysis of images and Lidar survey: a) 2-D mapping with Photoshop; b) 2-D map obtained from Lidar survey; c) comparison of the results for 3 difference self-cleaning designs.

4.6. Experimental matrices targeted by the study

As mentioned in previous sections, the flume configurations (see Section 4.2) and phasing of the experiments (See Section 4.4) have continuously evolved during the project lifetime to accommodate the decisions of the TAC as the project progressed. These changes in turn led to a variety of tests not uniformly applied throughout the study. For example, there were self-cleaning configurations and types of sand and event hydrographs that were originally proposed for the investigation and later on cancelled as well as some few additions to the experimental program as was found necessary. The experimental matrices presented below sum up all types of culvert designs, event hydrographs, and sediment characteristics used in the study. Specifications for individual experimental tests are uniformly coded with acronyms that facilitate the discussion of the results, their intercomparisons, as well as tracking the progression of the study. Consequently, the matrices are presented first for the IMM flume configurations followed by NMU ones. Tables 8 – 11 provide the self-cleaning configurations, the modeled hydrographs, sediment characteristics, and the sensitivity tests conducted for the IMM flume setting. Tables 12 provides culvert configurations, event hydrographs, and the sensitivity tests for the NMU flume arrangements for the three tested stream-to-culvert angles: 0.3, 2 and 4 degrees. The experimental matrices specified in Tables 8 to 13 are related to Phases 2, 3 and 4 of the study described in Table 6 while the test execution does not follow the study chronology.

Table 8. Self-cleaning configurations for the IMM flume arrangement

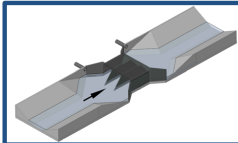
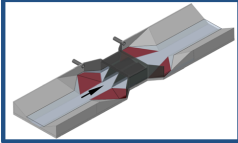
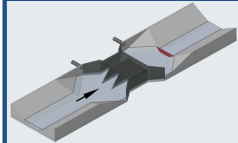
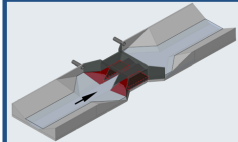
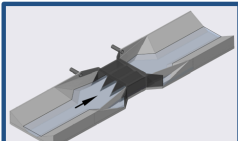
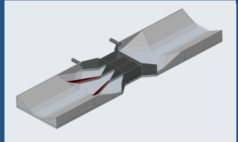
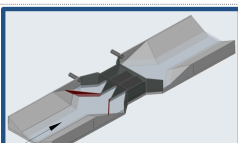
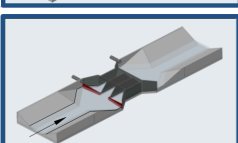
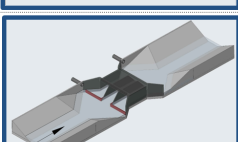
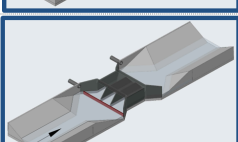
Iowa-Missouri-Mississippi (IMM) flume setting. Stream & culvert slope = 0.3 degrees		
Culvert configuration	Description	Tested
1 AIMM (As-is)	 Triple Reinforced Concrete Box (RCB) with 15° flared wingwalls (Iowa typical design)	Yes
2 FILS	 Fillets in the side areas of expansion/contraction	Yes
3 CWDX	 Downstream low-head weir	No
4 RIEB	 Higher invert elevations for side boxes	Yes
5 SWIN	 Straight wingwalls	Yes
6 CWLT	 Curtain wall long tapered (only side boxes)	Yes
7 CWMT	 Curtain wall medium tapered (only side boxes)	Yes
8 CWST	 Curtain wall short tapered (only side boxes)	Yes
9 CWSF	 Curtain wall short flat (only side boxes)	Yes
10 CWXF	 Curtain wall across flat	Yes

Table 9. Modeled hydrographs and sediment characteristics for the IMM flume arrangement

Storm	Description	Flow & sediment rates
1LS	One light & short storm*	50 gpm steady flow** & steady sediment rate
1LL	One light & long storm*	50 gpm steady flow & steady sediment rate
1HS	One heavy & short storm*	100 gpm steady flow & steady sediment rate
1HL	One heavy & long storm*	100 gpm steady flow & steady sediment rate
2LS	Succession of two light storms	2X 50 gpm steady flows & steady sediment rate
2HS	Succession of two heavy storms	2 X 100 gpm steady flows & steady sediment rate
1RE	Aggressive storm event (ramping)	50-100-50 gpm unsteady & unsteady sediment rate

* The distinction between light and heavy storm is based on flow discharge; the distinction between the short and long storm is based on the duration of the storm. These combinations of scenarios enable to account for various climatic and morphologic situation specific to various geographic areas at the TPF partnering states (i.e., perpetual vs. ephemeral).
** Base flows (~ 25 gpm) do not significantly mobilize the bedload. Flows > 25 gpm mobilize sediment.

Sand	Type	Sand diameter range
FS	Fine sand	0.3-0.85 mm (uniform)
CS	Coarse sand	0.2-2.0 mm (non-uniform)
NB	neutrally buoyant (crushed nut shells)	0.76 mm (uniform)

Table 10. Sensitivity tests for various storms, sand types and loads for the IMM flume arrangement

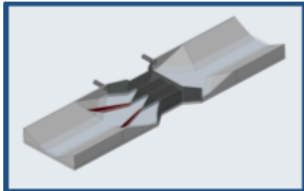
Self-cleaning design sensitivity tests		Culvert configuration description
CWLT		Long-tapered curtain wall (only side boxes)
Sand	Type	Sand diameter
CS	Coarse sand	0.2-2.0 mm (non-uniform)
NB	Neutrally buoyant	0.76 (uniform)
Test	Storm description	Flow & sediment rates
S1 (CWLT - NB)	One light and short storm	25 gpm steady flow & steady sediment rate
S2 (CWLT - NB)	One heavy and short storm	50 gpm steady flow & steady sediment rate
S3 (CWLT - NB)	Aggressive storm event (ramping)	25-100-25 gpm unsteady & unsteady sediment rate
S4 (CWLT - CS)	Upstream feeder & low feed rate	50 gpm steady flow & 1.5 sediment loads
S5 (CWLT - CS)	Upstream feeder & high feed rate	50 gpm steady flow & 2 sediment loads
S6 (CWLT - CS)	Downstream feeder & low feed rate	50 gpm steady flow & 3 sediment loads
S7 (CWLT - CS)	Downstream feeder & high feed rate	50 gpm steady flow & 5 sediment loads
S8 (CWLT - CS)	Downstream feeder & high feed rate	100 gpm steady flow & 2.5 sediment loads
S9 (CWLT - CS)	Downstream feeder & high feed rate	100 gpm steady flow & 5 sediment loads

Table 11. Sensitivity tests with fine sediment in the IMM flume arrangement

Sediment type sensitivity tests			
Sand	Type	Diameter range	Gradation
FS	Fine sand	0.3-0.85 mm	uniform
Code	Tested	Code	Tested
S10 (AIMM-1LS)	Yes	S41 (CWLT-1HL)	Yes
S11 (AIMM-1LL)	Yes	S42 (CWLT-2LS)	Yes
S12 (AIMM-1HS)	Yes	S43 (CWLT - 2 HS)	Yes
S13 (AIMM-1HL)	No	S44 (CWLT - 1 RE)	Yes
S14 (AIMM-2LS)	Yes	S45 (CWMT - 1 LS)	Yes
S15 (AIMM-2HS)	Yes	S46 (CWMT - 1LL)	Yes
S16 (AIMM-1RE)	Yes	S47 (CWMT - 1HS)	No
S17 (FILS - 1LS)	No	S48 (CWMT - 1HL)	No
S18 (FILS - 1LL)	No	S49 (CWMT - 2 LS)	Yes
S19 (FILS - 1HS)	No	S50 (VWMT - 2 HS)	No
S20 (FILS - 1 HL)	No	S51 (VWMT - 1 RE)	No
S21 (FILS - 2 LS)	No	S52 (CWST - 1 LS)	Yes
S22 (FILS - 2 HS)	No	S53 (CWST - 1LL)	Yes
S23 (FILS - 1RE)	No	S54 (CWST - 1HS)	Yes
S24 (RIEB - 1LS)	Yes	S55 (CWST - 1HL)	Yes
S25 (RIEB - 1LL)	Yes	S56 (CWST - 2LS)	Yes
S26 (RIEB - 1 HS)	Yes	S57 (CWST - 2HS)	Yes
S27 (RIEB - 1HL)	Yes	S58 (CWST - 1RE)	Yes
S28 (RIEB - 2LS)	Yes	S59 (CWSF-1LS)	No
S29 (RIEB - 2HS)	Yes	S60 (CWSF - 1LL)	No
S30 (RIEB - 1RE)	Yes	S61 (CWSF - 1 HS)	No
S31 (SWIN - 1LS)	Yes	S62 (CWSF - 1HL)	No
S32 (SWING - 1LL)	Yes	S63 (CWSF - 2LS)	No
S33 (SWIN - 1 HS)	Yes	S64 (CWAFF - 2HS)	No
S34 (SWIN - 1 HL)	No	S65 (CWSF - 1RE)	No
S35 (SWIN - 2LS)	Yes	S66 (CWXF - 1LS)	No
S36 (SWIN - 2 HS)	Yes	S67 (CWXF - 1LL)	No
S37 (SWIN - 1 RE)	Yes	S68 (CWXF - 1 HS)	No
S38 (CWLT - 1 LS)	Yes	S69 (CWXF - 2LS)	No
S39 (CWLT - 1 LL)	Yes	S70 (CWXF - 2 HS)	No
S40 (CWLT - 1 HS)	Yes	S71 (CWXF - 1 RE)	No

Table 12. Experimental matrices for the 0.3, 2 and 4 degrees NMU flume arrangement

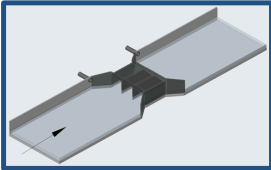
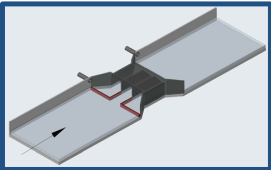
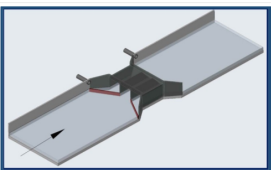
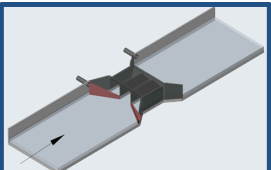
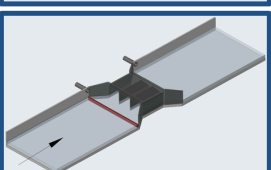
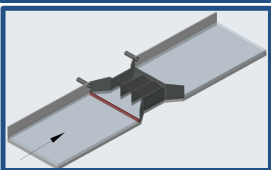
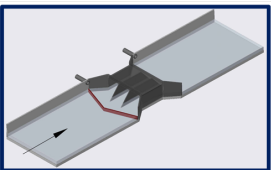
New Mexico - Utah (NMU) flume setting. Stream-to-culvert slope = 0.3 degrees				
Culvert configuration		Description	Tested	
1	ANMU (As-is)		Triple Reinforced Concrete Box (RCB) with 15° flared wingwalls	Yes
2	CWSF		Curtain wall short square flat (only side boxes)	Yes
3	CWAF		Curtain wall short angled flat (only side boxes)	Yes
4	CWAT		Curtain wall short angled tapered (only side boxes)	Yes
5	CWXF		Curtain wall across flat	Yes
6	CWXF(F)		Curtain wall across flat & filled river bed upstream	Yes
7	CWXV		Curtain wall across flat V-shaped	No
Storm	Description	Flow & sediment rates		
1LL	One light & long storm *	100 gpm steady flow & steady sediment rate, Hyper-concentrated flows		
1RE	Aggressive storm event (ramping)	50-200-50 gpm unsteady & unsteady sediment rate, hyper-concentrated flows		
2RE	2 Aggressive storm events (ramping)	50-200-50 gpm unsteady repeated 1 time with 2 minute gap & unsteady sediment rate, hyper-concentrated flows		
3RE	3 Aggressive storm events (ramping)	50-200-50 gpm unsteady repeated 2 times with 2 minute gaps & unsteady sediment rate, hyper-concentrated flows		
* Base flows (~ 50 gpm) do not significantly mobilize the bedload. Flows > 100 gpm mobilize sediment.				
Sand	Type	Sand diameter		
CS	Coarse sand	0.2-2.0 mm (non-uniform)		

Table 12 (continued). Experimental matrices for the 0.3, 2 and 4 degrees NMU flume arrangement

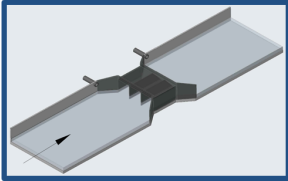
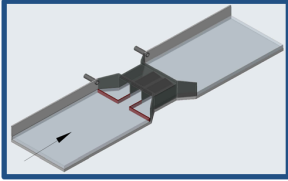
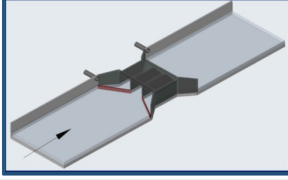
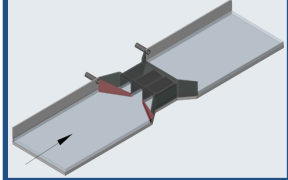
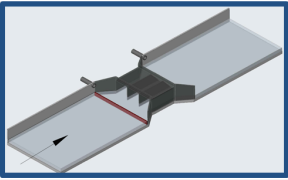
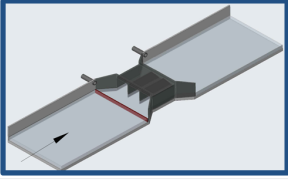
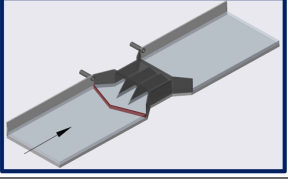
New Mexico - Utah (NMU) flume setting. Stream-to-culvert slope = 2 degrees		
Culvert configuration	Description	Tested
1 ANMU (As-is)	 Triple Reinforced Concrete Box (RCB) with 15° flared wingwalls	Yes
2 CWSF	 Curtain wall short square flat (only side boxes)	No
3 CWF	 Curtain wall short angled flat (only side boxes)	Yes
4 CWAT	 Curtain wall short angled tapered (only side boxes)	Yes
5 CWXF	 Curtain wall across flat	Yes
6 CWXF(F)	 Curtain wall across flat & filled river bed upstream	Yes
7 CWXV	 Curtain wall across flat V-shaped	No
Storm	Description	Flow & sediment rates
1RE	Aggressive storm event (ramping)	50-200-50 gpm unsteady & unsteady sediment rate, hyper-concentrated flows
2RE	2 Aggressive storm events (ramping)	50-200-50 gpm unsteady repeated 1 time with 2 minute gap & unsteady sediment rate, hyper-concentrated flows
* Base flows (~ 50 gpm) do not significantly mobilize the bedload. Flows > 100 gpm mobilize sediment.		
Sand	Type	Sand diameter
CS	Coarse sand	0.2-2.0 mm (non-uniform)

Table 12 (continued). Experimental matrices for the 0.3, 2 and 4 degrees NMU flume arrangement

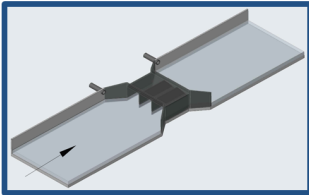
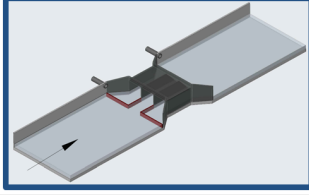
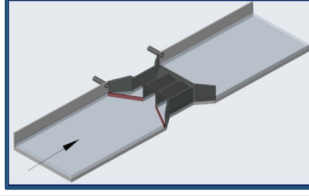
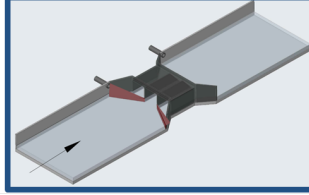
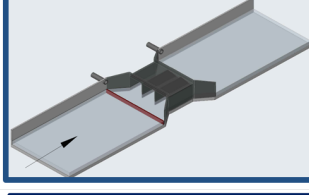
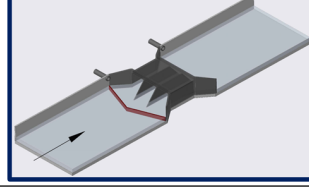
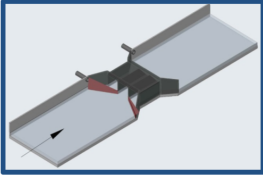
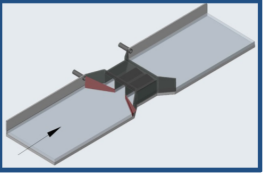
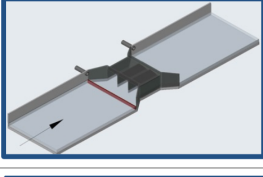
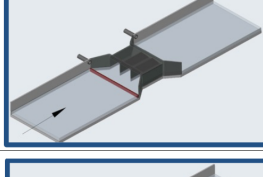
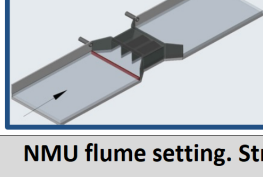
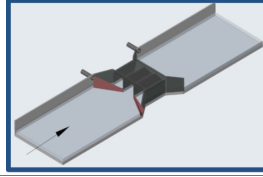
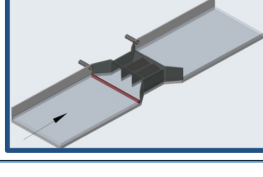
New Mexico - Utah (NMU) flume setting. Stream-to-culvert slope = 4 degrees		
Culvert configuration	Description	Tested
1 ANMU (As-is)	 Triple Reinforced Concrete Box (RCB) with 15° flared wingwalls	Yes
2 CWSF	 Curtain wall short square flat (only side boxes)	No
3 CWF	 Curtain wall short angled flat (only side boxes)	Yes
4 CWAT	 Curtain wall short angled tapered (only side boxes)	Yes
5 CWXF	 Curtain wall across flat	Yes
6 CWXV	 Curtain wall across flat V-shaped	No
Storm	Description	Flow & sediment rates
1RE	Aggressive storm event (ramping)	50-200-50 gpm unsteady & unsteady sediment rate, hyper-concentrated flows
* Base flows (~ 50 gpm) do not significantly mobilize the bedload. Flows > 100 gpm mobilize sediment.		
Sand	Type	Sand diameter
CS	Coarse sand	0.2-2.0 mm (non-uniform)

Table 13. Sensitivity tests for various culvert configurations, event hydrographs, and stream-to-culvert slope for the NMU flume arrangement

Self-cleaning design sensitivity tests		
Sand	Type	Sand diameter
CS	Coarse sand	0.2-2.0 mm (non-uniform)
Test	Culvert configuration	Storm description
NMU flume setting. Stream-to-culvert slope = 0.3 degrees		
S72 (CWAT-2RE)		2 Aggressive storm events (ramping)
S73 (CWAT - 3 RE)		3 Aggressive storm events (ramping)
S74 [CWXF(F) - 1RE]		Aggressive storm event (ramping)
S75 [CWXF(f) - 2RE]		2 Aggressive storm events (ramping)
S76 [CWXF(F) - 3RE]		3 Aggressive storm events (ramping)
NMU flume setting. Stream-to-culvert slope = 2 degrees		
S77 (CWAT - 2 RE)		2 Aggressive storm events (ramping)
S78 (CWAT - 3 RE)		3 Aggressive storm events (ramping)

5. EXPERIMENTAL RESULTS FOR PRODUCTION TESTS

5.1 Overview

The experimental study for this project entailed 180 stand-alone experimental tests conducted in two flume layouts, i.e., Iowa-Mississippi-Missouri (IMM) and New Mexico-Utah (NMU). The tests include 8 and 6 self-cleaning culvert (SCC) designs for the IMM and NMU flume layouts, respectively (see Tables 8 and 12). The list of the tests categorized by their purpose is provided in Table 14. The experimental program followed the phasing discussed in Section 4.4 while the results of the tests in Table 14 are presented following roughly an inverse progression as the tests were first conducted for the IMM flume layout followed by NMU one.

The screening tests referred to in Table 14 entails the so-called “production” experiments that are central to this report. This group of tests contains experiments that contributed to the establishment of the hydrologic scenarios replicating aggressive runoff events (see Tables 9 for IMM and 12 for NMU) associated with the most severe increase of the sediment deposits. The assessment of the storm severity on sedimentation is informed by direct field information for the IMM culverts (with cases observed through field trips in Iowa) and by inspecting video-documentation for the NMU area. Unfortunately, neither area benefits from quantification of the impact of single or multiple storms on sediment deposition as such studies are rarely available. Instead, intercomparison of the sedimentation amount and pattern distributions for various hydrologic scenarios simulated in the hydraulic model were used to determine the most impactful storm events.

The SCC sensitivity tests (corresponding to Phase 4 of the study – see Table 6) are grouped in the second category listed in Table 14. These tests explored the response of the sedimentation patterns to changes in the characteristics of the hydrological events (atypical conditions) for one of the IMM self-cleaning design (see Table 10). The number of sensitivity tests for atypical conditions modelled in the NMU flume layout (see Table 13) was smaller per the decisions of the project TAC (see Section 4.1). The model sensitivity tests were conducted only for the IMM flume layout to observe the behavior of the sedimentation patterns when a finer sediment was used in the tests (see Table 9). The debugging (corresponding to Phase I of the study) and unsuccessful tests are not included in the present report. Unsuccessful tests were subsequently repeated to complete the experimental program as planned.

Table 14. Summary of the experimental tests conducted through the study

Test type	Flume layout		Experimental program phase (see table 6)
	IMM	NMU	
SCC Screening (“production” tests)	62	18	Phase 3
SCC sensitivity	9	7	Phase 4
Model sensitivity (baseline tests)	40	-	Phase 2
Debugging	31	13	Phase 1
Unsuccessful	8	8	
	Total tests	196	

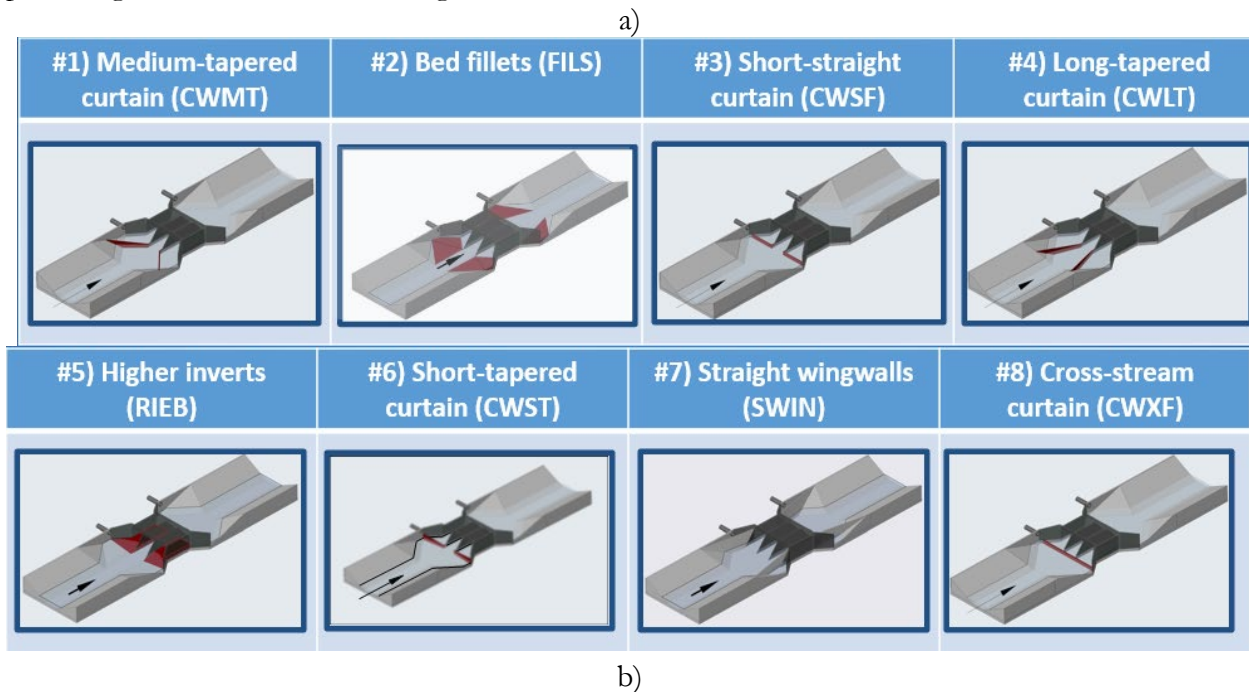
The discussions in this chapter are focused on the production tests for the two flume layouts. The sensitivity tests are discussed in the next chapter. The large number of cases and the wealth of measurements and visual information acquired during the production tests preclude a thorough analysis of all aspects of the test results (i.e., quantification of the changes of flow hydrodynamics and sediment transport processes) for each culvert configuration. While there are various ways to present the study results, we chose a top-down presentation approach that presents first the ranking of the SCC which represents the most important practical results of the study. Subsequently, we present the

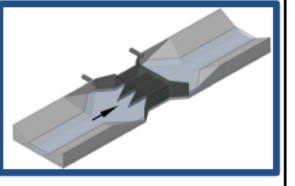
results of the 80 screening tests conducted with coarse sand across all SCC configurations for IMM and NMU layouts. Given that the SCC designs for the IMM flume layout benefitted from additional funding they are analyzed with a higher level of detail. The result discussion is structured as follows:

- ranking of the SCC in terms of reducing the amount of sediment at the culvert entrance
- illustration of the performance of the optimum SCC for the most detrimental storm events
- illustration of the SCC performance grouped by SCC designs.

5.2 Results of the IMM production tests

The ranking of the SCC designs for the IMM flume layouts illustrated in Figure 34a is based on the production tests listed in table contained in Figure 34b. The “Sediment retention reduction (%)” column of the table defines the amount of sediment passed by individual SSC compared to the original (“As-is”) culvert (lacking any mitigation measure). It is deemed that the higher the retention reduction percentage, the better the SSC design.



SCC configuration		Sediment conveyance (%)		Ranking	Reference (AIMM)
Code	Short description	1 light-long storm*	1 aggressive storm**		
AIMM	"As-is"	n/a	n/a	Reference	
CWMT	Medium-tapered curtain	57	72	1	
FILS	Bed fillets	48	67	2	
CWSF	Short-straight curtain	49	59	3	
CWLT	Long-tapered curtain	49	55	4	
RIEB	Higher inverts	34	36	5	
CWST	Short-tapered curtain	27	31	6	
SWIN	Straigh wingwalls	23	21	7	
CWXF	Cross-stream curtain	6	2	8	

* based on Areas #1, 2, 3, and 4
** based on Areas #1 & 2

Figure 34. Ranking of the SCC for the IMM flume layout: a) SCC configurations; b) SCC ranking based on the results of two severe runoff events (see also Figure 35)

The ranking is the result of testing all the SCC designs developed for the IMM flume layouts for two severe sediment transport events: **1 light-long storm (1LL)** and **1 aggressive (1RE) storm** is provided in Table 9. The overall ranking reflected by column 5 of the table is based on the comparison of the areal distribution of the sediment accumulated in Areas #1, #2, #3, and #4 of the culvert vicinity (see Figure 35) for the above-mentioned hydrological events. The areal distribution is determined with Photoshop software (2D quantitative evaluation) as the Lidar scanning (3D quantitative evaluation) was not available for the IMM flume. Separate quantification of the sediment deposition in each identified areas in Figure 35 was accomplished through supplementary funding contributed to the study by the Mississippi DOT is reported in the next chapter. The ranking of the IMM SCCs reported in Figure 34 are based on the Photoshop analysis conducted separately for Areas #1, 2, 3 and 4 of the culvert vicinity. The quantitative areal estimation of the sediment distribution per areas of culvert vicinity provides a much stronger piece of information for decision making regarding the sediment cleanup efforts for various implemented SCCs.

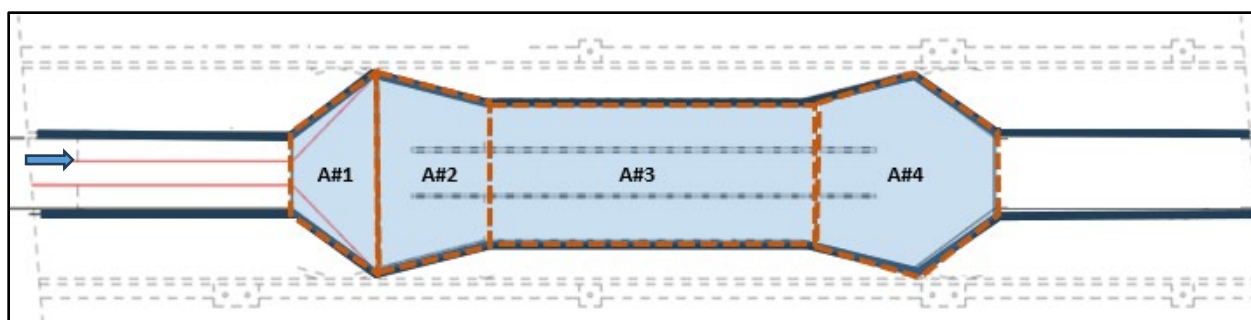


Figure 35. Delineation of the areas for the analysis of sedimentation in the vicinity of the culvert body for the IMM flume layout

While the sub-rankings of the SCC efficiency listed in columns 3 and 4 in the table (see Figure 34b) are relatively consistent for the two hydrological events, it is noted that the light & longer (1LL) steady flow storm is more detrimental for SCC efficiency than the aggressive storm (1RE). This realization is indicated by the consistently lower sediment retention percentage for the 1LL compared to 1RE storm (excepting the SWIN and CWXF configurations). This differentiation is associated with the fact that high flows occurring on the rising limb of the storm hydrograph (see Figure 24) moves downstream a larger amount of sediment in the initial phases of the storm. Given that the aggressive storms are more likely to occur than light & long steady flow storms in natural conditions, in this chapter we will only consider the aggressive storm (1RE) as common denominator for analysis of the SCC efficiency for both IMM and NMU flume layouts.

Another readily observable feature of the ranking is that the least efficient SCC is the cross-stream culvert design (CWXF) which is a shear reflection that the principles of self-cleaning culvert design for this design depart mostly from the considerations presented in Section 1.4 of the study. It also can be noted that the SCCs ranked 1-4 offer a sediment accumulation reduction of about 50% or larger while the SCCs ranked 5-9 offer a reduction less than 50%. This realization is important for practical implementation. Moreover, the SCCs “bed fillets” and “short-straight curtain” ranked in the first efficiency group are also easier to implement based on the comments of TAC members. A final note can be made on the fact that, excepting CWXF SCC, all the other designs allow unobstructed flow through the central barrel, a feature that is making them friendly for the aquatic habitat.

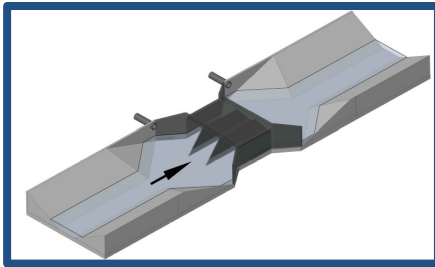
Considering a broader perspective with respect to the performance of individual SCCs for both IMM and NMU flume layouts, there are several approaches in tackling the discussion of the production test results. Given that for the present study the overall goal is to reduce sedimentation at

the culvert entrance (the area that triggers a detrimental operation of the culvert in long term), the tracking of the sedimentation process during its development under different scenarios is considered herein of secondary importance. Consequently, the experimental facility was equipped with the minimum of necessary measurements to control the overall water and sediment movement in the flume rather than acquiring continuous measurements of the flow variables during the tests for determining spatial distributions of the velocities and depths in the areas of interest. With this perspective in mind, the original design of the experimental program emphasized the acquisition of photo-evidence that can be readily inspected visually to lead to the ranking of the proposed SCCs with only parsimonious analyses. The photo-evidence inspection (a qualitative estimation of the sedimentation) is complemented with quantitative means to estimate the spatial distribution of the sedimentation. For the IMM SCC the quantitative analysis was executed with Photoshop software (see Section 4.5 and Figure 31 for details). For NMU SCC the quantitative analysis of the sedimentation deposition was executed with Lidar surveys (see Section 4.5. and Figure 32 for details).

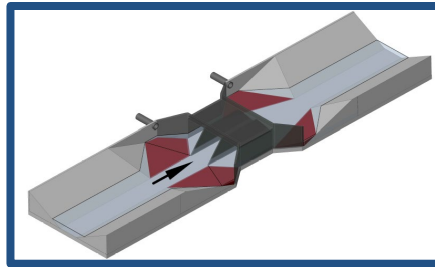
The visualization of the experiments for the IMM and NMU flume layouts was attained by a comprehensive program that entailed: a) acquisition of time-lapsed videos that capture the culvert vicinity in one image frame, and, b) acquisition of still photos from three distinct locations along the culvert length. The images garnered from these two sources serve as the primary information to determine the impact of various SCC on the inception and mitigation of sedimentation at culverts as an overall process. Before delving in more discussions on the sediment transport feature under the action of the SCC, it is found appropriate to illustrate the evolution of the actual experiments. As described in Section of the report (Section 4.2 and Figure 20), each of the conducted tests were recorded from the beginning to the end to illustrate the initiation and progression of sedimentation process. Using the recorded time-lapsed videos, we extracted images taken at $\frac{1}{4}$, $\frac{1}{2}$, and at the end of the experiment for the first 3 ranked SCCs exposed to one aggressive storm (1RE). Figure 36 displays snapshots extracted from these tests. The snapshots are powerful illustrations of the progression of sedimentation for each SCC and enable comparison of the sedimentation process across SCCs. Collectively, the results of the quantitative analysis indicate critical area of action early in the process development (i.e., the side area of the culvert expansion) and areas that are of secondary importance for mitigation (i.e., the body of the culvert).

The time-lapse videos also strengthen the confidence that the analysis of the photo-evidence made at the end of the tests is a reliable procedure for assessing the performance of individual SCCs overall. In order to illustrate this statement, samples of still photos acquired at the end of the experiment for one flow scenarios acting on two IMM SCCS are shown in Figure 37. The inspection of the photos in this figure indicates that while the sediment in the culvert body is similar for the “as-is” culvert design and the CWMT SCC design, the amount of sediment passed downstream in the expansion area at the culvert entrance is obviously larger for CWMT SCC than for the as-designed culvert structure. Based on the above argumentation, from this point on of our discussion most of the illustrations and discussions are focused on the photo-evidence acquired at the culvert entrance where the SCCs have to act efficiently all along the storm propagation duration.

#1: Medium, tapered curtain, aggressive storm (CWMT-1RE)



#2: Bed fillets, aggressive storm (FILS - 1RE)



#3: Short-straight curtain, aggressive storm (CWSF - 1RE)

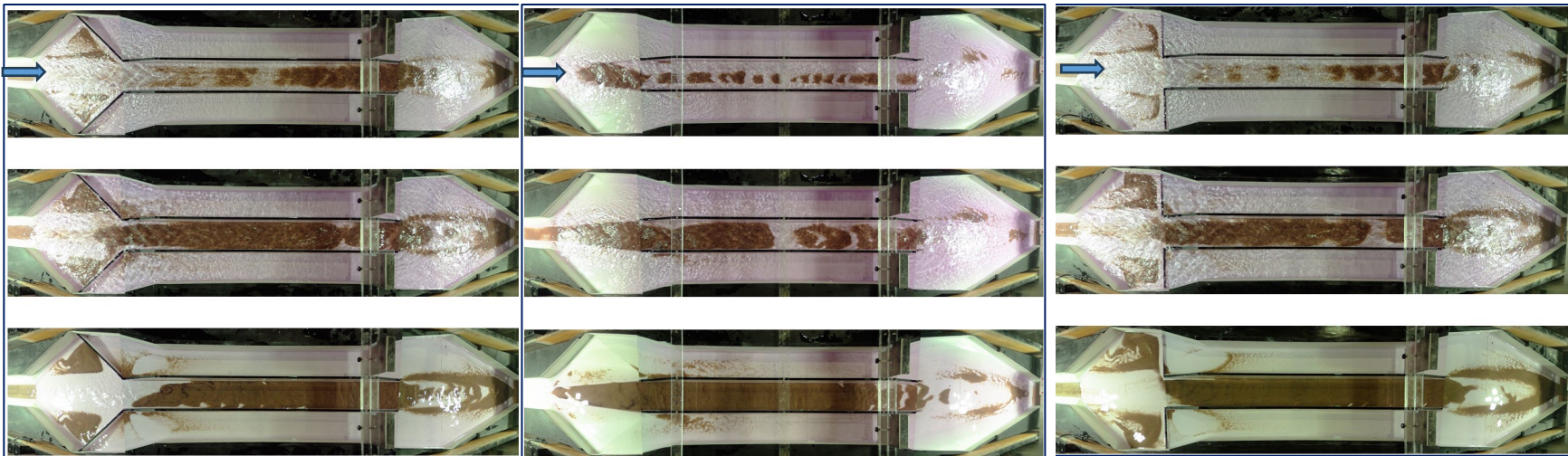
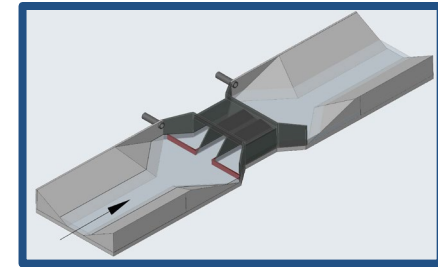


Figure 36. Snapshots of the first 3 ranked SCC tested for the IMM flume layout acquired during the tests at $\frac{1}{4}$ (the first row), $\frac{1}{2}$ (the second row), and at the end of the experimental runs (the third row) using time-lapsed movies captured with the webcam. Note: while all the illustrated SCCs retain sand in the culvert body, the least amount of sedimentation at culvert entrance is produced by CWMT SCC.

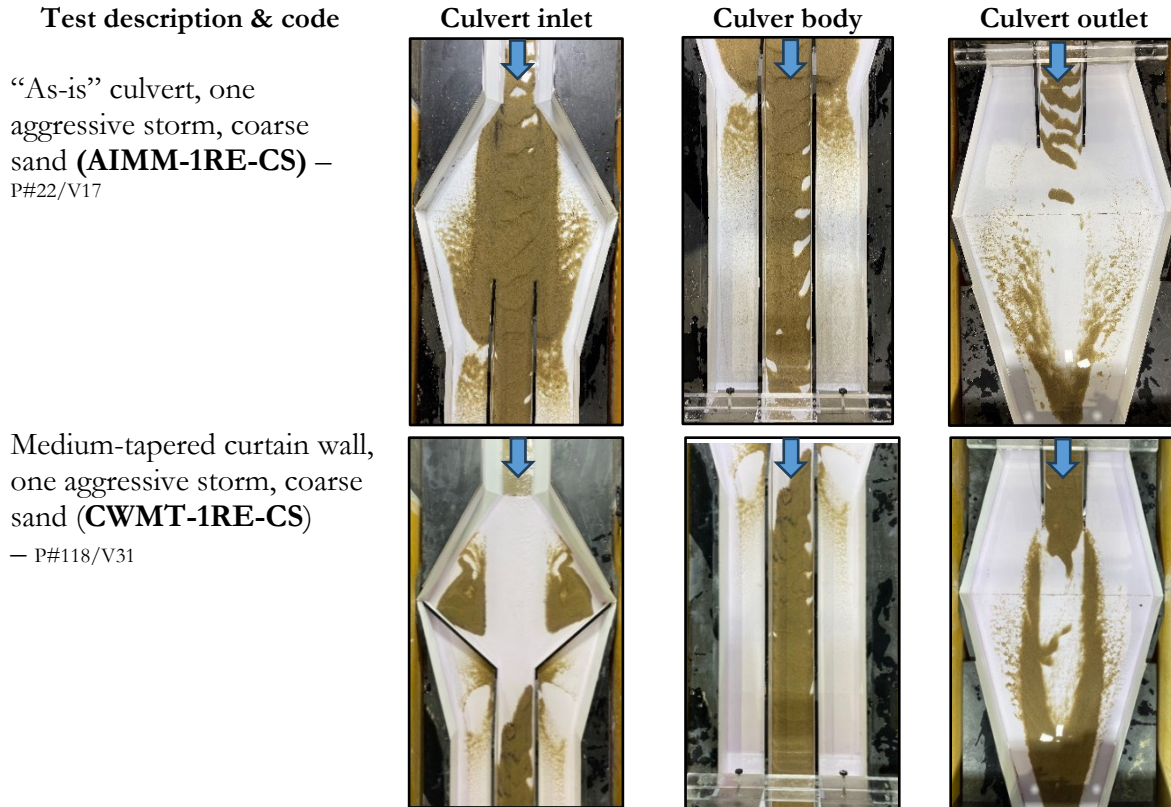


Figure 37. Sample still photos for two IMM CSSs subjected to an aggressive storm (1RE)

The next discussion item is focused on the performance of all IMM SCCs based on the photo-evidence of the sediment deposition at the flume entrance resulting at the end of the individual tests. This type of qualitative analysis was the core of the discussion during the TAC meetings and, basically the most powerful argument for selecting optimum CSS configurations for both flume layouts. Presented in Figure 38 is photo-evidence for the most unfavorable flows tested for IMM SCC ranking (see Figure 34b). Figure 38a displays the results of all IMM SCCs for one light & long storm (1LL), while Figure 38b displays the results for all IMM SCCs for one aggressive storm (1RE). The “as-is” culvert configuration is included for grounding the comparison. Typical comments made on the photo-evidence in Figure 38 are provided below to illustrate the type of inferences observed and subsequently used in SCC ranking by the TAC technical experts:

- with the flow rate increase (i.e., 1RE peaks at 150 gpm compared with the 1LL steady flow of 50 gpm) more sediment is moved downstream, less sediment is captured at the entrance, more sediment is protruding in the central barrel and washed downstream the culvert.
- the sediment conveyance through the central culvert barrel is due to the strong jet effect created by the stream-to-culvert expansion.
- the aggressive storm (1RE) and the light-long storms (1LL) are resulting in a similar footprint sediment deposition overall with the former developing higher deposit depths.
- the tapered curtain walls are the most efficient un reducing (medium-length and short-length configurations, CWMT and CWST, respectively) or totally eliminating the sedimentation in the side boxes (long tapered curtain – CWLT). The tapered curtain walls are not easy to implement.
- the straight-wingwall culverts are practically performing similarly to the oblique wingwall ones

This type of analysis can be applied to any pair or group of SCCs as illustrated in Section 6.3.1. Figure 39 provides all the production tests conducted for the SCCs tested in the IMM flume layout.

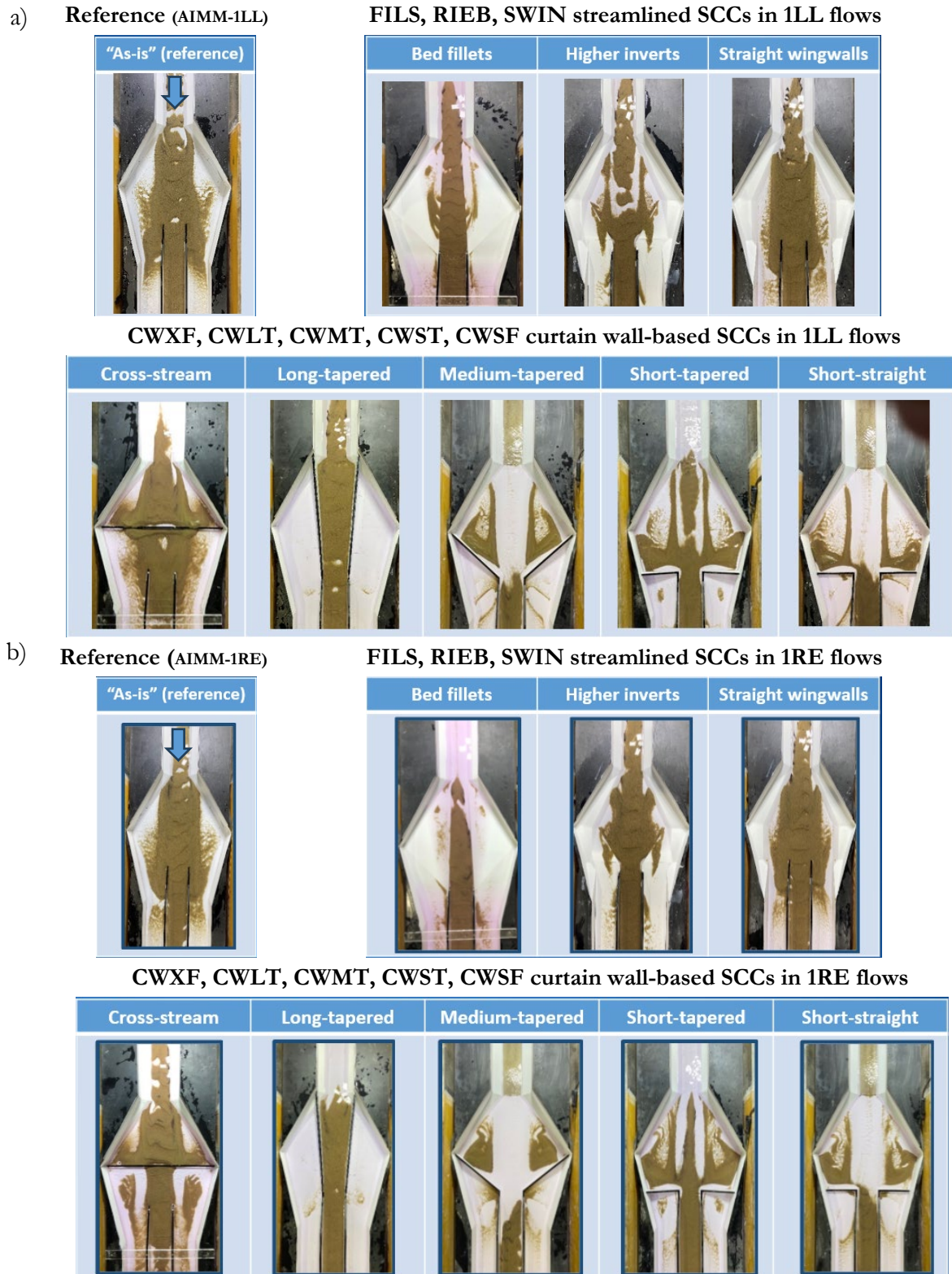


Figure 38. IMM SCCs tested with: a) one light & long storm flow (1LL), and b) one aggressive storm scenario (1RE)

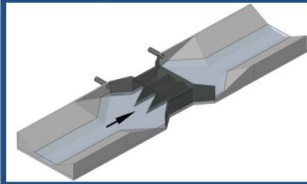

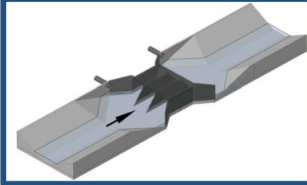

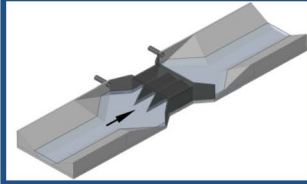

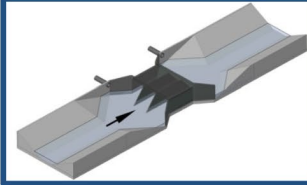

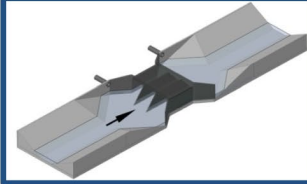

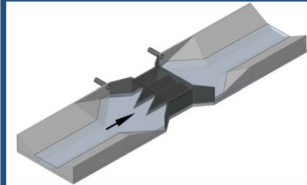

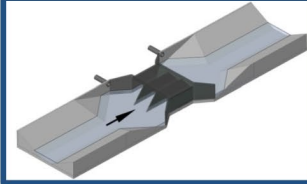

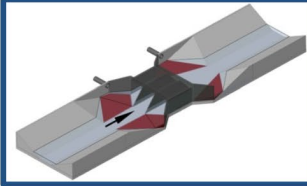
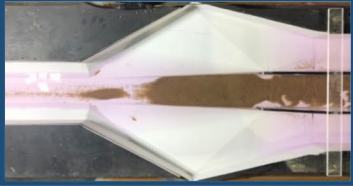
Test Code	Configuration Sketch	Sedimentation entrance area
AIMM-1LS		
AIMM-1LL		
AIMM-1HS		
AIMM-1HL		
AIMM-2LS		
AIMM-2HS		
AIMM-1RE		
FILS-1LS		

Figure 39. Synoptic view of all IMM SCC production tests

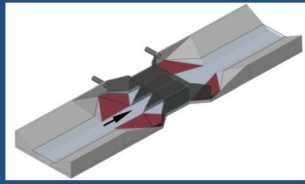

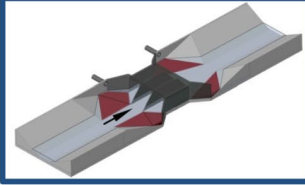
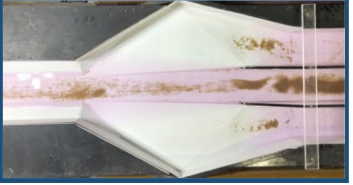
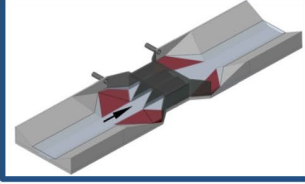
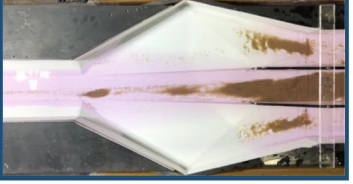
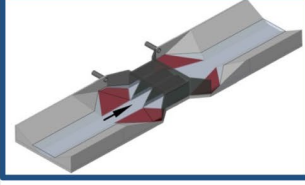

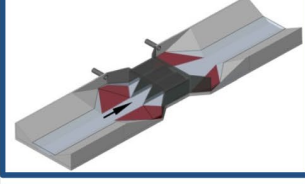
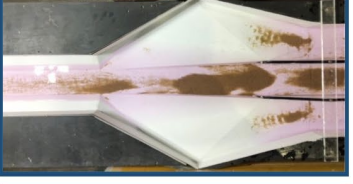
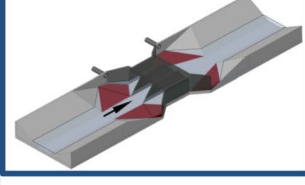

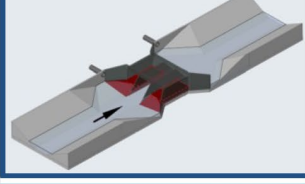

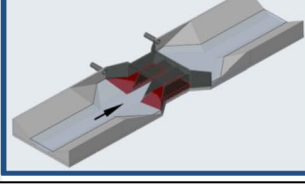

Test Code	Configuration Sketch	Sedimentation entrance area
FILS-1LL		
FILS-1HS		
FILS-1HL		
FILS-2LS		
FILS-2HS		
FILS-1RE		
RIEB-1LS		
RIEB-1LL		

Figure 39 (continued). Synoptic view of all IMM SCC production tests

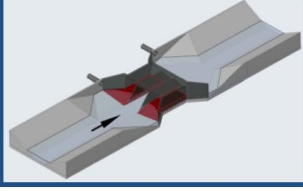

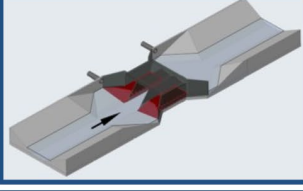

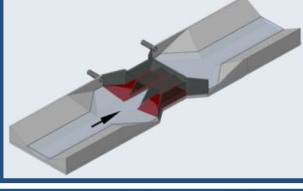

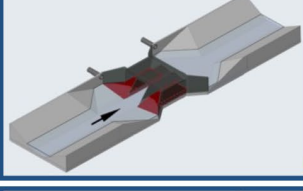
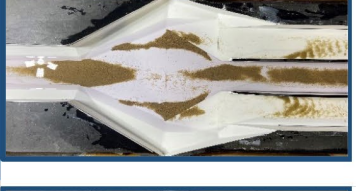
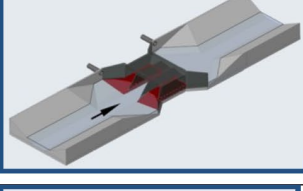
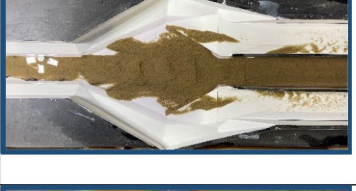
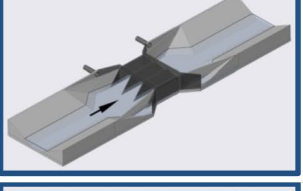
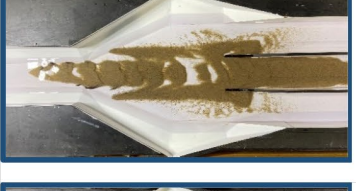
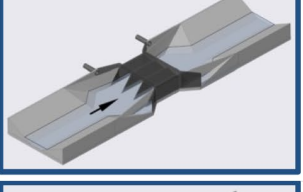
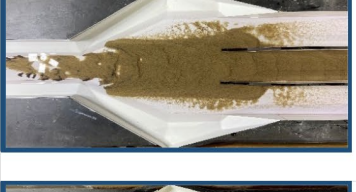
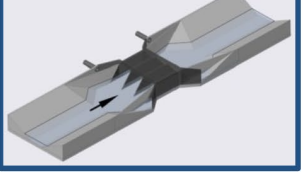

Test Code	Configuration Sketch	Sedimentation entrance area
RIEB-1HS		
RIEB-1HL		
RIEB-2LS		
RIEB-2HS		
RIEB-1RE		
SWIN-1LS		
SWIN-1LL		
SWIN-1HS		

Figure 39 (continued). Synoptic view of all IMM SCC production tests

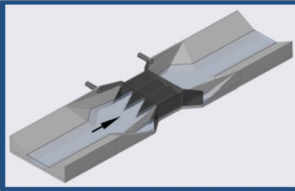

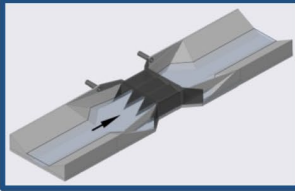

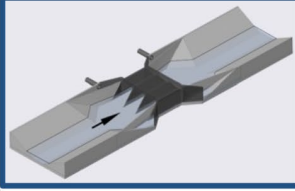

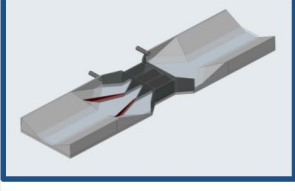

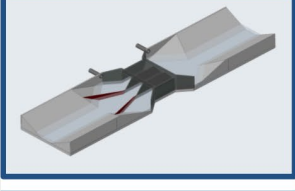

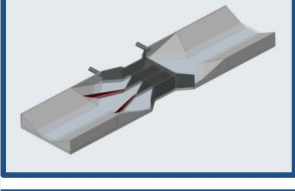

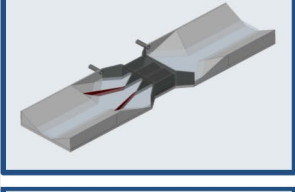

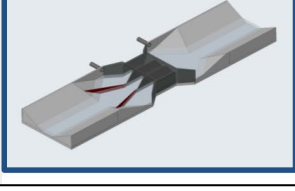

Test Code	Configuration Sketch	Sedimentation entrance area
SWIN-2LS		
SWIN-2HS		
SWIN-1RE		
CWLT-1LS		
CWLT-1LL		
CWLT-1HS		
CWLT-1HL		
CWLT-2LS		

Figure 39 (continued). Synoptic view of all IMM SCC production tests

Test Code	Configuration Sketch	Sedimentation entrance area
CWLT-2HS		
CWLT-1RE		
CWMT-1LS		
CWMT-1LL		
CWMT-1HS		
CWMT-1HL		
CWMT-2LS		
CWMT-2HS		

Figure 39 (continued). Synoptic view of all IMM SCC production tests

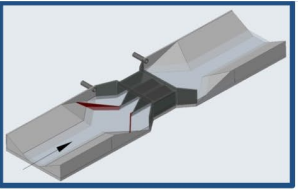

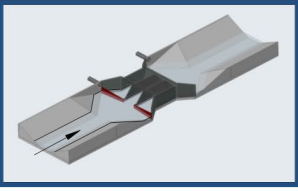

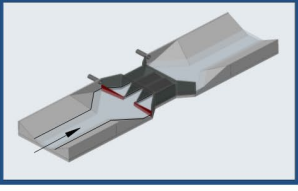

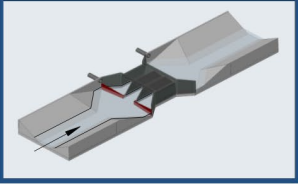
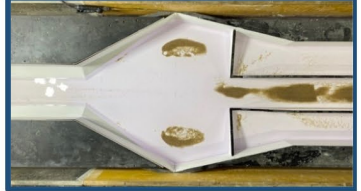
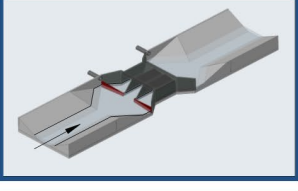
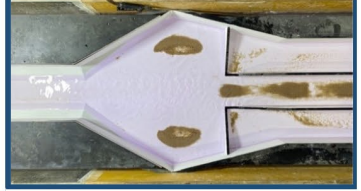
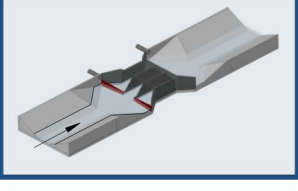

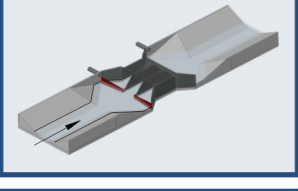

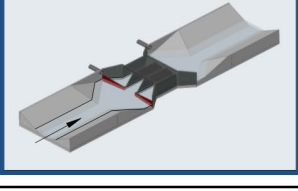
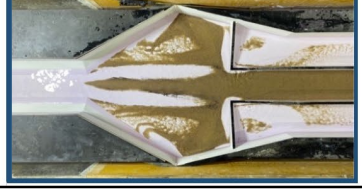
Test Code	Configuration Sketch	Sedimentation entrance area
CWMT-1RE		
CWST-1LS		
CWST-1LL		
CWST-1HS		
CWST-1HL		
CWST-2LS		
CWST-2HS		
CWST-1RE		

Figure 39 (continued). Synoptic view of all IMM SCC production tests

Test Code	Configuration Sketch	Sedimentation entrance area
CWSF-1LS		
CWSF-1LL		
CWSF-1HS		
CWSF-1HL		
CWSF-2LS		
CWSF-2HS		
CWSF-1RE		
CWXF-1LS		

Figure 39 (continued). Synoptic view of all IMM SCC production tests

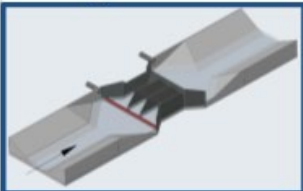
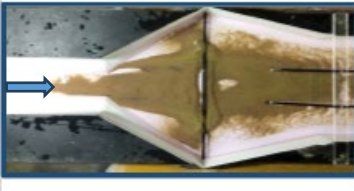
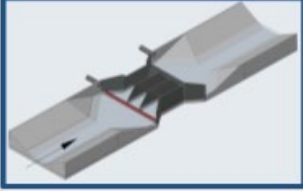
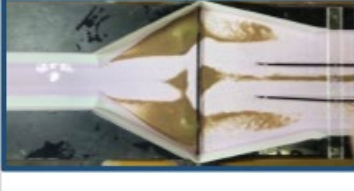

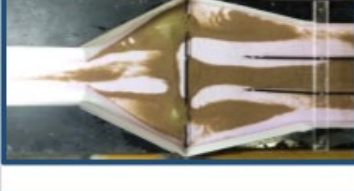




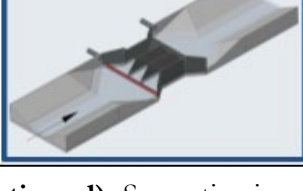

Test Code	Configuration Sketch	Sedimentation entrance area
CWXF-1LL		
CWXF-1HS		
CWXF-1HL		
CWXF-2LS		
CWXF-2HS		
CWXF-1RE		

Figure 39 (continued). Synoptic view of all IMM SCC production tests

The series of images included in Figure 39 provide a wealth of information about the production tests conducted for the IMM flume layout. The resources available for the project do not give room for individual or cross-SCC analysis such as the discussion presented above for the snapshots in Figure 38. At the level of general observations, some considerations are worth mentioning:

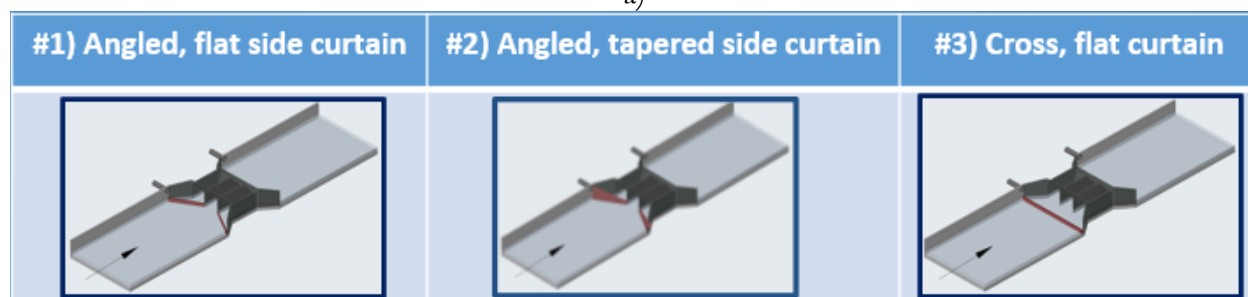
- the photo-evidence for each individual test contains distinct features that can qualitatively analyzed to infer flow and sediment transport characteristics,
- the symmetry of the sediment distribution patterns confirms the quality and stability of the flow during the tests. Relatedly, it should be noted that the large number of repeated tests listed in Table 14 is the result of rejecting experiments that have not providing symmetric flow patterns.
- the tests could be confidently repeated using the strict protocols for experiment execution.

5.3 Results of the NMU production tests

The number of the production tests for NMU is about 1/3 compared to the IMM flume layout counterpart. The ranking of the NMU SCCs is based on the production tests for all three stream-to-culvert angles and one aggressive storm (see 1RE in Table 12). The presentation of the production tests for the NMU flume follows closely the structure of Section 5.2 narration. Presented first is the ranking of the SCC designs for the NMU flume resulting from the production tests (see Figure 40). The overall ranking of the NMU SCCs classifies individual structures based on their capacity to convey sediment through the culvert structure (the same criterion used for ranking the IMM SCCs). The best performing NMU SCCs based on this study are listed in Figure 40a (in descending order): angled – flat curtain (CWF), angled, tapered curtain (CWAT), and the cross-sectional curtain (CWXF).

The overall ranking for the IMM SCCs combines the self-cleaning structure capability to extract sediment from the culvert entrance (Area #1 in Figure 41) and move the sediment through the whole structure (Areas #1 and #2 in Figure 41). The first performance indicator is based on the volume of sediment removed from the deposit created at the culvert entrance compared to the total volume of sand added in the model (column 3 of the table in Figure 40b). The volumes are obtained from 3-D Lidar surveys. The second indicator is the percentage amount of weight of sediment washout by the culvert compared to the total weight of the sand released in the model (column 4 of the table in Figure 41b). The protocol for capturing and assessing the amount of washout is described in Section 4.2.

a)



b)

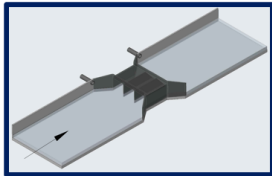
SCC configuration		Sediment conveyance (%) - 1 RE*		Ranking	Sediment retention (%)	
Code	Short description	Lidar scanning **	Sediment washout**			
Channel and culvert slope = 0.3 degrees (0 degree difference)						
ANMU		n/a	n/a	Reference	 <p>* 1RE = 1 aggressive storm ** based on Areas #1 and #2</p>	
CWXF	Cross flat curtain	0	0.07	3		
CWAF	Angled, flat side curtain	10	0.20	1		
CWAT	Angled, tapered side curtain	5	0.11	2		
Channel-to-culvert slope difference = 2 degrees						
ANMU		n/a	n/a	Reference		
CWXF	Cross flat curtain	13	0.16	3		
CWAF	Angled, flat side curtain	17	0.44	2		
CWAT	Angled, tapered side curtain	24	0.70	1		
Channel-to-culvert slope difference = 4 degrees						
ANMU		n/a	n/a	Reference		
CWXF	Cross flat curtain	12	0.80	3		
CWAF	Angled, flat side curtain	22	2.10	1		
CWAT	Angled, tapered side curtain	20	1.20	2		

Figure 40. Ranking of the SCC for the NMU flume layout: a) SCC configurations; b) SCC ranking based on the production test results for one aggressive runoff event (see also Figure 35) conducted in all stream-to-culvert angle settings.

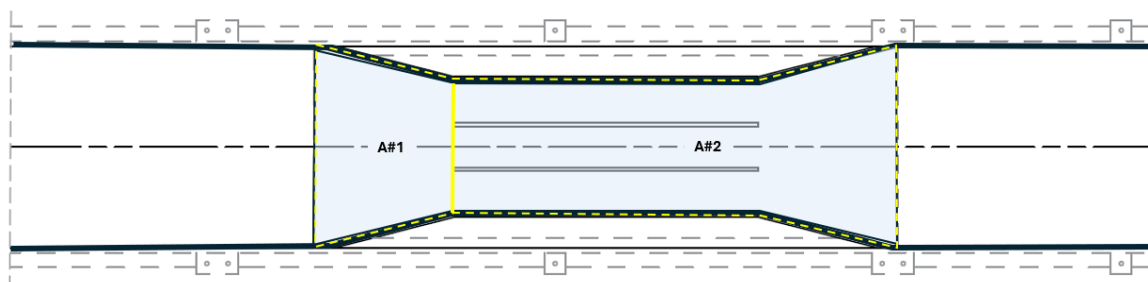


Figure 41. Delineation of the analysis areas for evaluating sedimentation for the NMU flume layout

The ranking was applied to the CWXF, CWAF, and CWAT designs for all the stream-to-culvert angles for one flow scenario, i.e., one aggressive storm event (1RE) using uniformly applied protocols. The overall ranking provided in column 5 of the table indicate that the cross-section curtain with flat edges (CWXF) is the least performant self-cleaning design out of all SCCs tested for the NMU conditions. The overall ranking classifies the angled flat curtain wall (CWAF) as the optimum option as it is ranked such for two of the 3 stream-to-culvert angles. angled tapered curtain wall (CWAT) for the three channel-to-culvert angles, the quantitative result, i.e., 0.3 degrees and 4 degrees. The observed that values for sediment conveyance reported in columns 3 and 4 are in close agreement in terms of trends, confirming that both measurement types are reliable for the scope of the study.

The numerical values listed in column 3 of Figure 40b indicate a relatively small range for the sediment conveyance through the culvert entrance (i.e., between 0% and 24%). This situation does not favor a differentiation of the performance of the sedimentation mitigation solutions with the same assurance as accomplished for the IMM SCCs. This is a direct reflection of the lower capability of the NMU SCCs to cope with the large amount of sediment incoming to the culvert.

The poorer conveyance performance of the NMU SCCs can be better understood if we analyze the production tests with more details. This subsequently attempted by illustrating the sedimentation progression in individual tests and across the flow and sitting conditions tested in the study. Figure 42 contains snapshots from the recorded time-lapsed videos extracted at $\frac{1}{4}$, $\frac{1}{2}$, and at the end of the experiments used for the NMU SCCs exposed to one aggressive storm (1RE). The visualized tests pertain to the NMU arrangement with 2 degrees stream-to-culvert angle that is in the middle of the range over which this angle was varied (i.e., from 0.3 to 4 degrees). The snapshots at the end of the experiments illustrated in Figure 42 (the third row of the snapshots) unequivocally indicate that all the NMU SCCs retain a large volume of the sand released in the model at the entrance of the culvert (i.e., Area #1). Larger volumes of sediment retained in the culvert body are observed for the CWXF and CWAF culvert configurations. Smaller volumes of sediment in the side boxes can be noticed for the CWAF and CWAT SCCs as both configurations entail unobstructed central barrel opening.

The overall feature of sand retention cannot be solely attributed to the installation of the SCCs. Instead, it is a shear reflection of the fact that the amount of sediment approaching the NMU culverts exceeds the sediment transport capacity of the as-designed culverts. This situation is partly explained by the shape of the NMU culvert configuration that is akin to a “funnel” that attempts to pass a large amount of material through the narrower area created by the oblique wingwalls positioned at the culvert entrance. The funnel-like shape at the culvert inlet produces accumulation of sediment not only for the 2 degrees stream-to-culvert sitting (as seen for the ANM-1RE sequence on the left of Figure 42), but it is a common feature of the NMU “as-is” culverts for all the stream-to-culvert angles tested in the present study as will be seen in abundant illustrations presented below. Illustrations in Figure 42 show that while all the SCCs retain the sand at the entrance and within the culvert body, there is much less sand accumulated in the side boxes for the CWAF and CWAT SCCs.

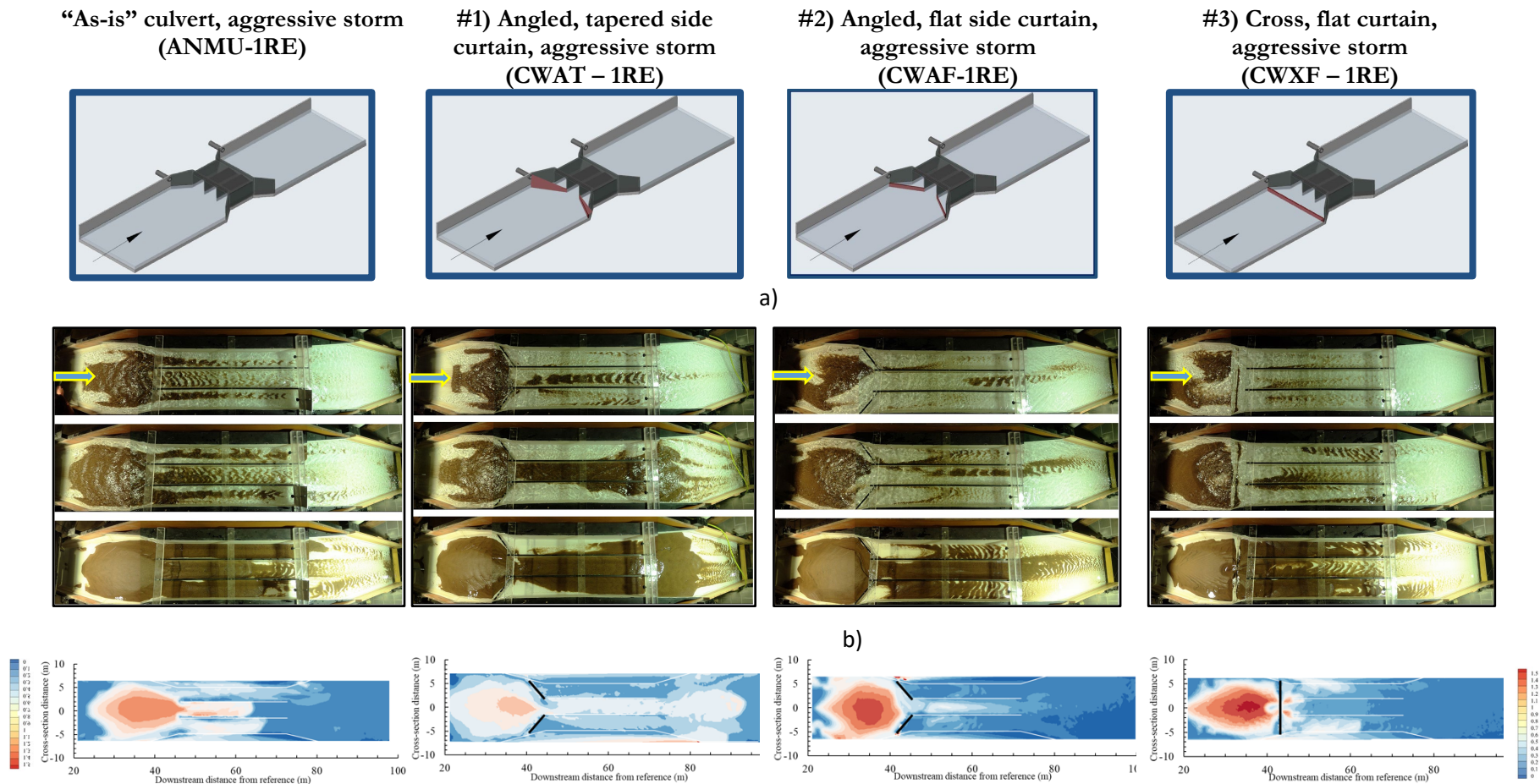
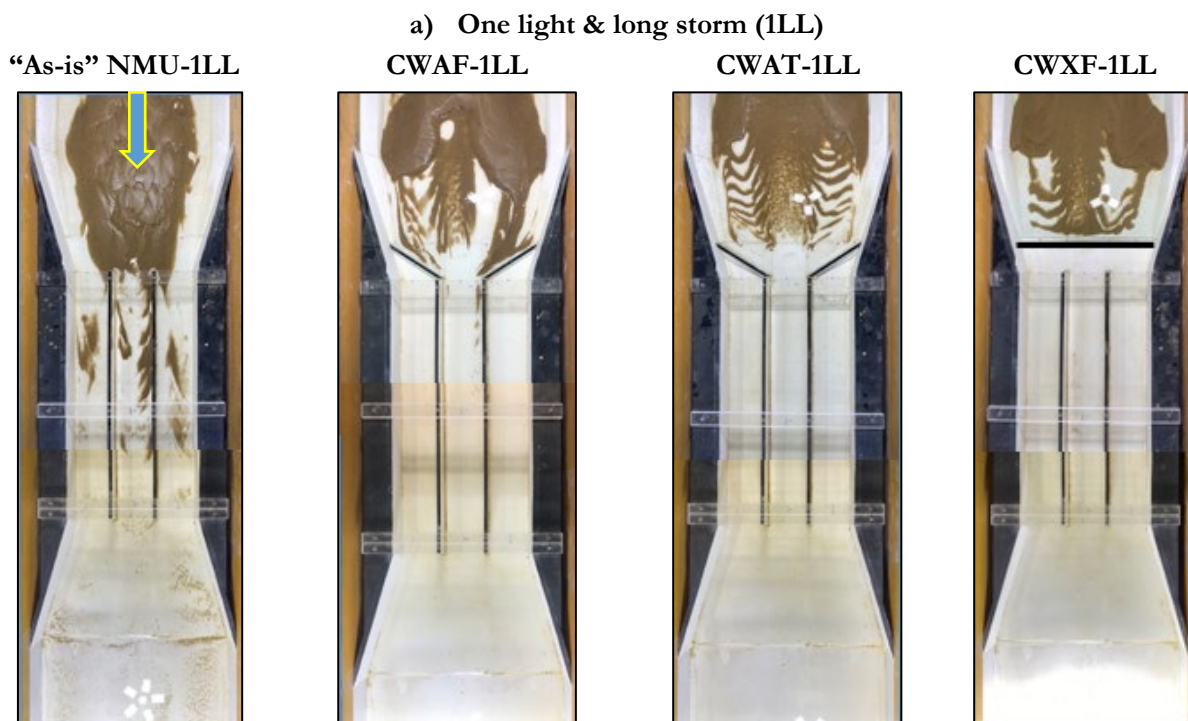


Figure 42. Production test results for the ranked NMU SCC sedimentation pattern distribution (extracted from the group of tests with a stream-to-culvert angle of 2 degrees (the second block of production tests in the table of Figure 40b): a) snapshots of the sedimentation footprints acquired during the tests at $\frac{1}{4}$ (first row), $\frac{1}{2}$ (the second row), and at the end of the experimental runs (the third row) using time-lapsed movies captured with the webcam; b) Lidar maps of the sediment deposits in the vicinity of the culvert structures for the production tests in Figure 42a.

Additional illustrations of the production tests for SCC designs are provided in Figure 43 for the NMU culvert with the stream and culvert aligned at 0.3 degree slope exposed to two types of storms: one light & long storm (1LL) and one aggressive storm (1RE) described in Table 12. The illustrations are made with still photos taken from two locations above the model culvert. A companion illustration is offered in Figure 44 where the quantitative estimation of the sediment volumes visualized were used to quantify the volumes of sediment accumulated in the vicinity of the culvert in Figure 43 is provided by 3-dimensional maps obtained from Lidar surveys. The Lidar maps for one aggressive storm were used for establishing the SCCs conveyance performance (see column 4 of the table in Figure 40b).

While the Lidar survey covered the entire flume length, we chose to focus our maps on the culvert entrance, culvert body, and downstream the culvert areas. For this purpose, the Lidar survey maps presented from this point on are visualized using the same reference line located about 20 m (prototype dimensions) upstream from the culvert structure. Moreover, the vertical elevation scale used for representing the sediment deposits was kept the same for all SCCs tested in the 0.3 degree stream and culvert angle, 2 degrees and 4 degrees stream-to-culvert angle flume arrangement. The vertical scale is also graduated in prototype dimensions. The reason for this selection choice is to be able to compare the sediment distribution patterns in the same xyz coordinate system. Selection of a scale for production tests grouped based on the stream-to-culvert angle would have better substantiated the differences in the topography of various SCCs for the same angle but would have less relevance when comparing the sediment distributions across the three stream-to-culvert angles.

The sedimentation distribution patterns illustrated in Figure 43 confirm that the NMU SCCs set on a slope of 0.3 degrees (the same slope as for IMM flume) retain most of the sediment carried by the storm at the culvert entrance for both the light and long storm (see Figure 43a) as well as for one aggressive storm (see Figure 43b). Overall, it can be stated that all SCCs practically eliminate deposition in the culvert boxes for one storm occurrence. The impact of repeated storms is illustrated in Section 6.2.2. The sedimentation patterns in Figure 43b for one aggressive storm illustrate the similarity of sediment deposit patterns for the CWF and CWAT ranked first across all stream-to-culvert angles.



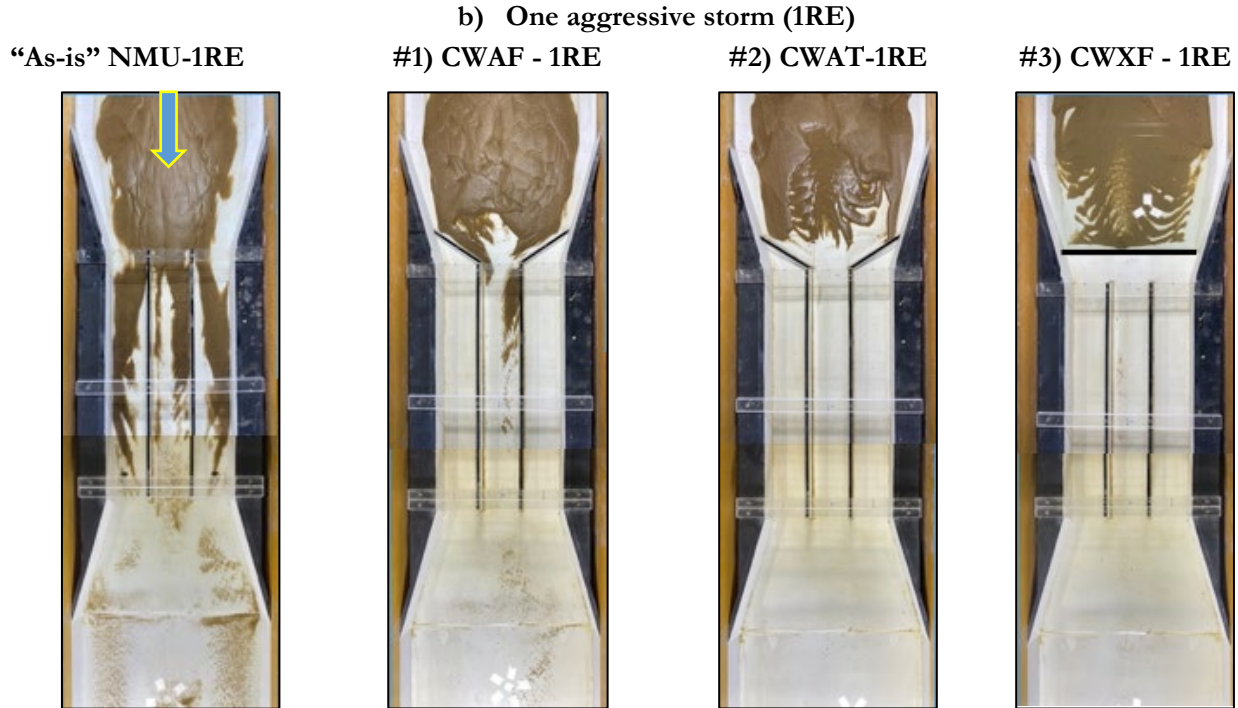


Figure 43. Ranking of NMU SCCs for two types of storms: a) one light & long storm, and b) one aggressive storm. Bed slopes for the stream and culvert are same (0.3 degrees).

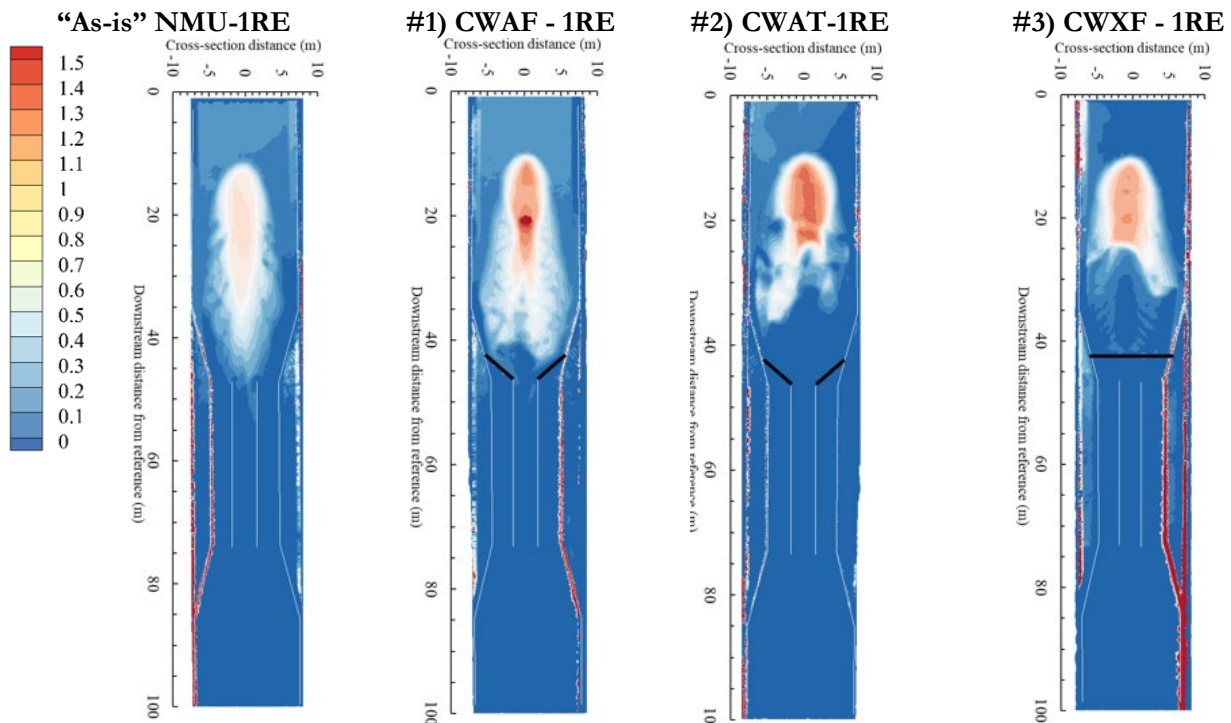


Figure 44. Lidar survey maps for the stream and culvert slopes set at a 0.3 degree (i.e., no difference between the stream and culvert bed slope)

The last group of still photos and the Lidar survey maps is presented in Figure 45 for the NMU SCCs set at 4 degree stream-to-culvert angle exposed to one aggressive storm (see Figure 26, Section 4.4). The notable feature of these illustrations is the considerable larger amount of sand accumulated

throughout the culvert area compared to the 0.3 degree slope and the 2 degree stream-to-culvert angle production tests presented above. This situation is direct results of the largest water and sediment transport rates of this sub-group compared with the flatter stream-to-culvert flumes.

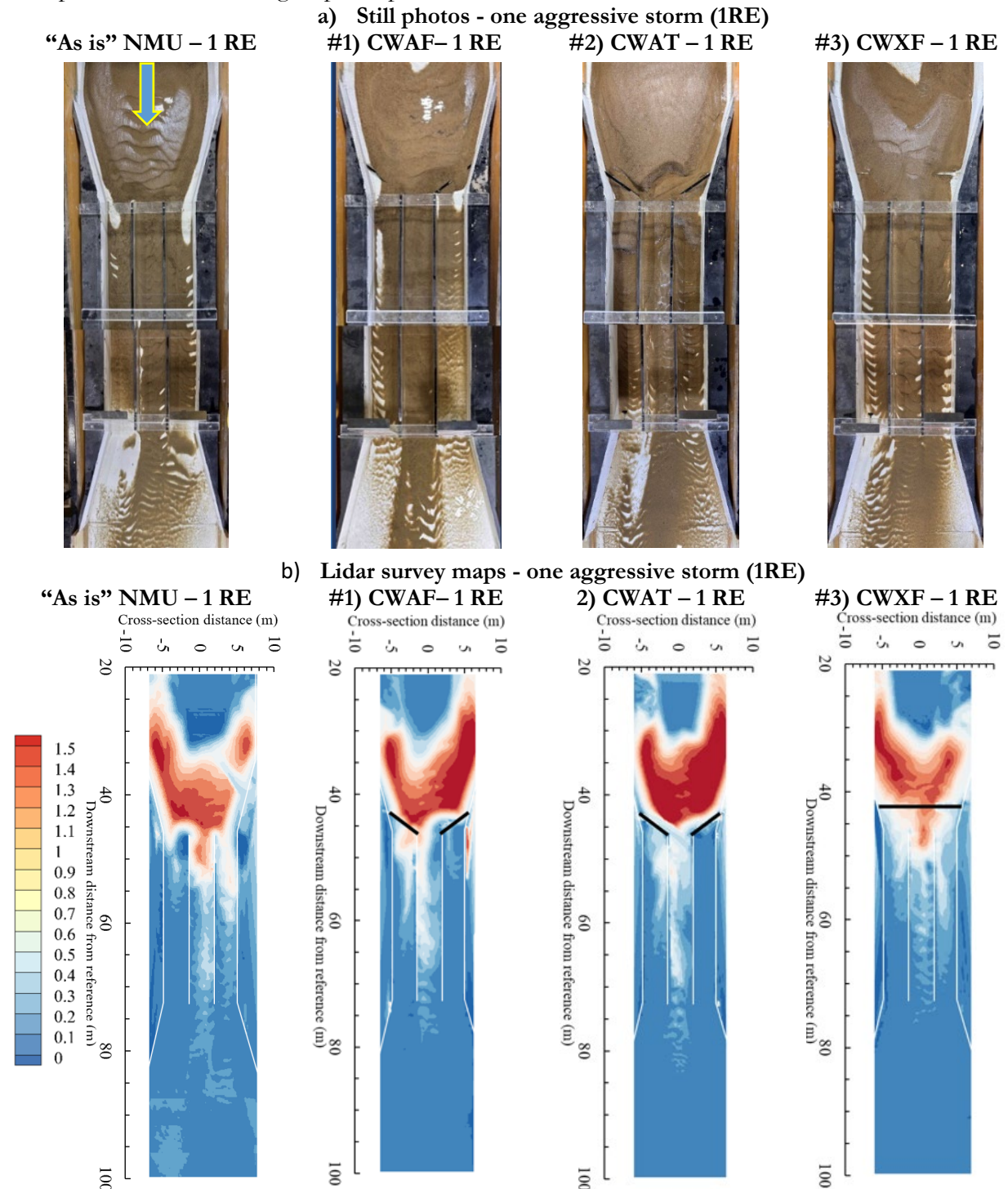


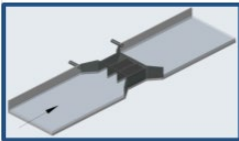

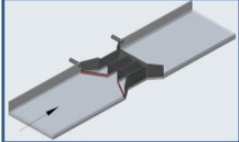

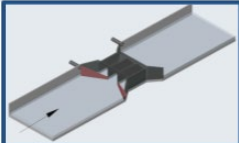


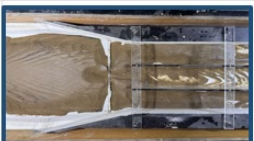
Figure 45. Ranking of NMU SCCs for one aggressive storm in the 4-degree stream-to-culvert angle

Finally, an alternative synoptic view of all the production tests conducted for the NMU flume are presented in Figures 46 and 47 (see Table 12 for the description of the acronyms).

Test Code	Configuration Sketch	Sedimentation entrance area
ANMU-1LL		
ANMU-1RE		
CWSF-1LL		
CWSF-1RE		
CWAF-1LL		
CWAF-1RE		
CWAT-1LL		
CWAT-1RE		
CWXF-1LL		
CWXF-1RE		

Figure 46. Synoptic view of all NMU SCC production tests in the 0.3 degree slope layout

a) 2 degree stream-to-culvert angle

Test Code	Configuration Sketch	Sedimentation entrance area
ANMU-1RE		
CWAF-1RE		
CWAT-1RE		
CWXF-1RE		

b) 4 degree stream-to-culvert angle

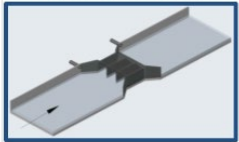

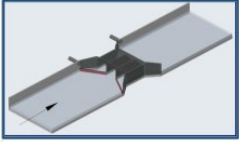

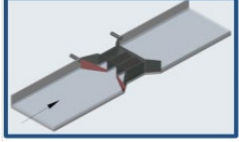
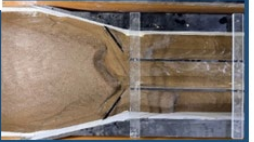
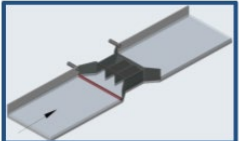
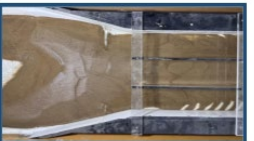
Test Code	Configuration Sketch	Sedimentation entrance area
ANMU-1RE		
CWAF-1RE		
CWAT-1RE		
CWXF-1RE		

Figure 47. Synoptic view of the NMU SCC production tests in the: a) 2 degree stream-to-culvert flume layout, and b) 4 degree stream-to-culvert flume layout

Similarly to the IMM production tests, the series of results presented in this section for the NMU flume layout provide a wealth of information about the flow and sediment behavior for various culvert geometry and hydrodynamic conditions. The symmetry of the sediment distribution patterns confirms the quality and stability of the flow during the tests. The reported photo-evidence contains multiple features that can be used to infer more details on the flow and sediment transport characteristics.

6. SENSITIVITY AND SYNTHESIS ANALYSES

6.1 Overview

This section complements the illustrations and ancillary discussions presented in Chapter 5 by diving deeper into aspects of the study beyond the experimental evidence highlighted by the production test results. The presentation encompasses both the IMM and NMU Self-Cleaning-Culverts (SSC) concepts by illustrating the results of the sensitivity studies conducted through the experimental study and documenting hydro-morphological features of the test results that underpin the difference between the influence induced by the installation of various SCCs on the flow and sediment transport at culverts exposed to sedimentation. Similarly to Chapter 5, the experimental evidence is rich in data and information which offers possibilities to analyze multiple analyses on various sedimentation processes aspects on a case-by-case basis (e.g., areal and 3-D extend of the sand deposits, response of the sedimentation process in the culvert vicinity to the changes in the flow field driven by SCC geometry).

Given the practice-focused nature of the study, the large number of SCC tests for the IMM and NMU flume arrangements, and the extent of the project resources for the experimental program the synthesis analyses discuss a sub-section of the study outcomes that are strictly relevant to the project goals. Consequently, the results of the preliminary tests (grouped under the “Debugging tests” in Table 14) are not presented in the report, despite that some of them (e.g., the dye injection tests) offer insights into flow mechanics that can trigger additional inferences on the flow dynamics changes. The coverage and the detail for the illustrations and analysis for the IMM and NMU components of the study are also different as the resources available for the IMM flume arrangement were larger than those for the NMU counterpart. The data acquired for the study (made available upon request) enable to extract more information and inferences about the complex flow process of water and sediment transport at culvert, especially that this area of water engineering is still understudied.

6.2 Sensitivity tests

6.2.1 IMM flume layout

The first set of sensitivity tests presented in this section aims to demonstrate the similarity of the sedimentation patterns for different types of transport, i.e., suspended load vs bedload. In natural rivers the two types of sediment transport are closely connected. The accurate hydraulic modeling of these two sediment transport types is however challenging, if even possible, using natural sand as transported matter. It is hypothesized that the bedload is the main form of transport responsible for the creation of the sediment accumulation at culverts. Given that the goal of this study is identifying the deposition matter of sediment from both transport types, we conducted preliminary tests with neutrally buoyant particles in the form of crushed walnut shells (NB) and the coarse natural sand (CS) used for the execution of the production tests for comparing their depositional patterns. The results of the sensitivity tests S1, S2, and S3 (see Table 10, section 4.6) illustrated in Figure 48 display the depositional patterns for the two transported materials. The tests were conducted on the long-tapered curtain wall (CWLT) SCC with three storm events: one light & short (1LS), one heavy & short (1HS), and one aggressive storm (1RE). For the tests with NB sand, it is obvious that strong washout precludes creation of deposits in the culvert vicinity, while for the CS tests the vast majority of the transported sand is confined within the area delineated by the curtain wall and the central barrel due to the good conveyance of the CWLT design. Minor deposition of sand outside these areas is shown for all tested cases. When deposition occurs, such as in S2 and S3 test cases, the location and amount of retained sand are similar for NB and CS tests (see the oval patches circling the sand deposition footprint) indicating that the two types of sediment transport are adding up over the same area of the culvert vicinity. This finding was used as an argument to continue the production tests studies using only natural sand transported as bedload.

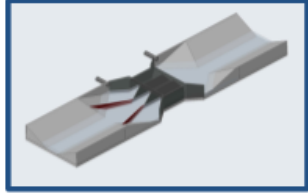

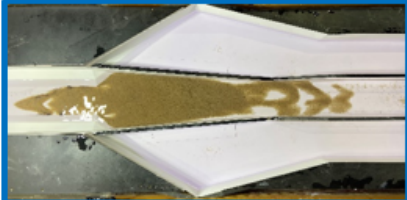




Culvert configuration		
Curtain wall long tapered exposed to various types of storms		
Sand	Type	Sand diameter
CS	Coarse sand	0.2-2.0 mm (non-uniform)
NB	Neutrally buoyant	0.76 mm (uniform)
Sensitivity tests		
Test code	NB	CS
S1 - One light & short (25 gpm)		
S2 - One heavy & short storm (50 gpm)		
S3 - One aggressive storm (25-100-25 gpm)		

Figure 48. Sensitivity test to illustrate differences in depositional patterns between suspended and bedload transport.

The IMM sensitivity tests S4 to S9 (see Table 10, Section 4.6) are aimed at checking the response of the SCC configurations to increased amounts of sediment approaching the culvert (hence, their labeling as stress tests). The stress tests were executed in the CWLT culvert configuration (proven to be one of the most efficient SCC designs), exposed to one light & short (1LS) and one heavy & short (1HS) flows loaded with gradually increased amount of sand compared to the standard load used for the production tests. The amount of sand was increased by adjusting the sediment rates for the two sand feeders (see Fig 19 in Section 4.2) to simulate the equivalent of 1.5 to 5 times the loads used in the production tests. The results of the stress tests (the first column of photos in Figure 48) compared with the reference cases, i.e., CWLT-1 LS for S4 to S7 (see first four photos in column two) and CWLT-1 HS for S8 and S9 (see the last two photos in column two). The stress test results illustrated that the CWLT design is operating efficiently under extreme sediment transport events, with minimum deposition occurring outside the curtain wall and the central barrel of the culvert.



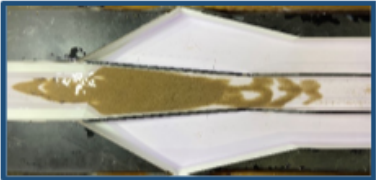





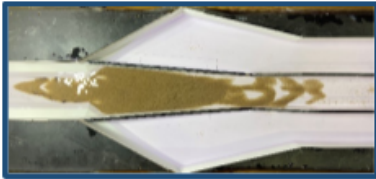

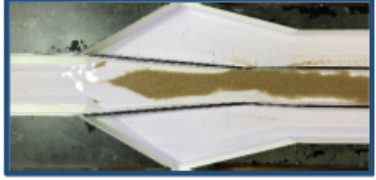

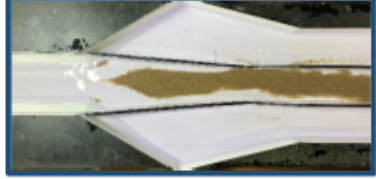
Culvert configuration		
Long-tapered curtain wall (CWL) exposed to various types of storms		
Sand	Type	Sand diameter
CS	Coarse sand	0.2-2.0 mm (non-uniform)
Test code	Stress test	Reference (1 sediment load)
S4 - One light - short storm (50 gpm) & 1.5 sediment load		
S5 - One light - short storm (50 gpm) & 2 sediment loads		
S6 - One light - short storm (50 gpm) & 3 sediment loads		
S7 - One light - short storm (50 gpm) & 5 sediment loads		
S8 - One heavy - short storm (100 gpm) & 2.5 sediment loads		
S9 - One heavy - short storm (100 gpm) & 5 sediment loads		

Figure 49. Stress tests for increased sand loads applied to IMM flume SCCs

The stress tests discussed in Figure 49 reveal the efficiency of the long-tapered curtain wall (CWL) under normal and extreme sediment loads by practically eliminating the sand deposition in the side areas at the culvert inlet for all tested cases. The self-cleaning efficiency of the CWLT design

is also remarkable over the whole culvert vicinity as illustrated in Figure 50a, where one light & short (1LS) and one heavy & short (1HS) are loaded with five times the amount of sand released in the production tests. The CWLT SCC design was found to be the most beneficial in keeping the side boxes clean being akin to a natural stream of reduced cross-section passing through the culvert. The downside of the CWLT design, as identified in the project TAC discussions about the hydraulic efficiency of these structures, is that its structure has to be protracted throughout the length of the culvert expansion area that implies high constructive costs and possibly other adverse operational considerations (due to scour along the curtain walls). Our literature review found that these structures are installed in some areas of US under layouts as illustrated in Figure 50b

a)




Culvert configuration		
Long-tapered curtain wall (CWLT) exposed to various types of storms		
Sand	Type	Sand diameter
CS	Coarse sand	0.2-2.0 mm (non-uniform)
Test description	Test result illustration	
One light - short storm & 5 sediment loads (S7)		
One heavy - short storm & 5 sediment loads (S9)		



Figure 50. Long-tapered curtain wall efficiency: a) stress tests for CWLT; b) CWLT concept installed in Los Angeles River (Photo source: Ted Soqui/SIPA USA AP).

The issue of sediment distribution along the culvert vicinity has been not included in the original scope of the study. However, the exiting data and processing procedures are in place to conduct such analysis. Using additional funding, the photo-evidence acquired for the IMM tests was analyzed with Photoshop software to determine the fraction of the sediment retained over various culvert zones (see

Figure 35). The numerical data presented on the sediment partitioning illustrated in Figure 51 usefully complement the information provided in Figure 34 regarding the IMM production tests.

SCC configuration			Fraction retention from total sediment deposit (%)				
Code	Short description	Sketch	Area #1	Area #2	Area #3	Area #4	Area 1 & 2
AIMM	"As-is"		16.1	29.2	29.2	35.5	45.2
CWMT	Medium-tapered curtain		8.2	8.4	35.5	48	16.5
FILS	Bed fillets		4.5	18.1	35.3	42	22.7
CWSF	Short-straight curtain		10.9	19.8	48.3	20.9	30.8
CWLT	Long-tapered curtain		15.3	16	43.2	25.5	31.3
RIEB	Higher inverts		11.6	23.5	29.2	35.8	35.1
CWST	Short-tapered curtain		18.2	25	39.3	17.5	43.2
SWIN	Straigh wingwalls		17.4	31.9	36.3	14.4	49.3
CWXF	Cross-stream curtain		30.1	30.1	24.5	5.3	60.3

Figure 51. Partitioning of the sediment deposit footprint per IMM culvert areas (see **Figure 35**)

The vast majority of the sensitivity tests for the IMM flume layout was conducted in the initial period of the project lifetime when an extensive testing program to assess the differences between coarse (SC) and fine (FS) sand on the creation of the sedimentation footprint was planned (see Tabel 11, Section 4.6). The results of the parallel sensitivity tests are illustrated in Figure 52.






















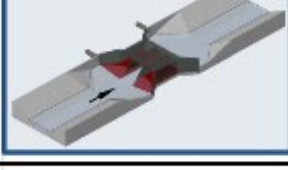
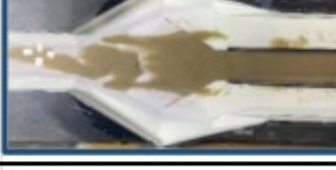
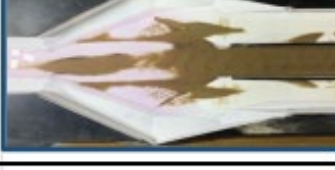
Test Code	Configuration Sketch	Sedimentation entrance area	
		"Fine" sediment	"Coarse" sediment
AIMM-1LS			
AIMM-1LL			
AIMM-1HS			
AIMM-2LS			
AIMM-2HS			
AIMM-1RE			
RIEB-1LS			
RIEB-1LL			

Figure 52. Sensitivity tests for highlighting the sand characteristics impact on sediment footprint in the IMM flume layout

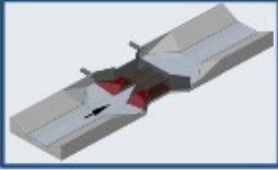
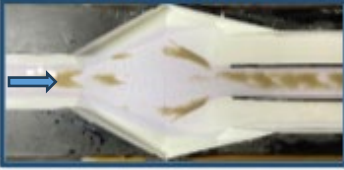
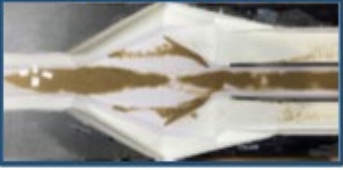

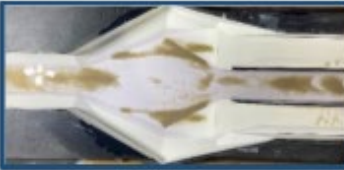
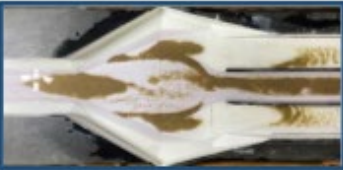
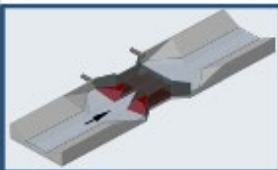


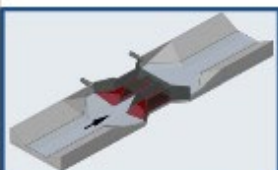














Test Code	Configuration Sketch	Sedimentation entrance area	
		"Fine" sediment	Coarse sediment
RIEB-1HS			
RIEB-1HL			
RIEB-2LS			
RIEB-2HS			
RIEB-1RE			
SWIN-1LS			
SWIN-1LL			
SWIN-1HS			

Figure 52. (continued) Sensitivity tests for highlighting the sand characteristics impact on sediment footprint in the IMM flume layout


















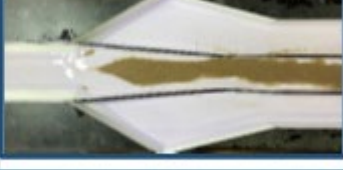






Test Code	Configuration Sketch	Sedimentation entrance area	
		"Fine" sediment	"Coarse" sediment
SWIN-2LS			
SWIN-2HS			
SWIN-1RE			
CWLT-1LS			
CWLT-1LL			
CWLT-1HS			
CWLT-1HL			
CWLT-2LS			

Figure 52. (continued) Sensitivity tests for highlighting the sand characteristics impact on sediment footprint in the IMM flume layout





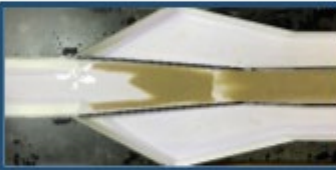



















Test Code	Configuration Sketch	Sedimentation entrance area	
		"Fine" sediment	"Coarse" sediment
CWLT-2HS			
CWLT-1RE			
CWMT-1LS			
CWMT-1LL			
CWMT-2LS			
CWST-1LS			
CWST-1LL			
CWST-1HS			

Figure 52. (continued) Sensitivity tests for highlighting the sand characteristics impact on sediment footprint in the IMM flume layout




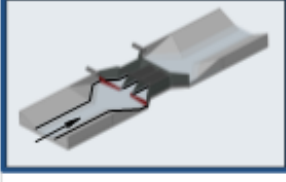


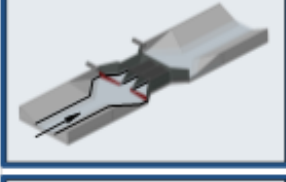


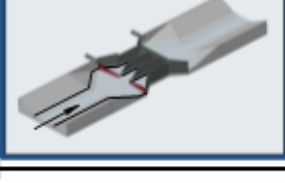


Test Code	Configuration Sketch	Sedimentation entrance area	
		"Fine" sediment	"Coarse" sediment
CWST-1HL			
CWST-2LS			
CWST-2HS			
CWST-1RE			

Figure 52. (continued) Sensitivity tests for highlighting the sand characteristics impact on sediment footprint in the IMM flume layout

Slight differences between the framing of multiple photos are due to the positioning and re-positioning of the camera over several months of executing the tests. The illustrations provided in Figure 52 reveals two important aspects. First, that the changes in the sediment granularity does not visibly affect the shape and positioning of the sediment deposits. Based on this observation the project TAC decided to stop the tests with two types of sediment for the subsequent tests. The second aspect is regarding the fidelity of the modeling results. The individual photos of the mosaic displayed in Figure 52 reveals that each of the 70+ snapshots of the tests result are symmetric with respect with model centerline and display unique features distinct from each other. that in turn attest the confidence in the outcomes of the modeling results.

6.2.2 NMU flume layout

As the degree of the sediment conveyance through the NMU culvert is drastically reduced compared to IMM flume layout, the focus of the sensitivity studies has been set to test the SCCs' designs for operation under the stress of larger loads passing through the culverts. This sensitivity focus become especially obvious following the site visit at culvert in New Mexico, where all the visited sites were massively clogged as illustrated in Figure 14. The stress tests S72, S73, S77 and S78 illustrated in Figure 53 are executed with gradually increased sediment loads on the culvert layout used for the NMU production tests executed for two stream-to-culvert angles. Inspired by the field site visits, a slightly modified flume layout was tested by simulating an extra layer fixed sand bed at the culvert entrance by setting a sand-painted board equivalent to the thickness of the clogged culverts observed in the field. These tests are illustrated by the results of the stress tests S74, S75, and S76 in Figure 53.

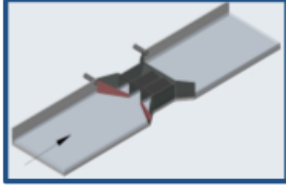
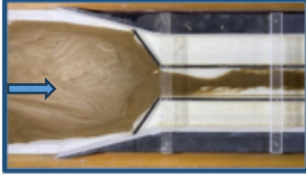



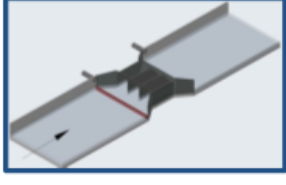
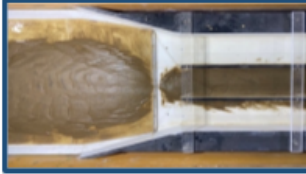

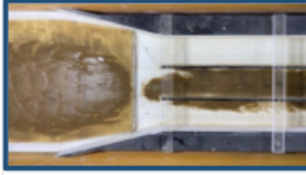

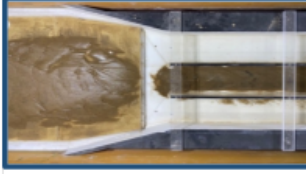

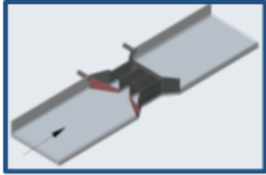
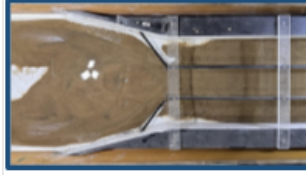

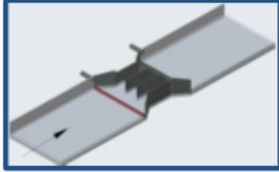

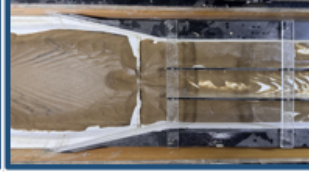
NMU SCC sensitivity tests			
Sand	Type	Sand diameter	
CS	Coarse sand	0.2-2.0 mm (non-uniform)	
Test	Stress test	Reference (1 agg.storm)	
0.3 degree for stream and culvert bed slope			
S72 - 2 aggressive storms	CWAT 		
S73 - 3 aggressive storms			
S74 - 1 aggressive storm on a clogged culvert	CWXF 		
S75 - 2 aggressive storms on a clogged culvert			
S76 - 3 aggressive storms on a clogged culvert			
Stream-to-culvert slope difference = 2 degrees			
S77 - 2 aggressive storms	CWAT 		
S78 - 3 aggressive storms	CWXF 		

Figure 53. Stress tests for increased sand loads and simulated culvert clogging applied to NMU flume SCCs

The most relevant aspect of the S72, S73, S77 and S78 the stress tests is that while the footprints of the sediment deposits remain quasi-similar in areal extend and distribution patterns, paractically covering the entire area of the culvert entrance. The increased sediment loads added to the tests resulted in an increase of the depth of the sand deposit on the original sedimentation footprint. A somewhat counterintuitive feature of the for S74, S75, and S76 stress tests is that the additional storms incoming over the clogged culvert where better handled as the repeated storms applied to original (clean) topography of the culverts. This feature is indicated by the smaller footprint of the sediment deposition running over the added sand-painted layer in the third, fourth and fifth photos of column 3 in Figure 53. The possible explanation for the improved conveyance is that the reduction of the stream and culvert cross sections due to previous runoff events leads to an increase the underlying flow velocity hence proportionally increasing the sediment transport through the structure.

A side inference from the production and sensitivity tests results reported in Chapters 5 and 6 for the NMU SCCs is that if the target of the installed structure would have been to retain rather than to convey the sediment, the appropriate ranking for the SCCs would be the reverse order, i.e., CWXF, CWF and CWAT (see also Figure 40b). Such alternative management option can be preferred if the criteria of easily cleaning the sediment after storm events is the adopted as chief strategy. Even if conveyance is used as chief criterion in selecting the optimum SCC configuration (see Figure 40b), the selection of the CWXF as the best self-cleaning option is made on the judgement that given the narrow bounds for differentiating between the conveyance efficiency for various NMU SCC configurations, it is easier to remove the sand in the open space at the entrance of the culvert than to retrieve sand from the farther away distances within the culvert body. It is apparent that deciding on a definitive ranking within the narrow quantitative bounds offered by the production tests is challenging and requires a multicriteria decision matrix that takes into considerations the quantitative results reflected in Figure 40b along with practical issues regarding the sediment removal which undoubtedly is needed for the NMU severely sedimented culverts.

6.3. Additional hydro-morphological considerations on the IMM & NMU tests

An essential aspect of the analysis of the hydraulic performance of the SCCs is observing the change in the flow field with the addition of various geometrical changes to the original culvert layout. These observations were made by capturing the velocity and depth distributions at critical control points throughout the hydraulic model and at additional points in the culvert vicinity. Based on the primary depth and velocity data, the main non-dimensional flow parameters governing the underlying open-channel flows were determined, i.e., the Froude (Fr) and Reynolds (Re) numbers. These non-dimensional numbers are also the main hydraulic model parameters used to scale up model results to prototype scale. The definitions of Fr and Re are as follows:

The diagram illustrates the definitions of the Froude number and Reynolds number. On the left, the Froude number equation is shown as $Fr = \frac{V_{mean}}{\sqrt{gR_h}}$. Arrows indicate that Fr is the Froude number, V_{mean} is the mean cross-sectional velocity, g is the gravitational acceleration, and R_h is the hydraulic radius. On the right, the Reynolds number equation is shown as $Re = \frac{V_{mean}R_h}{\nu}$. Arrows indicate that Re is the Reynolds number, V_{mean} is the mean velocity, R_h is the hydraulic radius, and ν is the kinematic viscosity. The word "and" is placed between the two equations.

These illustrations are made only for the main production tests for the NMU tests (i.e., the tests described in the Chapter 5 for determining the SCC ranking) and for all the production tests for IMM flume layout taking advantage of the additional funding provided for the investigation by the Mississippi DOT toward the end of the project lifetime.

6.3.1 IMM flume layout

Velocities and depths were simultaneously collected throughout the model extend for each executed tests for controlling the quality of the established flow in the model and document the hydraulic aspects of the original and modified culverts. Of interest herein is only the hydrodynamics of the culvert vicinity as illustrated in Figure 54. Velocities were only collected at a central point located at $0.6h$ from the free surface which is the typical sampling point for assessing the average cross-sectional velocity (bulk velocity).

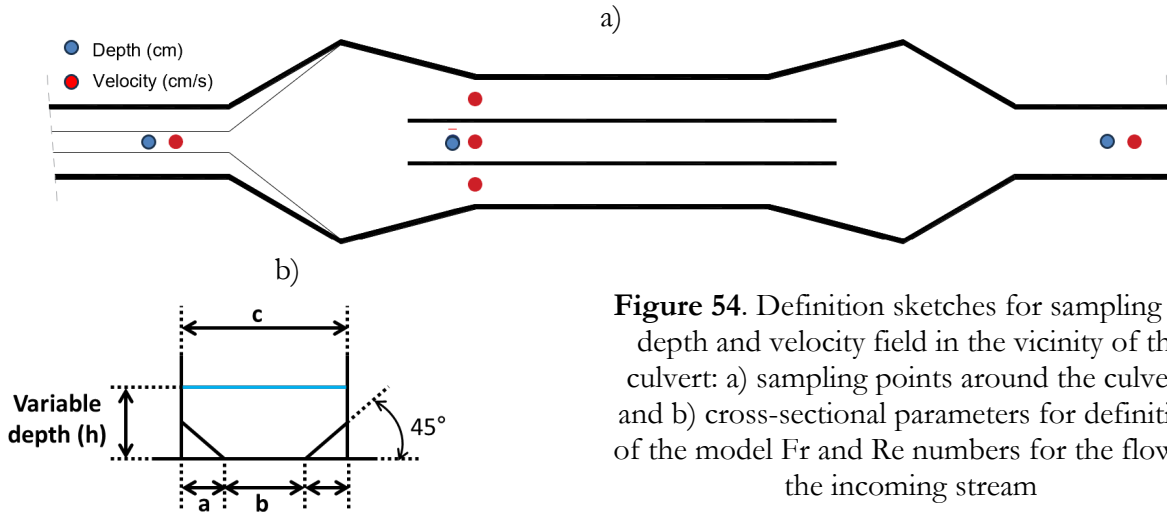


Figure 54. Definition sketches for sampling the depth and velocity field in the vicinity of the culvert: a) sampling points around the culvert, and b) cross-sectional parameters for definition of the model Fr and Re numbers for the flow in the incoming stream

Given that the IMM flume cross-section area is reduced by the fillets installed at the bottom corner of the flume, numerical simulations were used to estimate the relationship between the mean velocity and the velocity sampled over the cross section (i.e., point 6 in Figure 55). The relationship between the two velocities were estimated in a cross section located upstream the culvert expansion for the discharge range used in the experimental tests (i.e., 50 -100 gpm). The iso-velocity contours for the two discharges as obtained from numerical simulations are illustrated in Figure 55. The depth and velocity distributions along with Fr and Re for the IMM production tests are shown in Figure 56.

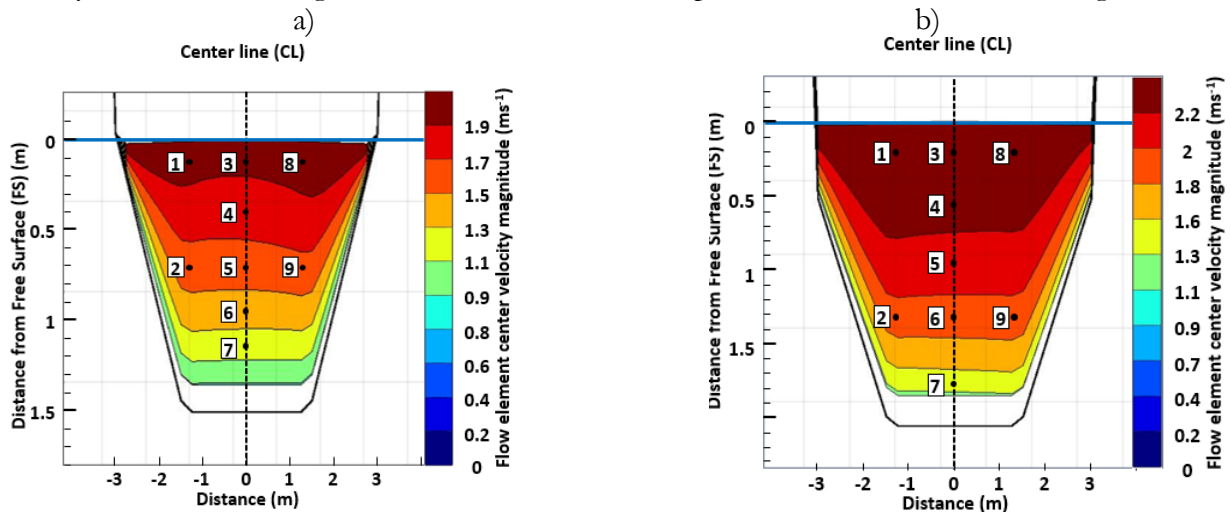


Figure 55. Numerical simulations results (in prototype scale) used for relating the central point velocity acquired in the model (i.e., point 6 in the figure) and mean velocities used for determining the Fr and Re numbers corresponding to model discharges of: a) 50 gpm, and, 100 gpm.

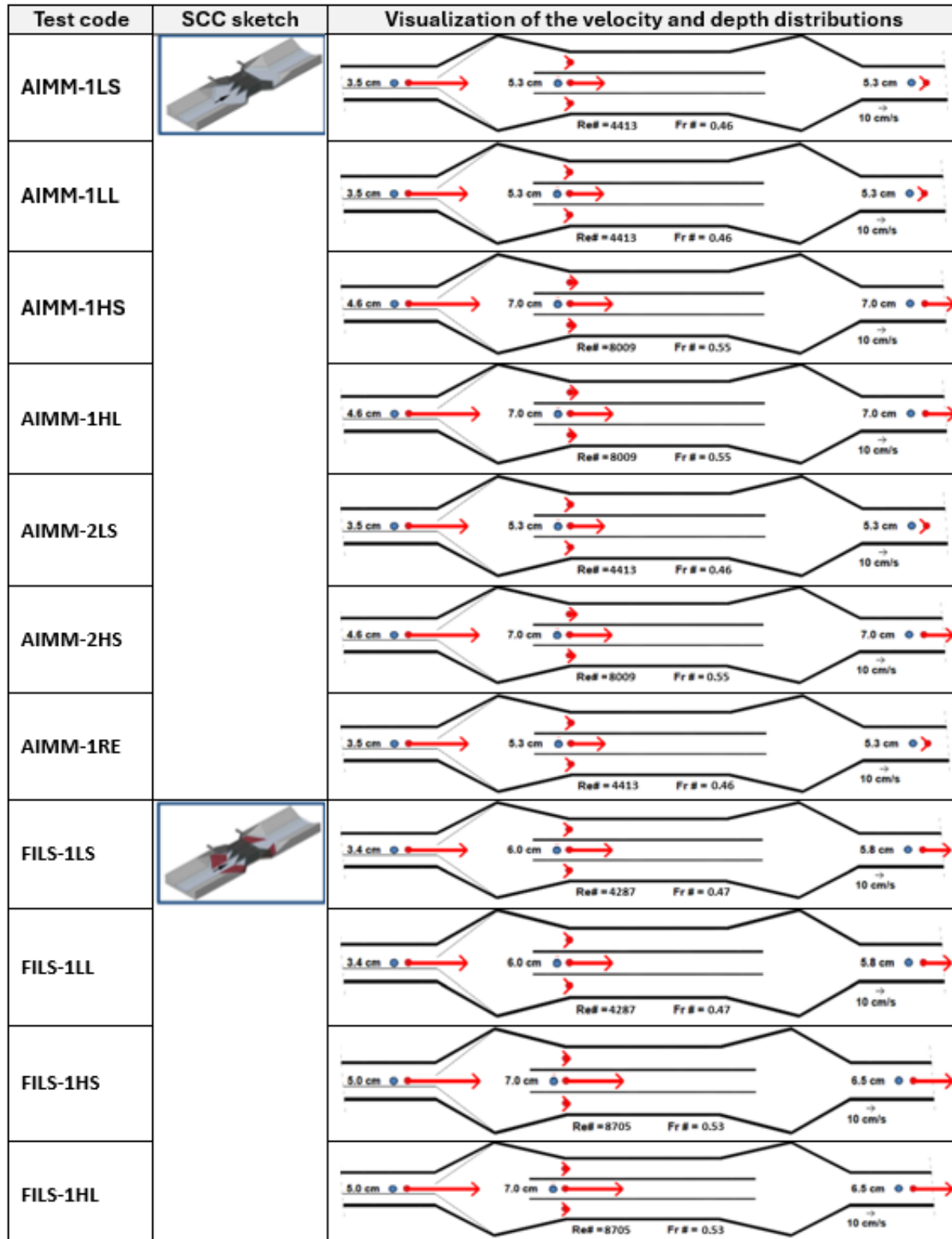


Figure 56. Numerical and graphical representation of the depths and velocities in the IMM SCCs' vicinity along with the Fr and Re numbers for the flow in the incoming stream. For varying flows (i.e., aggressive storms), the Fr and Re are only provided for the initial test stage.


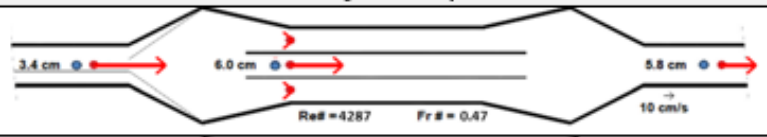
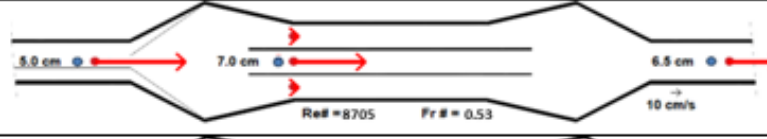
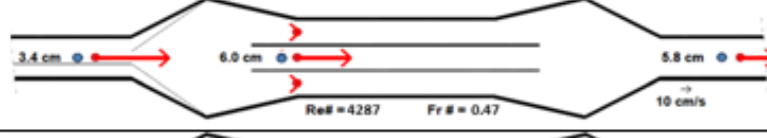

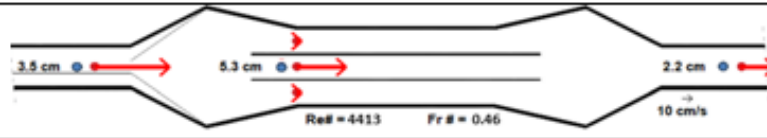
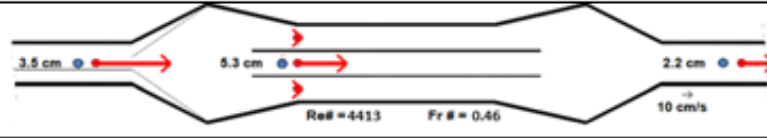
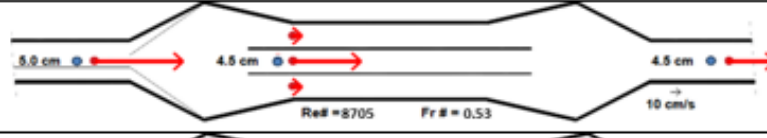
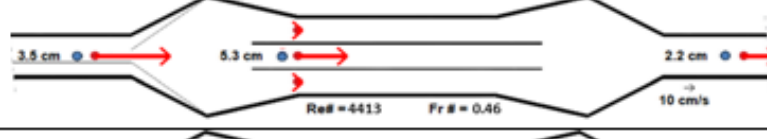
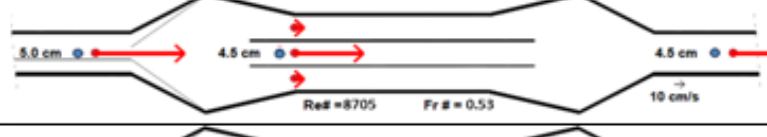
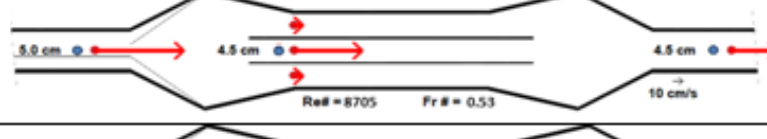


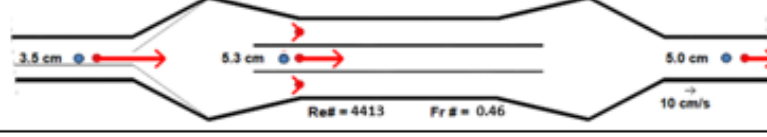
Test code	SCC sketch	Visualization of the velocity and depth distributions
FILS-2LS		
FILS-2HS		
FILS-1RE		
RIEB-1LS		
RIEB-1LL		
RIEB-1HS		
RIEB-1HL		
RIEB-2LS		
RIEB-2HS		
RIEB-1RE		
SWIN-1LS		

Figure 56 (continued). Numerical and graphical representation of the depths and velocities in the IMM SCCs' vicinity along with the Fr and Re numbers for the flow in the incoming stream. For varying flows (i.e., aggressive storms), the Fr and Re are only provided for the initial test stage.



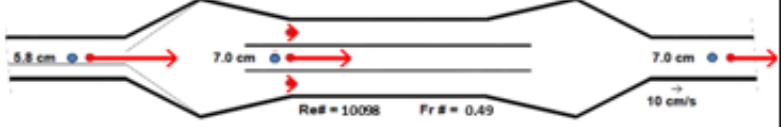




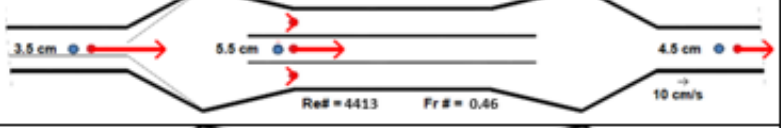
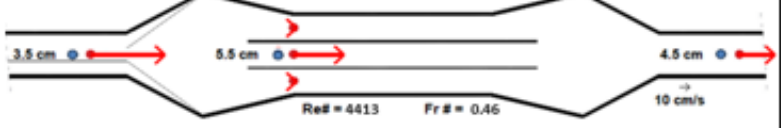
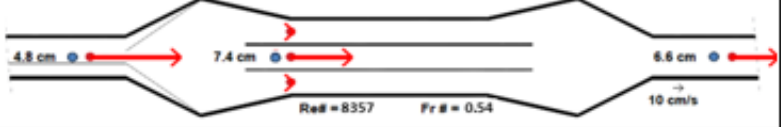
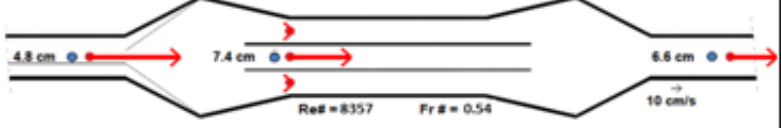


Test code	SCC sketch	Visualization of the velocity and depth distributions
SWIN-1LL		
SWIN-1HS		
SWIN-2LS		
SWIN-2HS		
SWIN-1RE		
CWLT-1LS		
CWLT-1LL		
CWLT-1HS		
CWLT-1HL		
CWLT-2LS		
CWLT-2HS		

Figure 56 (continued). Numerical and graphical representation of the depths and velocities in the IMM SCCs' vicinity along with the Fr and Re numbers for the flow in the incoming stream. For varying flows (i.e., aggressive storms), the Fr and Re are only provided for the initial test stage.


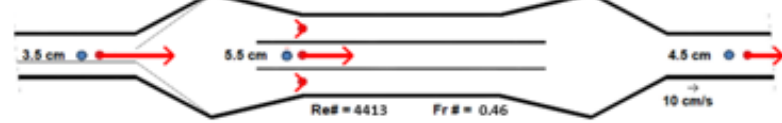


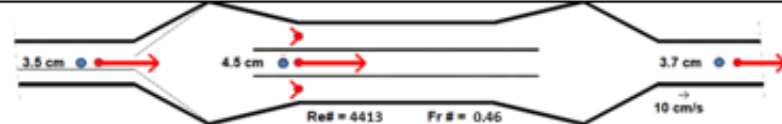

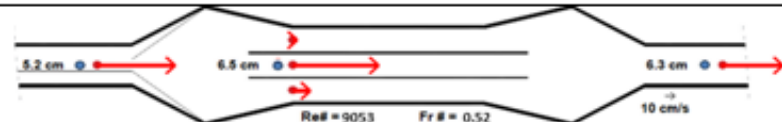
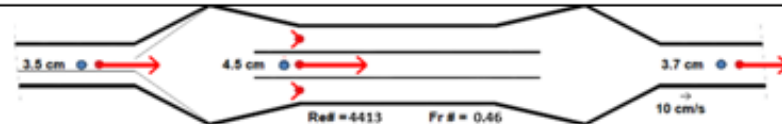
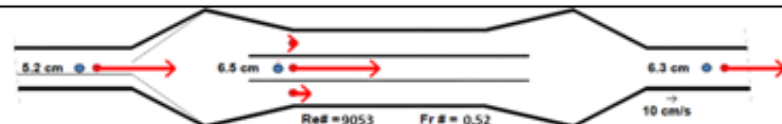
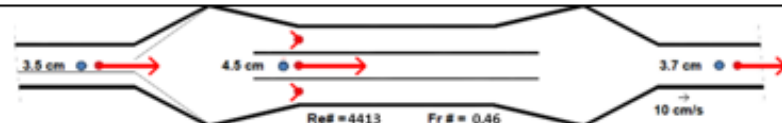

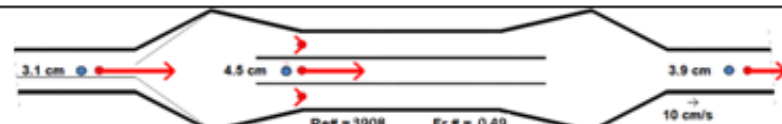
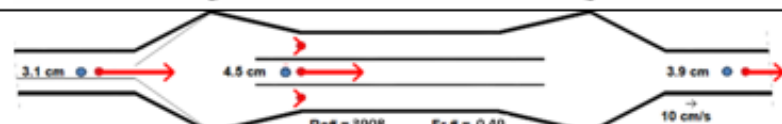
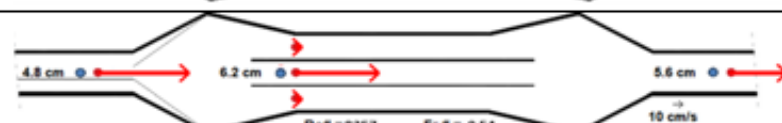
Test code	SCC sketch	Visualization of the velocity and depth distributions
CWLT-1RE		
CWMT-1LS		
CWMT-1LL		
CWMT-1HS		
CWMT-1HL		
CWMT-2LS		
CWMT-2HS		
CWMT-1RE		
CWST-1LS		
CWST-1LL		
CWST-1HS		

Figure 56 (continued). Numerical and graphical representation of the depths and velocities in the IMM SCCs' vicinity along with the Fr and Re numbers for the flow in the incoming stream. For varying flows (i.e., aggressive storms), the Fr and Re are only provided for the initial test stage.


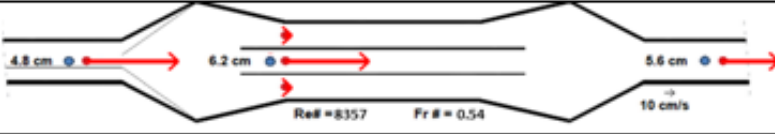
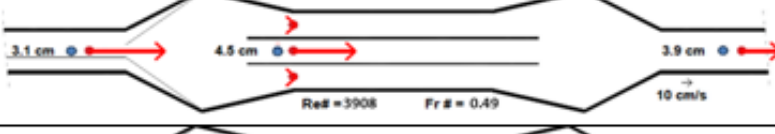

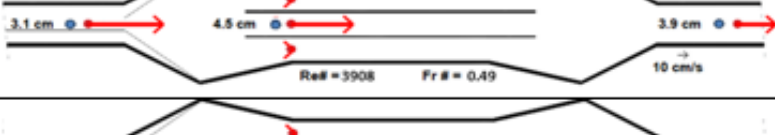

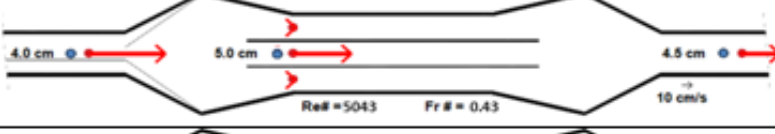
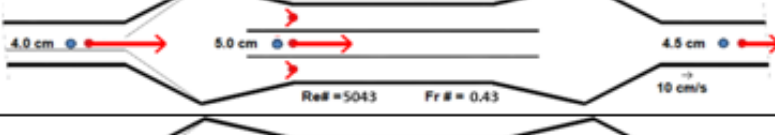
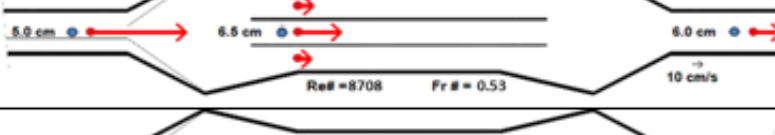
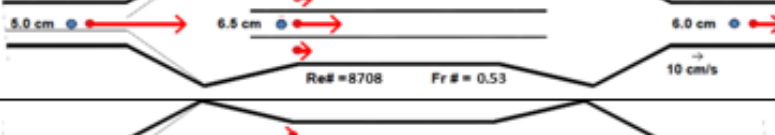
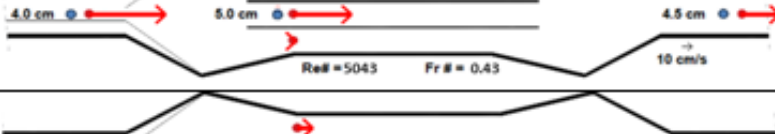
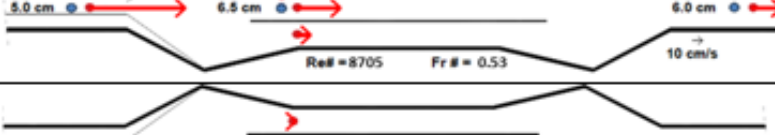
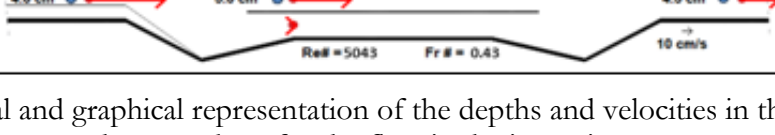
Test code	SCC sketch	Visualization of the velocity and depth distributions
CWST-1HL		
CWST-2LS		
CWST-2HS		
CWST-1RE		
CWSF-1LS		
CWSF-1LL		
CWSF-1HS		
CWSF-1HL		
CWSF-2LS		
CWSF-2HS		
CWSF-1RE		

Figure 56 (continued). Numerical and graphical representation of the depths and velocities in the IMM SCCs' vicinity along with the Fr and Re numbers for the flow in the incoming stream. For varying flows (i.e., aggressive storms), the Fr and Re are only provided for the initial test stage.

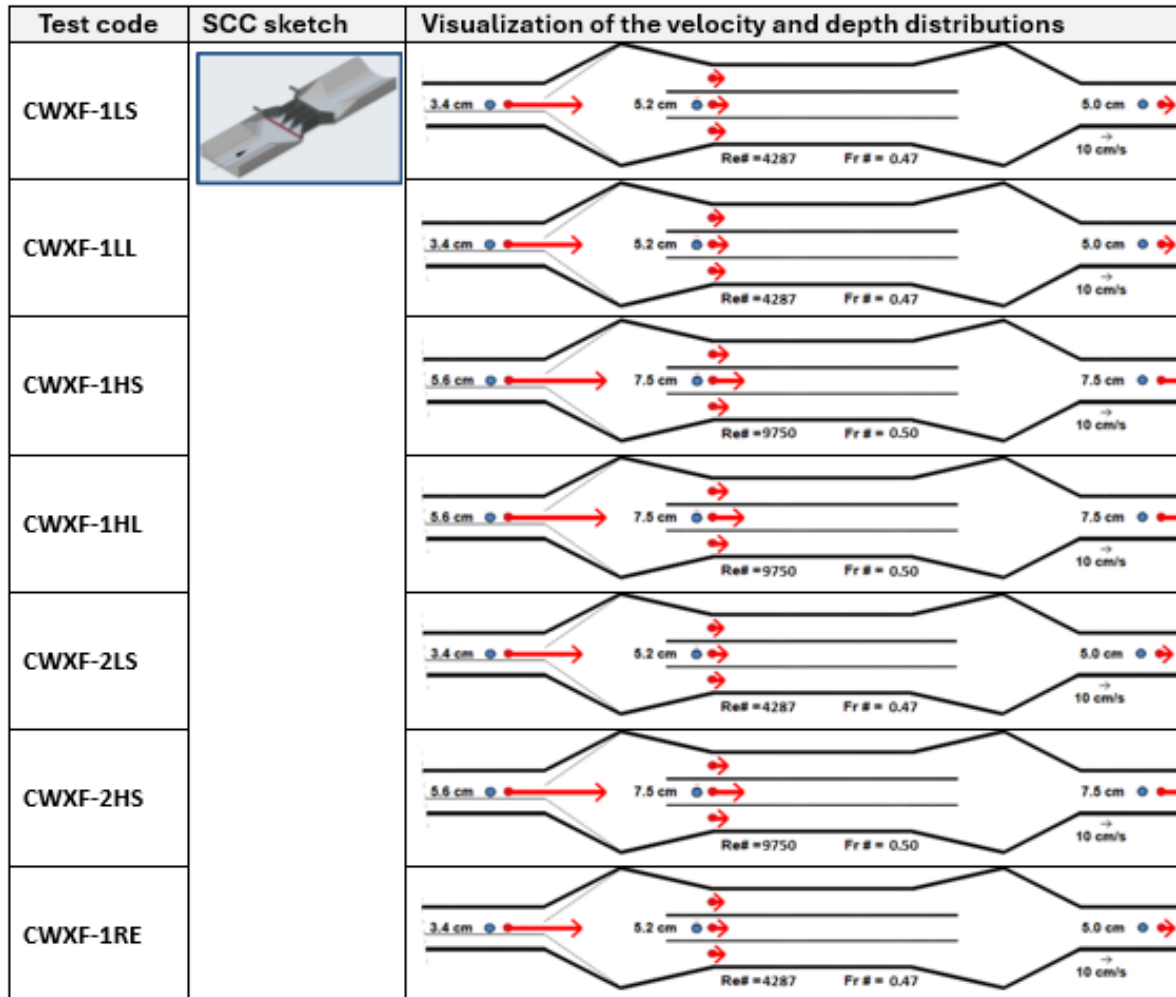


Figure 56 (continued). Numerical and graphical representation of the depths and velocities in the IMM SCCs' vicinity along with the Fr and Re numbers for the flow in the incoming stream. For varying flows (i.e., aggressive storms), the Fr and Re are only provided for the initial test stage.

The results illustrated in Figure 56 are obtained prior to the execution of the production tests with clear water. Slight changes are expected for the flows carrying sediment because of the presence of the bedload transport. The dimensions for the depths and velocities in the figure are the for direct measurements obtained in the hydraulic model. The Fr and Re numbers are the same for model and prototype. While the distributions have many common features across the modeled scenarios, they are unique for each test, similar to the results of sediment patterns illustrated in Figure 39.

There is a close connection between the flow hydrodynamics and the sediment transport induced by the underlying flow. Useful inferences on the transport of sediment in non-uniform and unsteady flows can be drawn if the data illustrated in Figure 56 is related to the quantitative mapping (2D or 3D) of the sediment deposits (see Figure 39). While such an analysis is beyond the scope of the present research, it is worth showing some samples of the change in the sediment footprint correlated with the flow distribution for clear water flow. Sample of such illustrations are shown in Figure 57 for flow cases not used so far (e.g., see Figure 38 for alternative comparisons). The quantitative exploration of this information is critically for calibration and validation of numerical simulations for these complex flows. Such information is scarcely available from controlled, well-prescribed experimental conditions.

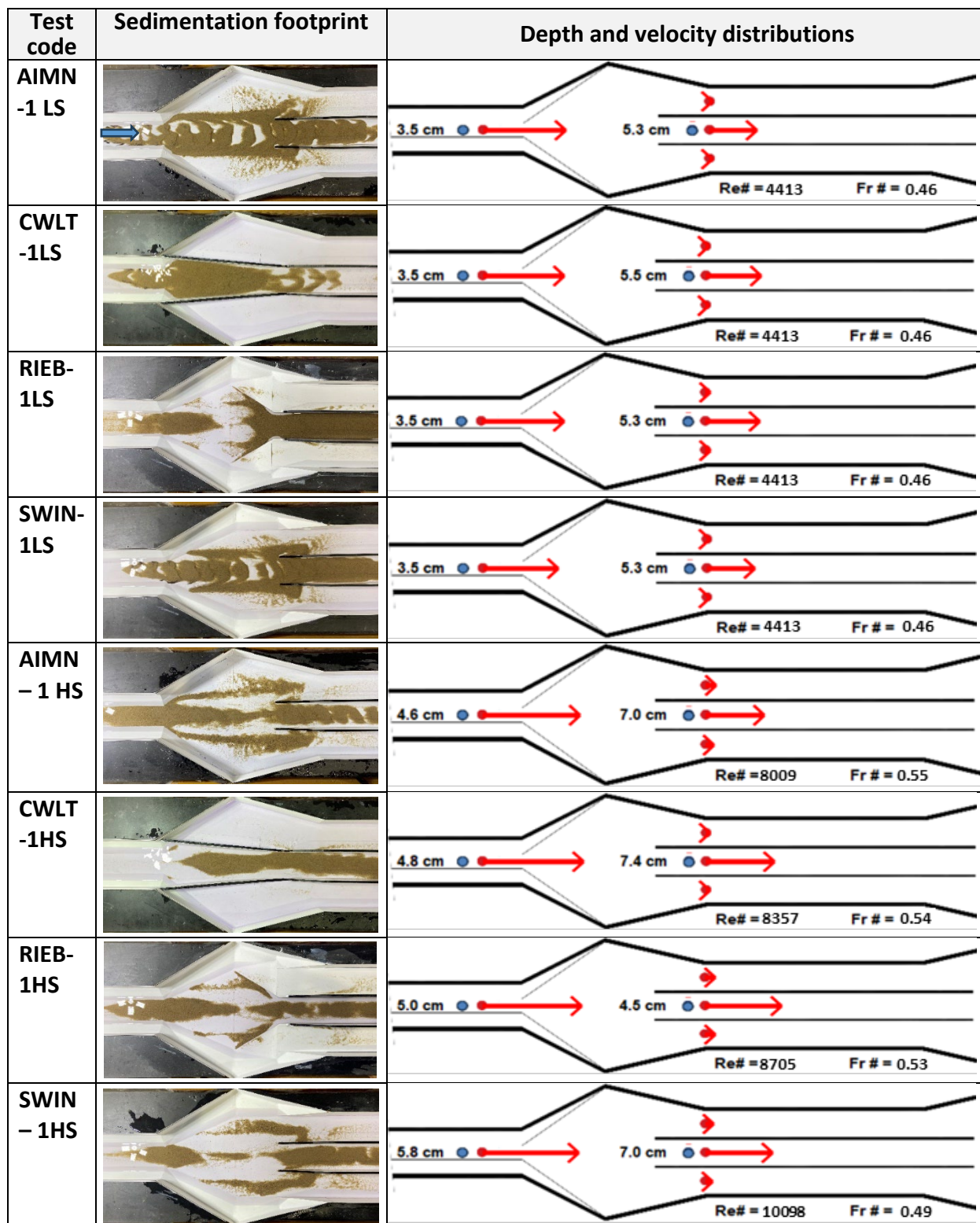


Figure 57. Pairing of the sedimentation footprint with the spatial distributions of depths and velocities in the culvert vicinity for selected flow and SCC combinations

The flow distribution at the culvert entrance for all the production tests substantiates an important hydraulic aspect of the culvert hydraulics at multi-box culverts that is not currently considered in the

design of this type of culverts. Specifically, it is apparent that the velocity in the central barrel is larger than the velocities in the side boxes which in turn favors sediment deposition in the lateral areas of the cross section and implicitly throughout the length of the outer boxes. The depths and velocities reported in Figure 56 can be used to determine the actual partitioning of the flow at the culvert entrance and evaluation of the ratios for flow discharge that should be attributed to each culvert box for an accurate sizing of the box geometry. Another hint of the depth and velocity distribution illustrated in this figure is that the hydraulic losses can be estimated if the energy equation is applied to the upstream end of the expansion to the culvert and the downstream end of the contraction at the culvert outlet. A reliable estimation of the losses calculated as mentioned above would require however, repetition of the tests to enhance the statistical pool used for the loss estimation.

6.3.2. NMU flume layout

Velocities and depths were simultaneously collected throughout the model extend for each executed tests for controlling the quality of the established flow in the model and document the hydraulic aspects of the original and modified culverts. Of interest herein is only the hydrodynamics of the culvert vicinity as illustrated in Figure 58. Velocities were collected in five points at the entrance of the culvert located at 0.6h from the free surface. The average cross-sectional velocity (bulk velocity), was estimated using a weighted average to account for the velocity distribution across the section.

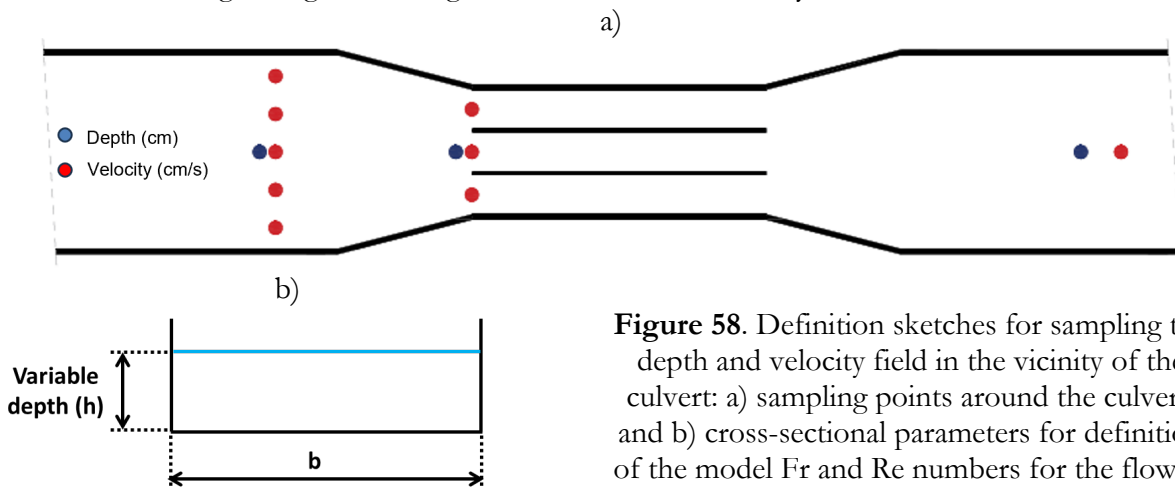


Figure 58. Definition sketches for sampling the depth and velocity field in the vicinity of the culvert: a) sampling points around the culvert, and b) cross-sectional parameters for definition of the model Fr and Re numbers for the flow in the incoming stream

The incoming stream for the NMU flume is a simple rectangle making the calculation of the Fr and Re numbers simpler as not adjustments for the cross-sectional geometry shape are needed (see Figure 58b). The non-dimensional numbers are calculated for the cross section located immediately upstream from the culvert inlet (along the line linking the tips of the culvert wingwalls) for the discharge range used in the experimental tests (i.e., 100 - 200 gpm). The numerical and graphical representation of the depth and velocity distributions along with Fr and Re for the NMU production tests are shown in Figure 59. The range for the Fr and Re numbers for all the tests conducted for the NMU model are provided in Table 15. Note that the Fr and Re numbers are continuously changing during variable flows such as the one aggressive storm, hence the minimum and maximum steady flows within the range are provided in the table. The common feature of the velocity distributions for all the stream-to-culvert angles is the “funnel-like” hydrodynamics described by a quasi-uniform velocity distribution at the culvert entrance that converges to higher value at the culvert inlet.

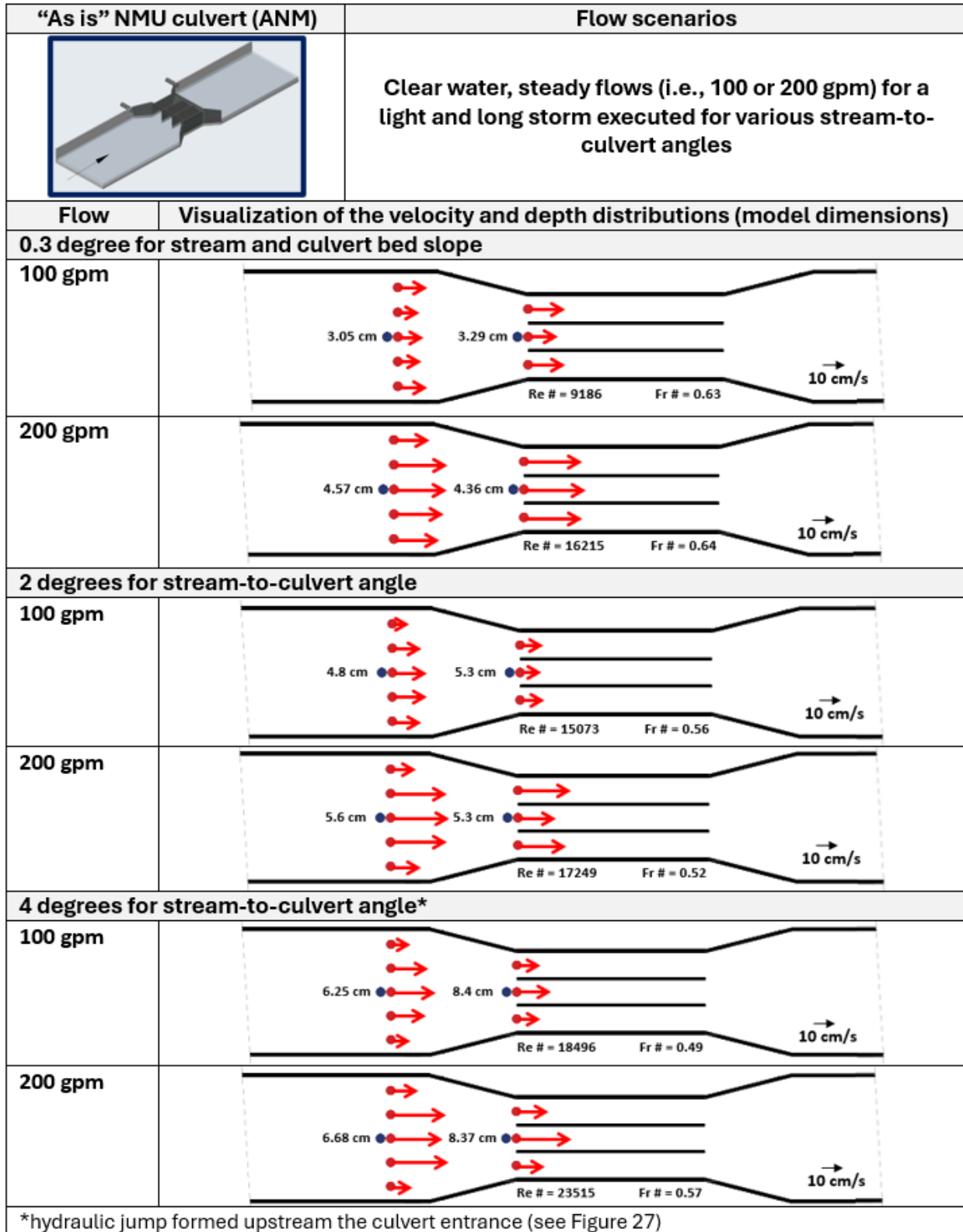


Figure 59. Numerical and graphical representation of the depths, velocities, Fr and Re for NMU tests

Table 15. Froude and Reynolds numbers for NMU SCCs tested for one aggressive storm (1RE)

SCC configuration		Froude #	Reynolds #
Channel and culvert slope = 0.3 degrees (0 degree difference)			
ANMU		0.63 ~ 0.64	9186 ~ 16215
CWAF		0.39 ~ 0.48	11785 ~ 20772
CWAT		0.27 ~ 0.43	11063 ~ 21180
CWXF		0.36 ~ 0.49	9830 ~ 21070
Channel-to-culvert slope difference = 2 degrees			
ANMU		0.56 ~ 0.85	15073 ~ 27990
CWAF		0.62 ~ 0.63	14484 ~ 24897
CWAT		0.65 ~ 0.79	18362 ~ 28472
CWXF		0.55 ~ 0.63	14897 ~ 29025
Channel-to-culvert slope difference = 4 degrees			
ANMU		0.49 ~ 0.57	18497 ~ 23517
CWAF		0.41 ~ 0.59	20947 ~ 29318
CWAT		0.39 ~ 0.55	17757 ~ 28811
CWXF		0.36 ~ 0.61	16358 ~ 29336

Connections similar to the IMM flume tests (as illustrated in Figure 57) can be explored to highlight the relationships between the flow hydrodynamics and the sediment transport induced by the underlying flow. However, considerably few experimental evidence is available for testing hypotheses related to this issue from the experiments in the NMU flume layout.

6.4. Closing comments on the experimental results

Research studies on both flow and sediment transport processes in highly variable unsteady and non-uniform pen-channel flows are real challenges for any of the available investigative tools, i.e., laboratory experiments, field observation, or numerical investigations. Given that the field observations are often constrained by acquiring multi-variable data in an unpredictable (and often unsafe) measurement environment and that the numerical simulations cannot be fully trusted without validation with field observations, the only reliable source of information on these complex flows are laboratory experiments. The lab experiments provide opportunities to observe and measure details of the process and to fine tune the process parameters to observe their impact on the study targets. This is not to say that the laboratory experiments are fully replicating the natural scale processes.

A rigorous research of sediment transport in such complex flow is notoriously complex being typically reduced to the investigation of uniform, steady flows (Rouse, 1940). Even for these much simpler studies it is often necessary to sacrifice even approximative hydraulic similarity given that the geometric modeling of the sediment size (typically defined as the mean diameter of sediment size frequency curve) must scale down to the dimensions of the involved transport processes: the bedload and suspended load. A further compromise is necessitated because the bedload and sediment load are modeled by different criteria. Specifically, the bedload transport is governed by Shields criteria governed by the ratio of mean sediment diameter to boundary-layer thickness with relationships obtained on a semi-empirical basis that cannot be easily generalized. The transport of suspended sediment is governed by flow turbulence that requires to relate the sediment-distribution function in terms of the fall-velocity characteristics of the sediment and the distribution of flow turbulence in the vertical. This intricate modeling conflicts results in the fact that most of the studies of sediment

movement have been arbitrarily restricted to cases in which little or no material is carried in suspension – the latter being a phenomenon the sediment geometry is not a pertinent factor.

Ensuing from the above consideration is that the experiments conducted for this study are of high complexity and difficulty entailing non-uniform unsteady channel flows. Our first-of-the-kind research of sediment-laden flows through culverts using variable sediment feeding rates lies in an uncharted area of study with only few publications informing on aspects of hydraulic modeling conducted in much simpler channel flows. Most of the research is of an exploratory nature as important process drivers are not sufficiently documented or completely lacking field data. Even if all the similitude criteria required for a full-fledged hydraulic study could not be fulfilled, the results of the hydraulic modeling presented in Chapter 5 and 6 of this study are deemed to at least can capture essential features needed for enabling screening of various changes in the sedimentation patterns brought about the self-cleaning culvert solutions. The qualitative evaluation based on images and time lapse videos provides powerful evidence of the sedimentation process initiation, development, and final degree of sedimentation and its areal distribution (useful for multi-criteria investigations). The quantitative evaluation (based on surface area or volume mapping of the sediment deposits) is useful for cost-benefit analyses and developing logistics for the culvert cleaning operations.

The reliability of the hydraulic model is proven by the sensitivity of the model response to changes in both culvert configurations and flow conditions used for the individual tests. The results presented in this study apply to multi-box culverts with an odd number of boxes with small degree of skew (i.e., the angle between the culvert installation and a line perpendicular to the highway centerline). The experimental evidence garnered through the study clearly demonstrates that each test has a unique, distinguishable sedimentation pattern, which is quasi-symmetric with respect to the flume centerline. Repetition of the tests for the same culvert configurations and flow conditions implemented using the precisely designed experimental protocols have confidently resulted in identical results.

There are some notable limitations of the IMM and NMU tests reported herein. Among them are:

- The study results are not readily applicable to multi-box culverts with more than three boxes, but nevertheless can guide their design.
- The study results are not applicable for multi-box culverts with even number of boxes as they require quite different SCC configuration designs (currently under investigations by these authors for an ongoing IDOT project).
- None of the flow scenarios tested in this study considered woody debris presence, a complexity factor that can drastically change the flow hydraulics in various stages of the storm propagation. Moreover, the presence of debris requires antagonistic design principles, i.e., retention of the debris at the culvert entrance and increased conveyance of sediment in the same area.
- The IMM test results are significantly more abundant in information compared to the NMU results as they benefitted more attention, research funding, and prior information for conducting the research from previous studies. The NMU flow scenarios were limited by lack of actual data on the flow hydrographs of ephemeral streams located in semi-arid areas which instead relied on extending the knowledge available for IMM settings using engineering judgement. Finally, there were experimental facility limitations that did not fully serve the testing of the NMU tests, as the initially planned for IMM flume configuration created a hydraulic jump at the culvert entrance for the 4 degree stream-to-culvert angle that most probably is not occurring in field conditions.

Ideally, this initial study should be continued with the development of performance curves that evaluate the hydraulic capacity of a culvert (i.e., flow discharges) for various headwaters and velocities at inlet and outlet velocities as investigated by Charbeneau et al. (2006). Given that the presented tests are among the first of the kind, they would benefit from a more extensive sensitivity tests that covers a much wider range of geometries, sand characteristics, and flow hydrographs informed by robust field observations.

7. PRACTICAL RECOMMENDATIONS

7.1 Inferences from the experimental tests

The info garnered through this experimental study aims at advancing the understanding of the flow and sediment transport behavior of a typical three-barrel culvert configuration set in a simple road-culvert-stream arrangement exposed to various meteorological conditions. Specifically, the inferences are strictly valid for a culvert to stream angle of $\alpha = 0$, a culvert-road angle of $\beta = 90$ degrees, with the stream and culvert cross section symmetrically arranged along a common centerline (see Figure 60). The generic sketch illustrated in Figure 60 is more representative for a an IMM stream-road-culvert crossing. The NMU culverts do not typically include an expansion at the culvert inlet rather collects runoff through a contraction-like transition described next. The large number of our study experiments for representative IMM and NMU settings exposed to various flow conditions provide a wide range of qualitative and quantitative inferences for supporting formulation of design specifications and offering practical information for routine culvert operations. For situations where the actual sites deviates more than ± 15 degrees from the $\alpha = 0$ and $\beta = 90$ alignments, additional evaluations and, possibly, further modelling is needed to investigate features reported in this study.

A common geometric feature of the IMM and NMU culverts in our study is the “expansion area” enclosed between the tips of the flared wingwalls set at the culvert inlet and outlet – an area that is typically enclosed in the culvert structure. The expansion areas are connected with the natural stream with “transition areas” that are delineated by the cross sections T_1 and T_2 upstream the culvert and cross sections T_3 and T_4 downstream (see Figure 60). The main attention of our study is the upstream transition-expansion area where the flow nonuniformity (defined by streamlines that are not straight and parallel) and flow recirculation trigger sedimentation processes that subsequently affect the culvert long-term operation.

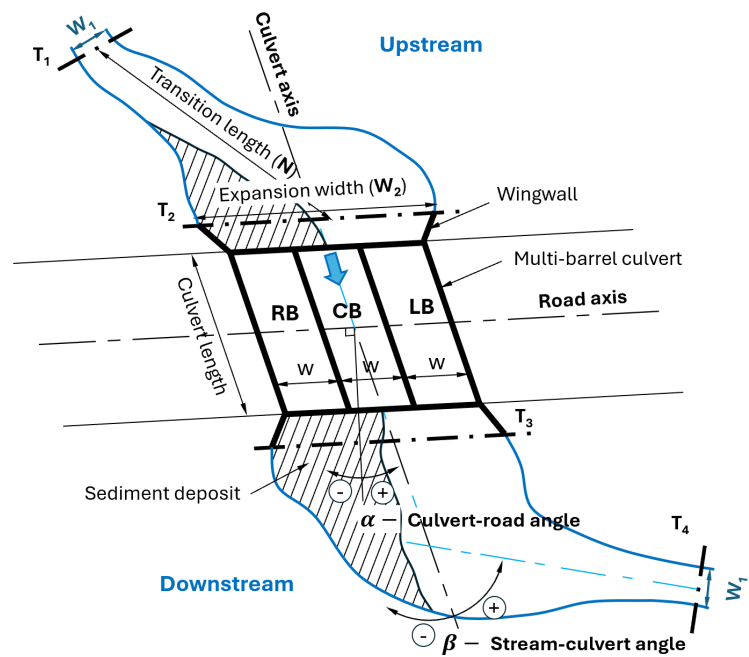


Figure 60. Terminology for defining culvert road crossing

The presence and degree of flow nonuniformity (i.e., divergence/convergence of the streamlines for a given streamflow) in the transition-expansion areas is a flow complexity that depends on the areal extent of these areas. Two non-dimensional parameters, i.e., the Stream-to-Culvert Width ratio, $SCW = W_2/W_1$ (defined in Section 3.1 and Figure 3) and the Transition Length to Culvert Width ratio, $TLCW = N/W_2$ are used to quantify the degree of flow nonuniformity. The values for the two ratios determine the distribution of the velocity at the culvert inlet and the allocations of the design flow to discharges passing through individual culvert barrels. We assume that the parameters used for characterizing the flow nonuniformity (i.e., SCW and TLCW) can be also used for guiding the mitigation measures against sedimentation. Actually, a data-driven study on sedimentation at 250 culverts located in the State of Iowa found that SCW ratio is the most important factor in differentiating silted vs. non-silted culverts (Xu et al., 2019b). Another flow complexity involved in sedimentation at culverts is the presence of unsteady flows associated with the propagation of runoff events (see Section 3.1). Sediment transport under unsteady flows show differential bedload rates and

yield ratios during the rising and falling limb of the hydrographs (De Sutter et al., 2001; Hummel et al., 2012; Wang et al., 2019). The combination of the effects due to flow non-uniformity and flow unsteadiness decide where and when the sediment settling in the culvert vicinity will occur. The knowledge on these flow complexities is scant. Currently, there are considerable gaps in the theory regarding the non-uniform, unsteady, sediment-laden flows developing in three-dimensional culvert geometry. A review article published by Mrokowska & Rowinski (2019) points out that we still do not know if it is possible to quantify sediment transport in unsteady flow given that the sediment composition and characteristics of transient flow conditions do not allow more than qualitative observation of the relationships between various driving quantities. Lack of understanding and analytical tools for investigating complexities of this process combination makes it difficult to predict sedimentation at culverts.

As concluded in Section 6.4, addressing fundamental knowledge gaps and making progress in this area of engineering can be only obtained from laboratory studies. Even the experimental evidence is hard to come by. A handful of prior studies have investigated issues related to flow distribution and energy losses in the presence of flow nonuniformity in channel expansions at culverts (e.g., Charbeneau et al., 2006; Jones et al., 2006; Haderlie and Tullis, 2008). All these studies were conducted with clear-water tests. Another handful of tests has been conducted with addition of sediment transport (Howley, 2004; Ho et al., 2013; Rowley, 2014; Cafferata et al., 2017) under steady flow regimes. Our present study expands the prior laboratory work conducted by Ho et al. (2013) and the field-study inferences from Muste and Xu (2020) for investigating sediment transport through a subset of culvert geometries exposed to steady and unsteady flows with and without sediment transport.

This study is a new contribution tackling sedimentation at culvert with a comprehensive view that attempts to realistically replicate the processes occurring for typical IMM and NMU multi-barrel culvert configurations installed in two widely different morphological and hydrological conditions: perennial streams in temperate climate for IMM culverts and ephemeral streams in semi-arid regions for NMU culverts. A survey of the US DOTs found that 22 of the 35 states use multi-barrel culverts (Haderlie & Tullis, 2008). Our study does not however aim to be an all-encompassing generic investigation of the fundamental aspects of sediment transport processes but substantiate features of these processes that are important for practical considerations related to sedimentation processes. The study is novel and, to the knowledge of the authors, has not been tested experimentally before. Summarized next are several generic and individual hydraulic and sediment transport features of the IMM and NMU culvert models that are closely connected to the project goal.

The transition areas shown in Figure 60 can be shaped differently depending on the local conditions at the culvert sites. In our study, the IMM culvert is fitted with an expansion at the culvert inlet and a contraction at its outlet (like the situation illustrated in Figure 60). In contrast, the NMU layout is fitted with a contraction upstream and an expansion downstream the culvert. The degree of flow uniformity and, hence, the impact of sediment transport is decided by the SCW and TLCW ratios. Prior studies converge to the realization that a TLCW of 4:1 defines a “natural” transition, one where the energy losses are not considerably affected (Albertson et al., 1950). By extension, we can deem that flow non-uniformity effect is relatively mild up to this threshold ratio. An important remark on this aspect is that the culvert design is weakly addressing the sizing of the transition areas. This aspect is critical point not only for properly selecting the culvert configuration but equally relevant for the issues related to sediment transport that are rarely considered not considered part of the culvert design.

Achieving a natural-scale transition requires additional excavation work around the culvert which is not always possible due to costs and local site constraints (e.g., the size of the right-of-way at the culvert location). The culvert layouts accepted by the project TAC for our study display a TLWC of 2.7 for IMM and a ratio of 1.1 for the NMU culvert arrangements, which are distinctively different from the 4:1 “natural” transition. Accordingly, the flow nonuniformity for our tested scenarios is also

significant. Indeed, this feature is well illustrated in Figure 61 where a “jet” effect is substantiated for the IMM culverts, and a “funnel” effect is visible for the NMU culverts. The dye visualization patterns illustrated in Figure 61a are more persistent for the IMM flow conditions compared to NMU ones as the velocities for the latter case are significantly larger. The flow velocity and depth distribution unevenness illustrated in Figure 61b leads to uneven sediment accumulations in the vicinity and throughout the culvert body as abundantly illustrated with test results presented in Chapters 5 and 6. Despite the geometrical difference between the transitions for the two culvert configurations, there are favorable conditions created for developing sediment deposit in both cases albeit that this is done through different mechanisms. Specifically, sedimentation triggering is due to the presence of low-velocity areas on the lateral sides of the IMM culvert entrance, while for NMU the sedimentation is related to the convergence toward the culvert of flows heavily loaded with sediment.

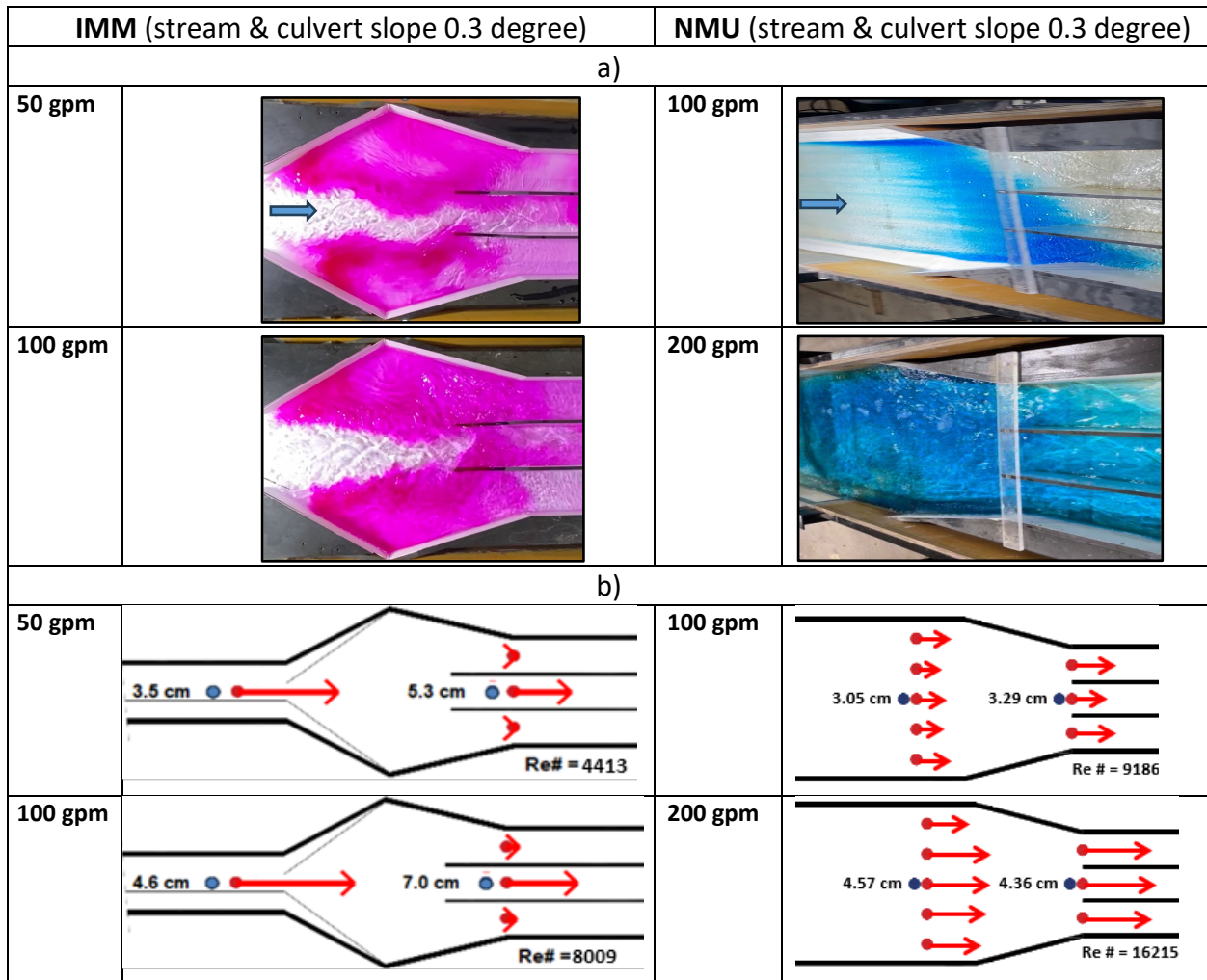


Figure 61. Illustration of the flow nonuniformity effect in the transition area from the stream to the IMM and NMU culvert entrance: a) dye visualizations; and, b) distribution of the measured depths and velocities at the culvert inlet (model dimensions).

Our findings on the jet effect occurring in the divergent transition area set at a multi-box culvert entrance to connect it with the undisturbed stream for in the tests with the IMM culverts are confirmed by an extensive study conducted with clear water experiments by Charbeneau et al. (2002). Their experiments were conducted with and without culvert set in the model. The velocity distribution across the model acquired at various distances from the stream entrance in the expansion showed the

persistence of the jet effect for both cases, with evidence of some broadening of the jet in the downstream direction, but without significant decrease of the centerline depth-averaged velocity. These patterns for cross-sectional velocity distribution indicate a much greater velocity entering the central barrel(s) of multi-barrel culverts and creation of favorable conditions for formation of flow recirculation zones on the side of the jet just upstream from the of the outer culvert barrels. The recirculation zones are the most likely contributors to the increased sedimentation in the outer barrels as constantly evidenced by our experimental tests. Extension of the experimental results with 2-D numerical simulations in the Charbeneau et al. studies indicated that with the increased of the TLWC ratio the recirculation zones become elongated and move closer to the channel centerline with an overall effect of reducing their footprint. The TLWC ratio of 4:1 was found as optimal from the perspective of reducing the flow recirculation zones. Similar quantitative inferences for NMU are not available as there are no previous studies known to these authors of such culvert arrangements and our own tests are limited to just one fixed stream-culvert geometry.

The major inference related to the sediment transport in the tests on as-is culverts and culverts retrofitted with Self-Cleaning Culvert (SCC) designs is that once the sediment deposits are initiated, the deposition driven by the combined contribution of suspended and sediment loads builds up on basically the same footprint suggesting that these transport processes are cumulative rather than complementary. Under the combined effects of the hydraulic drivers and the stabilization effect of the vegetation growth the sediment deposits reach a maturity topography that can be attained within 5 years from the culvert construction or cleanup in temperate climate conditions (Muste and Xu, 2022). Butler et al. (2003) argues that an initially clean culvert flowing as a free-surface flow can handle bedload transport without creating deposits. The presence of bedload transport increases the bed resistance causing an increase in depth and decreasing velocities. Intuitively, it might be assumed that a reduction in velocity would cause a reduction in the sediment-transporting capacity of the flow leading to further deposition and possibly blockage. In fact, laboratory evidence has shown that the presence of bedload results in a greater capacity for transporting sediment as bedload (May, 1993). This is because the degree of sediment transport is related to the width of the deposited bed, which can be much greater than the narrower stream without bedload. May concluded that presence of increased depth associated with the bedload presence may balance with the incoming sediment load and prevent further deposition. This surprising self-cleansing effect can be an acceptable reasoning for IMM culvert operations after deposit “fossilization” and for the surprising capacity of the NMU silted culverts to still convey sediment with just a fraction of the original culvert opening left open (see Figures 14a and 15d).

Another inference on the sediment transport at as-is the IMM and NMU culverts is that the sedimentation patterns observed in the tests are different for the two flume arrangements. The IMM arrangement favors sand deposition in the outer area at the culvert inlet and in the side boxes while it is much more uniformly distribution in the NMU tests. These flow-driven patterns have been abundantly confirmed by field observations at culverts located in the two climatic zones. Additional field observations highlight that a large number of the IMM culverts are displaying non-symmetry between the deposit footprint and size between the two outer areas of the culvert. This feature results from the unique hydromorphological unevenness in the road-culvert-stream conditions (i.e., values of the angles, stream bed substrate, etc.) that decides a preferential flow path for the flow stream early after the culvert is built or cleaned that is subsequently maintained during the accelerated maturation of the deposits due to vegetation growth. From the few visits at NMU culverts, it is found that the sediment deposits are typically flat and continuous across individual barrels due to the high stream power produced by the “funnel” effect and limited presence of the vegetation due to the transported material nature. The SCCs configurations developed for this study specifically targeted the experimental evidence inferred from the combined laboratory-field observations.

7.2. Culvert design considerations

7.2.1 *Culvert hydraulics with consideration of sediment transport*

Conventional culvert design has traditionally based on hydraulic conveyance for clear water conditions, safety and cost. There is a plethora of design considerations for single- and multi-box culvert for handling clear-water flows are well described and extensively verified with experimental and numerical studies. Summarized below are the steps of conventional culvert design to provide a robust backbone for the design aspects related to sediment transport through culverts.

At the onset of the hydraulic design, special attention must be paid to the recent increase of more intense and frequent precipitation events that not only affect the estimation of design water flows but also culvert vulnerability to sediment transport. The recent study conducted by Mukherjee et al. (2025) using an ample ensemble modeling accounting for hydro-morphological and hydroclimatic factors signals that more careful consideration of the assessment of the culver vulnerability to flood-induced soil erosion. Specifically, they found that culverts located in the Eastern US forested area are hydrologically vulnerable (undersized) to floods. Following the establishment of the design flows with consideration of climate change projections, the hydraulic sizing is performed along with simultaneous consideration given to the proposed culvert installation procedures, including alignment checks, stream dimension verification for bank-full discharge, and substrate composition evaluation (e.g., Gillespie et al., 2014).

In current practice, the multi-barrel culverts are designed using single-barrel culvert design procedures and summing the individual flow capacities through simple superposition (e.g., Jones et al. 2006). The amount of skew, nonuniformity in the upstream flow approach, and the inlet geometry are also an integral part of determining the final design. The sizing of a culvert is made under two types of flow conditions: (a) inlet control; and (b) outlet control. The hydraulic theories and design procedures differ for inlet and outlet controls. In design, both conditions are separately analyzed, and the design alternative predicts the largest headwater value is assumed to govern. Many culverts are built without hydraulic considerations of the inlet because design guidelines do not explicitly state the performance benefits of an optimized inlet design.

Given that all the SCC modifications at culverts are made at the culvert entrance, the design under consideration herein is the inlet control. The headwater height under inlet control is determined by the flow rate, the cross-sectional area, the shape and the inlet configuration of the culvert. Expansions, reductions, or any other modifications at the culver inlet have significant impact on the flow distribution and culvert performance and relatedly on the sediment transport through the culvert. For both hydraulic and sediment efficiency it is critical to check for flow uniformity of the selected culvert geometry set in the local arrangement. If the main flow uniformity criterion is satisfied (e.g., TLCW close to a 4:1 ratio) consider that that superposition of equal discharges at individual boxes is reasonable. i.e., within $\pm 5\%$ of the analytical assumptions (Haderlie and Tullis, 2008). The average - barrel discharges for individual boxes can be based on the single-barrel hydraulic design. For nonuniform flow conditions a physical model is recommended when determining the culvert sizing as the standard design specifications do not cover this type of flows.

The multiple-barrel culverts should be connected with the natural channel with minor widening to avoid conveyance loss through sediment deposition in some of the barrels. The culvert slope should generally match the channel slope, if practical. Minimum culvert slopes should not be flatter than 0.3% if ground conditions permit. Maximum culvert slopes should not be greater than 6% for reinforced concrete surfaces. Culvert slopes can be further adapted for accommodating sedimentation and aquatic habitat passage considerations. For sediment consideration a critical requirement is to ensure the verification of the minimum flow velocity that ensure “self-cleansing” (Butler et al, 2003). Several additional considerations regarding the changes that the sediment induces on the hydraulic gradient and the friction factor can be found in (UDOT, 2017).

Traditionally, specification of the minimum “self-cleansing” velocity is unrelated to the characteristics and sediment concentration. A robust evaluation of the minimum velocity requires to determine the sediment-transporting capacity “that is sufficient to maintain a balance between the amounts of sediment entrainment, deposition and erosion, with a time-averaged depth of sediment deposit that minimizes the combined costs of construction, operation, and maintenance” (Butler, 2003). While the three sediment transport components are covered with a large body of analytical formulas, their implementation for culvert design purposes is a complex endeavor, if practical at all for design purposes. To illustrate the level of complexity for determining the relationship between sediment mobility and hydraulic performance at culverts Figure 62 summarizes the steps involved in a systematic approach to relate self-cleansing criteria to the main drivers of culver hydraulics (Ackers et al. 1996). It should be noted that these relationships are obtained for uniform, piece-wise steady open-channel flows. In the absence of easier to apply specifications, we suggest adoption of ODOT (2014) recommendations for a minimum velocity of 3ft/s in order to ensure sediment mobility for various types of sediment characteristics and for preventing sediment settlement in the culvert barrels.

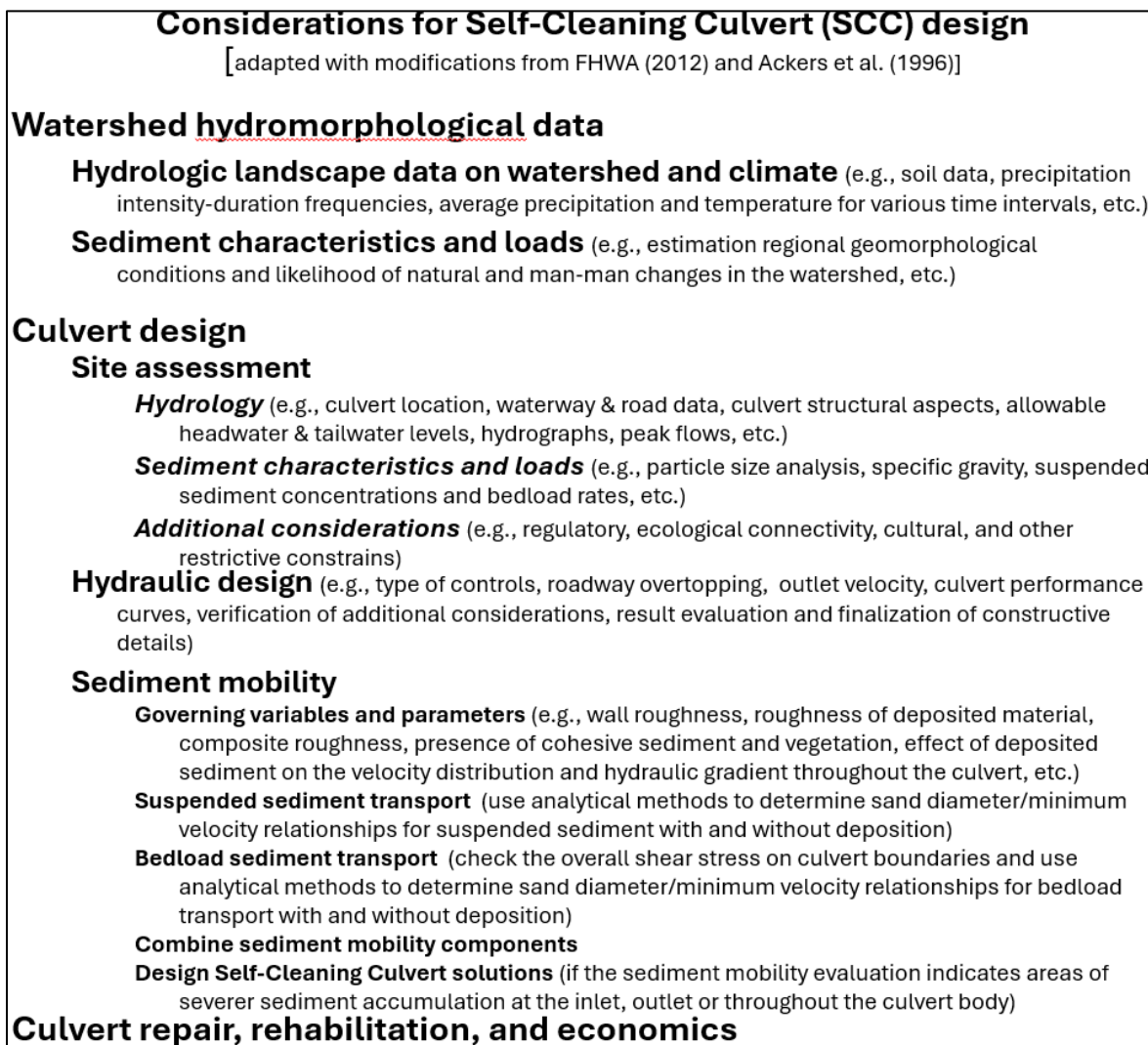


Figure 62. Flowchart for SCC design with considerations on sediment transport

7.2.2 *Hydromorphological considerations on SCCs*

The main focus of our experimental tests in the IMM and NMU flume arrangement is on substantiating the impact of the SCC designs on the sediment transport and ranking the sedimentation degree for tests design alternatives. A common geometric feature of the IMM and NMU SCCs is that the transition zones to culverts is extended by the presence of the flared wingwalls. This feature is widely present in multiple DOTs but possibly phasing out under the current proliferation of pre-cast culvert alternatives (SWIN) that, in most of the cases, have the wingwalls straight. Given that the flared wingwall installation increases the “effective” SCW ratio up to 25% (depending on the flare angle) the study’s conclusions & ranking can be considered conservative for culverts with straight wingwalls. Another common SCC design concept enforced in our study was to adopt SCC solutions with minimum modification of the culvert geometry. By following this principle, it is ensured that the developed solutions are valid for both new and existing culverts (as this approach does not require structural changes to the culvert geometry). Finally, one more feature relevant to the present analysis for the IMM and NMU SCCs were designed using a “low” hydrodynamic profile, i.e., their height varied between 2 and 5 ft (prototype dimensions) using tapered shapes. The maximum SCC height does not exceed $0.25w$, where w is the width of an individual barrel (see Figure 60).

The high-level considerations regarding the applicability of the IMM and NMU tests are listed in Section 6.4 and will be not replicated here. The exploratory tests on the SCC were developed based on understanding of the culvert hydraulics underpinning the flow and sediment transport and engineering judgement rather than on large amount of data. Given that the overall goal of this research was to identify and screen as many as possible SCC solutions that fit specific purposes, our measurement program was continuously adjusted to acquire experimental evidence that can be quickly assessed based on engineering judgement. Consequently, the data acquisition program entailed measurements of aspects to quantify the modeling input, the model operation, and the modeling results. The end result of this combination of factors is that the design considerations for SCCs are not as rich in recommendations as the ancillary tests are obtained from pioneering experiments supported by parsimonious measurements and insufficient sensitivity analysis (i.e., much less sensitivity tests for optimization of SCC geometry than the comprehensive ones on impact of sediment characteristics).

The SCC ranking provided in Sections 5.2 and 5.3 are based on frugal datasets with prevalence given to the qualitative and quantitative information on sediment footprint distribution rather than on detailed quantification of flow characteristics. Until new experimental tests of this kind are made available and complementary measurements are obtained, we offer a summary of the test considerations in lieu of definitive recommendations for better informing the SCC design and practice. The presented recommendations should be used with caution and tempered by engineering judgement as the results rely on a limited number of experiments applied to a subset of the possible hydraulic conditions at the culvert-road-stream crossings. Specifically, the recommendations are formulated using a fixed set of geometrical parameters for the SCCs installed in the culverts and for predetermined types of flow and range for their variation. However, during the propagation of flood waves the geometrical parameters (as well as the non-dimensional ratios associated with transition extension, i.e., SCW and TLCW) are continuously changing, an essential aspect that it is not captured in our end-to-end result (Figure 39 for IMM and 46-47 for NMU) but can be further analyzed in the time-lapsed photo (see Figures 36 for IMM and 42 for NMU). Moreover, definitive recommendations cannot be truthfully issued without a cost-benefit analysis that include additional aspects that are beyond improving the flow and sediment conveyance (e.g., maintenance costs, ensuring of a healthy and aesthetically-pleasing appearance of the streams at road crossings, and safety of the aquatic habitat).

The generic recommendations for the design IMM and NMU culverts that are subject to SCC implementation entail the following elements:

- Choose a culvert width as close as possible to the width of the natural channel approaching the culvert to restrict the development of nonuniform flow.
- Install culverts with a slope close to the natural channel to avoid adding geometric complexities.
- Avoid oblique stream-to-culvert angles by setting the culvert along the channel direction. The initial cost increase might pay off when the culvert sedimentation is not becoming a concern in operation.
- Keep the headwater depth at the culvert inlet at half-full (and no more than two-thirds) of the culvert height. Assumption of culvert operation with submerged inlet control further complicates the analytical assessment of the hydromorphological conditions (i.e., combination of flow through orifices developing downstream as open-channel flows).

The first three recommendations listed above (especially the first) are not different from the considerations required for the hydraulic sizing of the culverts. They are repeated here as currently there are few considerations to account for sediment issues in multi-box culvert design and the ones listed above are essential to assure better sediment conveyance, thereby reducing the risk of structural failure. These generic guidelines can be definitely considered in the preliminary culvert design and for retrofitting silted culverts.

More specific recommendations for designing SCCs stem from testing 9 designs for IMM and 5 designs for NMU. Similarly to the more generic recommendation listed above, their extension to other configurations and test conditions requires caution and engineering judgement. Presented next are specific inferences on the SCCs tested in the IMM and NMU flumes.

IMM SCCs

- Given the nonuniformity of the flows approaching IMM culverts, the SCC designs should aim to further direct the flow toward the central barrel and enhance the turbulence level in the outer boxes to keep the sediment in suspension during the flow-sediment movement through the culvert.
- Changes of the side box geometry at the culvert entrance produced by short-straight curtain walls (CWSF and CWSI) or bed fillets (RIEB) are the most efficient for mitigating sedimentation at the culverts (see additional results and additional comments in Sections 5.2 and 6.2.1 of the report). The bed-fillet solution implementation at an Iowa culvert in 2010 has proven long-term efficiency to date.
- The tapered curtain walls are streamlining better the flow; the long-tapered curtain wall (CWLTI) outperforms all tested SCC configurations, but based on the assessment of the project TAC it is not practical for implementation
- The long duration and light storm can be more detrimental for sedimentation than a heavy and short storm as the second type of event have a cleansing role as described by Butler et al. (2003).
- The best ranked IMM SCC configurations are relatively easy to construct and operate.
- The best ranked IMM SCC configurations performed well in sensitivity studies (extended storm durations, repeated storms, various sand characteristics).

One aspect observed in the field trips at IMM Culvert that might be important for enhancing the SCC design is the investigation of the dynamic equilibrium occurring through the preferential deposition occurring “naturally” under the stream action over long-time intervals (over seasons and year of operation). This self-cleaning approach was proposed for this study (CWDX) but was not tested (see Table 8). Devising SCC that strikes a balance between bed layer growth and bedload conveyance might “naturally” change the sediment deposits distribution over the multi-box culverts by reducing sedimentation in some parts of the culvert areas and enhancing its capability to flush the sediment in other areas. Favoring sediment transport using the natural approach proved to be efficient in field conditions when the headwater could be maintained at a levels that ensured that the transition areas toward and away from culvert were flooded at all times, including the minimum flow (Muste and Xu, 2020).

NMU SCCs

- The flow approaching the NMU culverts displays a quasi-uniform behavior with the flow velocity distribution more balanced over the culvert boxes than for IMM culverts.
- The funnel-like transition at NMU culverts considerably increase the velocities at the culvert entrance requiring to considerably increase the amount of sand added to the tests, i.e., amounts up to 5 times than those used in IMM were found necessary to replicate patterns observed in the field.
- The 2 and 4 degrees stream-to-culvert NMU flume arrangement required an almost double amount of sand than those used in the 0.3 degree.
- Changes made upstream the culvert entrance slowed velocities in this area favoring increased sediment retention rather than the increased sediment conveyance targeted for the IMM SCCs.
- All curtain-wall designs (CWXF, CWSF, CWAT, and CWAF) are effective in keeping the sediment out of outer boxes for an initial storm (see Sections 5.3 and 6.2.2). Subsequent storms flowing over a raised bed at the culvert entrance increase the sediment conveyance as the curtain walls filled upstream with sands act as a downward curtain wall that has been proven effective in multiple instances observed in the field studies conducted at IMM culvert sites.
- The cross-section curtain (CWXF) is effective in retaining sediment upstream, but it is questionable if it is effective for long-term culvert service.
- The aggressive heavy storms are more detrimental compared with long duration and repeated storms due to the fact that the sediment in the deposits tested in the model are mobile and uniformly distributed across the width for the NMU flume
- The best ranked SCC configurations are relatively easy to construct and operate and performed well in sensitivity studies (extended storm durations, repeated storms)

8. CONCLUSIONS

This study aims at developing Self-Cleaning-Culvert (SCC) designs that limit or eliminate sedimentation at culverts, an operational and maintenance nuisance that affect the operation of multi-box culverts in many parts of the US. The experimental program developed for this purpose targets sedimentation formation at a typical three-box culvert configuration set on streams located in two distinct and quite opposite climate and morphological zones: perennial streams in temperate climate and ephemeral streams in semi-arid regions. The selection is strictly dictated by the funding agencies of the study: Iowa, Mississippi, and Missouri DOTs (collectively labeled IMM) and New Mexico and Utah DOTs (NMU). The experimental tests cover a range of precipitation events observed at culvert sites and realistically replicated the complex features of the resulting flows with controlled and replicable experimental protocols.

The sedimentation pattern and areal distributions for the as-is IMM and NMU culverts display consistently different patterns for a range of hydromorphological conditions tested in the hydraulic model. Specifically, the IMM culverts favor sedimentation in the outer area of the culvert entrance and of the culvert body while the NMU culverts display a much more uniform sediment distribution across the culvert barrels. The sedimentation footprint is closely connected to the nonuniform and quasi-uniform aspect of the flow distribution in the transition areas leading to the IMM and NMU culverts, respectively. Starting with the realization of these persistent features for the underlying flows at culverts, we designed and tested geometrical modification of the transition areas leading to culvert inlet using streamlined shapes that directed the flow through the central barrel with additional considerations given the constructability and maintenance costs.

The tested SSC showed a satisfactory sediment conveyance efficiency for the IMM culverts but a much-reduced efficiency for NMU culverts. Almost all the tested SCCs for IMM culverts showed capabilities to flush the sediment by more than 50%. The addition of geometry changes at the NMU culvert entrance have further hampered the capability of the structure to handle the much heavier

sediment load carried by flash floods compared with the IMM streams. Nevertheless, the NMU SCC have some beneficial impacts by elevating locally the stream bed to provide enhanced stream power during subsequent storms and by retaining the sediment upstream the culvert from where it can be easier removed in case of culvert operation failure. The qualitative and quantitative data and information accumulated through the experimental research enabled to clearly distinguish the self-cleaning potential of individual SCC designs allowing to rank the structures using various criteria, i.e., hydraulic and sediment transport efficiency, upfront and during operation costs, or secondary-induced effect on stream aesthetic appearance and ecological aspects.

The 80 production and 44 sensitivity tests produced by this innovative and comprehensive experimental study produced a vast amount of data from that have been just partially explored commensurate with the goals and available project resources. The analysis of the research results is reported with the end-user in mind focusing more on the practical needs of engineers (notably from state and federal transportation agencies, and consultancies in the US) engaged in the design, monitoring, or trouble-shooting culvert maintenance. The abundant information delivered by the study can be further explored through additional analyses to more substantially advance the understanding these complex flow and sediment transport through culverts located in a variety of hydrological and geomorphological conditions. Due to the complexity of these complex multi-phase flows, laboratory experiments remain the best source of information for developing analytical and numerical tools for practical applications.

REFERENCES

- Ackers, J. C., Butler, D. and May, R. W. P. (1996). Design of sewers to control sediment problems. CIRIA Rep. No. R141, CIRIA, London, UK.
- Albertson, M.L., Dai, Y.B., Jensen, R.A. and Rouse, H. (1950): Diffusion of submerged jets, Transactions American Society of Civil Engineers, 115, pp. 639-664.
- Armstrong, A., Sousa, L.R., Haggerty, C., Fischer, C. and Wagenlander, W. (2012). An integrated approach to sustainable roadside design and restoration, Report No. FHWA-WFL/TD-13-01, Federal Highway Administration, Federal Lands Highway Coordinated Technology Implementation Program, Vancouver, WA.
- AASHTO (1975). Guidelines for the hydraulic design of culverts, Task Force on Hydrology and Hydraulics AASHTO Highway Subcommittee on Design, American Association of State Highway and Transportation Officials, Washington, D.C.
- ASCE (2000). Hydraulic modeling: concepts and practice. ASCE Manuals and Reports on Engineering Practice No.97, American Society of Civil Engineers, R. Ettema Editor, Reston, VA, ASCE Publications.
- ASCE (2008) Sedimentation Engineering: Processes, measurements, modeling and practice, ASCE Manuals and Reports on Engineering Practice, No. 54. Garcia M. (editor), New York, NY, ASCE Publications, doi.org/10.1061/9780784408148.
- Butler, D., May, R., & Ackers, J. (2003). Self-cleansing sewer design based on sediment transport principles, J. Hydr. Eng., 129(4), 276–282, [doi.org/10.1061/\(ASCE\)0733-9429\(2003\)129:4\(276\)](https://doi.org/10.1061/(ASCE)0733-9429(2003)129:4(276))
- Brunner, G. W. (2016). HEC-RAS, river analysis system hydraulic reference manual. USACE, Hydrologic Engineering Center, Davis, CA.
- Cafferata, P., Lindsay, D., Spittler, T., Wopat, M., Bundros, G., Flanagan, S., Coe, D., and Short, W. (2017). “Designing watercourse crossings for passage of 100-year flood flows, wood, and sediment”, California Forestry Report No. 1, Department of Forestry and Fire Protection, Pebble Beach, CA.

- Charbeneau, R. J., Henderson, A. D., Murdock, R. C., and Sherman, L. C. (2002). "Hydraulics of channel expansions leading to low-head culverts.," Report FHWA/TX-03-2109-1, Texas Center for Transportation, Research, Austin, TX.
- Charbeneau, R. J., Henderson, A. D., and Sherman, L. C. (2006). Hydraulic performance curves for highway culverts, *J. Hydraulic Engineering*. 132 (5): 474-481. doi:10.1061/(ASCE)0733-9429(2006)132:5(474).
- Demir, I., Muste, M. and Xu, H. (2019). Transfer of the Iowa DOT Culvert web-tool prototype to Iowa DOT mainframe, Report for project TR-744, Iowa Highway Research Board Department of Transportation, The University of Iowa, Iowa City, IA
- De Sutter, R., Verhoeven, R., and Krein, A. (2001). Simulation of sediment transport during flood events: laboratory work and field experiments, *Hydrological Sciences Journal*, 46:4, 599-610, DOI: 10.1080/02626660109492853
- Ercicum, S., Crookston, B., Bombardelli, F., Bung, D.B., Felder, S., Mulligan, S., Oertel, M. and Palermo, M. (2021). Hydraulic structures engineering: An evolving science in a changing world. *WIREs Water*. 8(2), e1505.
- Faqiri, K. (2014). Hydraulic capacity of culverts under sediment transport – Multibarrel setup, PhD Thesis, Norwegian University of Science and Technology, Trondheim, Norway
- Fearn, R.M., Mullin, T. and Cliffe, K.A. (1990), Nonlinear flow phenomena in a symmetric sudden expansion, *J. Fluid Mechanics*, 211, doi.org/10.1017/S0022112090001707, pp. 595 - 608
- FHWA (1972). Hydraulic design of improved inlets for culverts, HEC No. 13, Hydraulics Branch, Bridge Division, Office of Engineering, FHWA, Washington, D.C. (L.J. Harrison, J.L. Morris, J.M. Normann and F.L. Johnson).
- FHWA (2012). Hydraulic Design of Highway Culverts, Third Edition, Federal Highway Administration publication # HIF-12-026, Washington, D.C.
- FHWA (2014). "Culvert management case studies: Vermont, Oregon, Ohio and Los Angeles County, Federal Highway Administration Report FHWA-HIF-14-008.
- Foltz, R. B., Yanosek, K. A., & Brown, T. M. (2008). Sediment concentration and turbidity changes during culvert removals. *Journal of Environmental Management*, 87(3), 329-340.
- Fuller, I. C., Basher, L. R., Murray Hicks, D. (2014). "Towards understanding river sediment dynamics as a basis for improved catchment, channel, and coastal management: the case of the Motueka catchment, Nelson, New Zealand." *International Journal of River Basin Management*, 12(3), DOI: 10.1080/15715124.2014.885437, pp. 175-192.
- French, J.L. (1966a). Fifth Progress Report on Hydraulics of Culverts Nonenlarged Box Culvert Inlets; NBS Report, Volume 9327. Washington, DC.
- French, J.L. (1966b). Sixth Progress Report on Hydraulics of Culverts: Tapered Box Culvert Inlets; NBS Report, Volume 9355, U.S. Department of Commerce, National Bureau of Standards: Gaithersburg, MD.
- French, J.L.; Bossy, H.G. (1967). 7th Progress Report on Hydraulics of Culverts: Tapered Box Culvert Inlets with Fall Concentration in the Inlet Structure; National Bureau of Standards: Washington, DC.
- Fujita, I., Muste, M. and Kruger, A. (1998). Large-Scale Particle Image Velocimetry for Flow Analysis in Hydraulic Applications, *J. Hydr. Res.*, 36(3), pp. 397-414.
- Furniss, M. J., Ledwith, T. S., Love, M. A., McFadin, B. C., & Flanagan, S. A. (1998). Response of Road-Stream Crossings to Large Flood Events in Washington, Oregon, and Northern California (No. 9877 1806-SD/IDC)
- Gillespie, N., Unthank, A., Campbell, L., Anderson, P., Gubernick, R., Weinhold, M., Cenderelli, D., Austin, B., McKinley, D., Wells, S., Rowan, J., Orvis, C., Hudy, M., Bowden, A., Singler, A.,

- Fretz, E., Levine, J. and Kirn, R. (2014). Flood effects on road–stream crossing infrastructure: economic and ecological benefits of stream simulation designs. *Fisheries* 39,
- Goodridge, W. H. (2009). Sediment Transport Impacts Upon Culvert Hydraulics, Master Thesis, Utah State University, Logan, Utah.
- Haan, C. T., Barfield, B. B., and Hayes, J. C. (1994). “Design hydrology and sedimentology for small catchments”, San Diego Academic Press, San Diego, CA, USA
- Haderlie, G. and Tullis, B.P. (2008). Hydraulics of multibarrel culverts under inlet control., *J. Irrigation and Drainage Engineering*, 134(4), doi: 10.1061/_ASCE_0733-9437_2008_134:4_507_
- Heller , (2011) Scale effects in physical hydraulic engineering models. *J Hydraul Res.*, 49(3), 293–306.
- Ho, H-C. (2010). “Investigation of unsteady and non-uniform flow and sediment transport characteristics at culvert sites”, PhD thesis, Civil & Environmental Engineering, The University of Iowa, Iowa City, Iowa, USA.
- Ho, H-C., Muste, M. and Ettema, R. (2013). Sediment Self-cleaning Multi-box Culverts, *J. Hydraul Res.*, 51(1), pp. 92-101.
- Howley, C. S. (2004). “The relationships among culvert characteristics and culvert sedimentation.” Master Thesis, University of Tennessee, Knoxville, TN.
- Hummel, R., Duan, J.G. and Zhang, S. (2012). Comparison of unsteady and quasi-unsteady flow models in simulating sediment transport in an ephemeral Arizona stream, *J. American Water Resources Association*, 48(5): 987-998. DOI: 10.1111/j.1752-1688.2012.00663.x
- Iqbal, U., Barthelemy, J., Perez, P., Cooper, J. and Li, W. (2021). A scaled physical model study of culvert blockage exploring complex relationships between influential factors, *Australasian Journal of Water Resources*, DOI: 10.1080/13241583.2021.1996679
- Jaeger, R., Tondera, K., Pather, S., Porter, M., Jacobs, C. and Tindale, N. (2019). Flow Control in Culverts: A Performance Comparison between Inlet and Outlet Control, *Water* 2019, 11, 1408; doi:10.3390/w11071408
- Johnson, P. A. and Brown, E. R. (2000). Stream assessment for multicell culvert use, *J. Hydraul. Eng.*, 126 (3), pp. 381–386.
- Jones, S., Kerenyi, K. and Stein, S. (2006). Effects of Inlet Geometry on Hydraulic Performance of Box Culverts Publication No. FHWA-HRT-06-138,
- Kantoush, S. A. (2008). Experimental study on the influence of the geometry of shallow reservoirs on flow patterns and sedimentation by suspended sediments. Doctoral dissertation. Laboratoire de Constructions Hydrauliques (EPFL). <https://doi.org/10.5075/epflthesis-4048>.
- Kosicki, A.J., Davis, S.R. (2001). Consideration of stream morphology in culvert and bridge design. *Transport. Res. Rec.: J. Transport. Res. Board* 1743(1), pp. 57–59.
- Kozarek, J. and Mielke, S. (2015). Sediment transport through recessed culverts: Laboratory experiments, Report for project 2015-08, Minnesota Department of Transportation, St. Paul, MS.
- Li, Z.J., Qian, H.L., Cao, Z.X., Liu, H.H., Pender, G. and Hu, P.H. (2018). Enhanced bed load sediment transport by unsteady flows in a degrading channel. *Int. J. Sediment Res.*, 33, pp. 327–339.
- Lord, M. L., Germanovski, D. and Allmendinger, N. E. (2009). “Fluvial geomorphology: Monitoring stream systems in response to a changing environment, in Young, R., and Norby, L., *Geological Monitoring: Boulder, Colorado*”, Geological Society of America: 69–103, doi: 10.1130/2009.monitoring (04).

- Lyn, D.A., Dey, S., Saksena, S. and Merwde, V. (2024). Culvert versus bridge hydraulics for larger-span or short culverts, *J. Hydraulic Engineering*, 150(2), DOI: 10.1061/JHEND8.HYENG-13650.
- May, R. W. P. (1993). Sediment transport in pipes and sewers with deposited beds, Rep. No. SR 320, HR Wallingford, UK.
- Merritt, W. S., Letcher, R. A., and Jakeman, A. J. (2003). "A review of erosion and sediment transport models". *Environmental Modelling & Software*, 18 (8), doi: [https://doi.org/10.1016/S1364-8152\(03\)00078-1](https://doi.org/10.1016/S1364-8152(03)00078-1), pp. 761-799.
- Miranzadeh, A. K. and Hossein, H. (2023) Blockage of box-shaped and circular culverts under flood event conditions: a laboratory investigation, *International Journal of River Basin Management*, 21(4), DOI: 10.1080/15715124.2022.2064483, pp. 607-616,
- Mrokowska, M. and Rowinski, P. (2019). Impact of unsteady flow events on bedload transport: a review of laboratory experiments, *Water*, 11, doi:10.3390/w11050907, 16 p.
- Mukherjee, S., Panda, S., Amatya, D.M., Dobre, M., Campbell, J.L., Lew, R., Caldwell, P., Elder, K., Grace, J.M. and Johnson, S.L. (2025). Hydro-geomorphological assessment of culvert vulnerability to flood-induced soil erosion using an ensemble modeling approach, *Environmental Modelling & Software*, 183, doi.org/10.1016/j.envsoft.2024.106243.
- Muste, M., Ettema, R., Ho, H-C. and Miyawaki, S. (2009). "Development of Self-Cleaning Box Culvert Designs," Report for Iowa Highway Research Board TR-545, The Iowa Department of Transportation, Ames, IA
- Muste, M., H-C. Ho, Mehl, D. (2010). "Insights into the Origin and Characteristics of the Sedimentation Process at Multi-Barrel Culverts in Iowa" IIHR-Hydrosience & Engineering Technical Report No., Iowa City, Iowa.
- Muste, M., Ho, H-C. (2012). "Determination of Entrance Loss Coefficients for Pre-Cast Reinforced Concrete Box Culverts," Iowa Highway Research Board, Ames, Iowa.
- Muste, M., Baranya, S., Tsubaki, R., Kim, D., Ho, H-C., Tsai, H-W. and Law, D. (2016). "Acoustic Mapping Velocimetry," *Water Resources Research*, 52, doi:10.1002/2015WR018354.
- Muste, M. and Xu, H. (2017a). "Mitigation of sedimentation at multi-box culverts", IIHR Report No. TR-655, Submitted to the Iowa Highway Research Board, Ames, IA, USA.
- Muste, M. and Xu, H. (2017b). "Sedimentation mitigation using streamlined culvert geometry", Report ST-001, Iowa Department of Transportation, Statewide Transportation Innovation Council, Federal Highway Administration, McLean, VA. 13
- Muste, M., Bacotiu, C. and Thomas, D. (2019). "Evaluation of the slope-area method for continuous streamflow monitoring," *Proceedings of the 38th World Congress*, September 1-6 2019, Panama City, Panama.
- Muste, M., Lee, K., Kim, D., Bacotiu, C., Rojas Oliveros, M., Cheng, Z. and Quintero, F. (2020). "Revisiting Hysteresis of Flow Variables in Monitoring Unsteady Streamflows" State-of-the-art Paper Series, *Journal of Hydraulic Research*; 58(6), pp. 867-887, <https://doi.org/10.1080/00221686.2020.1786742>
- Muste, M. and Xu, H. (2020). Development of self-cleaning box culverts, Iowa Highway Research Board Report for TR-719, Prepared for Iowa Department of Transportation, Ames, IA.
- Muste, M. and Xu, H. (2022). Multi-pronged Approach for Monitoring Sedimentation Processes at Multi-barrel Culverts, *Journal of Hydrology*, Special Issues on "In-river structures", <https://doi.org/10.1016/j.jhydrol.2022.127840>.
- Muste, M., Kim, K., Kim, D. and Fleit G. (2024). Decoding the hysteretic behavior of hydraulic variables in lowland rivers with multivariate monitoring approaches, Submitted to *Hydrological Processes*, Special Issue on "Hydrological processes in lowlands and plains".
- NCHRP (2011). Hydraulic loss coefficients for culverts, Project 15-24 (PI: B.L. Tullis).

- NCHRP (2019). Sustainable Highway Construction Guidebook, Research Report 916, National Cooperative Highway Research Program, <https://doi.org/10.17226/25698>
- ODOT (2014). Roadway drainage manual, Chapter 9: Culverts
(<https://oklahoma.gov/content/dam/ok/en/odot/documents/chapter-9-culverts.pdf>)
- Pyles, M. R., Skaugset, A. E. and Warhol, T. (1989). Culvert design and performance on forest roads. In 12th Annual Council on Forest Engineering Meeting, Coeur d'Alene, ID (pp. 82-87).
- Richardson, E.V., Simons, D.B., and Julien, P.Y. (1990). Highways in the river environment: Federal Highway Administration FHWA-HI-90-016, McLean, VA 719 p.
- Rowinski, P.M. and Czernuszenko, W. (1998). Experimental study of river turbulence under unsteady conditions, *Acta Geophys. Polonica XLVI*, pp.. 461-480.
- Rouse, H. (1940). Criteria for similarity in the transportation of sediment, *Proceedings of Hydraulics Conference, University of Iowa Studies in Engineering, Bulletin No. 20*, Iowa City, IA, USA, pp. 33–49,
- Rowley, K. J. (2014). “Sediment transport conditions near culverts”, M.S. Thesis Dissertation, Brigham Young University, Provo, UT.
- Safari, M-J-S., Aksoy, H., Unal, N.E. and Mohammadi, M. (2017). Non-deposition self-cleansing design criteria for drainage systems, *J. of Hydro-environmental Research* (14), pp. 76-84
- Schall, J.D., Thompson, P.L., Zerges, S.M., Kilgore, R.T. and Morris, J.L. (2012.) Hydraulic design of highway culverts. 3rd ed. Rep. No. FHWA/HIF- 12-026, HDS-5. Federal Highway Administration, Washington, DC
- Schumm, S. A. (1977). *The fluvial system*, John Wiley and Sons, New York, NY, 338p.
- Solomon, S. D., Qin M., Manning, Z., Chen, M., Marquis, K. B., Averyt, M. T., and Miller, H. L. (2007). “Contribution of working group i to the fourth assessment report of the intergovernmental panel on climate change”, Cambridge (UK), New York (NY USA), IPCC.
- Slater, L. J., and G. Villarini (2016). “Recent Trends in U.S. Flood Risk,” *Geophysical Research Letters*, 43(24), 12428-12436.
- Smith, C.R. and Kline, S.J. (1974). An experimental investigation of the transitory stall regime in two-dimensional diffusers, *J. Fluids Engineering*, pp. 11-15.
- Suszka, L. (1987). Sediment transport at steady and unsteady flow; a laboratory study, PhD Thesis, EPF Lausanne, Switzerland.
- Tetreault, J., Moore, I. D., Hoult, N. A., Tanzil, D., Maher, M. L. J. (2018). “Development of a sustainability evaluation system for culvert replacement and rehabilitation projects”, *Journal of Pipeline Systems Engineering and Practice* 9 (2): 1949–1204.
- Tsihrintzis, V.A. (1995). Effects of sediment on drainage culvert serviceability. *J. Perform. Constr. Fac.* 9(3), 172–183.
- UDOT (2017). Drainage manual, Appendix 9.C: Sedimentation at culverts, Utah Department of Transportation, Salt Lake City, UT
([https://www.udot.utah.gov/main/f?p=100:pg:0:::1:T,V:826,](https://www.udot.utah.gov/main/f?p=100:pg:0:::1:T,V:826))
- Villarini, G., Scoccimarro, E., Gualdi, S. (2013). “Projections of heavy rainfall over the central United States based on CMIP5 models”, *Atmospheric science letters* 14 (3): 200–205.
- Wang, L., Cuthbertson, A., Pender, G., & Zhong, D. (2019). Bed load sediment transport and morphological evolution in a degrading uniform sediment channel under unsteady flow hydrographs. *Water Resources Research*, 55, 5431–5452.
<https://doi.org/10.1029/2018WR024413>
- Wendling, R. (2019). “Cost of roadside ditch grading, personal communication,” Buchanan County Secondary Roads, Buchanan County.
- Xu, H. (2019). “Data-driven framework for forecasting sedimentation at culverts. PhD Thesis Dissertation,” The University of Iowa, Iowa City, USA.

- Xu, H., Muste, M. and Demir, I. (2019a). “Web-based Geospatial Platform for Analysis and Forecasting of Sedimentation at Culverts,” *J. Hydroinformatics*, 21(6), 1064-1081, doi: 10.2166/hydro.2019.068
- Xu, H., Demir, I., Koylu, C. and Muste, M. (2019b). “A Web-based Visual Analytics Framework for Identifying Potential Contributors to Culvert Sedimentation,” *Science of the Total Environment*, 692, 806-817, <https://doi.org/10.1016/j.scitotenv.2019.07.157>
- Wang, L., Cuthbertson, A.J.S., Pender, G. and Cao, Z. (2015). Experimental investigations of graded sediment transport under unsteady flow hydrographs. *Int. J. Sediment Res.*, 30, pp. 306–320.